RELATIVISTIC AND NON-RELATIVISTIC HOLOGRAPHY

BY

NAM NGUYEN HOANG

DISSERTATION

Submitted in partial fulfillment of the requirements
for the degree of Doctor of Philosophy in Physics
in the Graduate College of the
University of Illinois at Urbana-Champaign, 2010

Urbana, Illinois

Doctoral Committee:

Professor Scott Willenbrock, Chair
Professor Robert Leigh
Professor Charles Gammie
Professor John Stack

Abstract

Holography is one of the most interesting developments in String theory in the past few years. In this thesis, we discuss various aspects of the correspondence at the phenomenological and conceptual levels. At the phenomenological level, holographic duals of strong coupling QCD-like boundary theories is constructed using intersecting D-branes configurations Dq-Dp-$\overline{\text{D}p}$, in which the Dp's are probe branes under Dq's background geometry. Confinement, chiral symmetry phase transitions and their relation are carefully studied for various values of q, p and other parameters of the system. In terms of discrete symmetry, introducing torsion by adding the Nieh-Yan term (with space-time dependent coefficient) into 3+1 Einstein-Hilbert gravity is postulated to correspond to parity symmetry breaking in the boundary. A solitonic solution, which we call the torsion vortex as it resembles in many ways the Abrikosov vortex, is found in the bulk and believed to be dual to the parity breaking vacuum of the boundary theory. At the conceptual level, we deliberately tackle the boundary condition, variational principle and renormalization problems in non-relativistic holography. The systematic boundary condition formalism of Skenderis and Van Rees is extended to scalar field in Schrödinger space-time. In the same background, variational principle and renormalization procedures are constructed for fermions and vector fields, paying careful attention to the representation theory of the Schrödinger group. In any cases, 2-point functions for the dual operators are computed for various values of the parameter spaces.

To Mom, Dad and Sisters.

Acknowledgments

First and foremost, I would like to thank my father and sisters who have always been supporting my academic pursuit for so many years. Special dedication and gratitude to my mother who has directed, encouraged me and loved me so much.

I would like to express my gratitude to my advisor Robert Leigh, for dragging me to the whole new world of the fascinating theoretical Physics, for being patient listening to my ideas and tolerant with my frequent missing deadlines, and finally for always giving invaluable insights and perspectives to my research.

I would like to thank Anastasios Petkou and Mohammad Edalati who were my very friendly and creative collaborators. Many thanks to my wonderful officemates: Sean Nowling, Josh Guffin, Shiying Dong and Juan Jottar. Needless to say, I have learned most of my knowledge from the seminars, the blackboard discussions and casual chats with you. Thank you for always being helpful and supportive.

Thanks to the Graduate and High Energy office staffs who have been very spontaneously helpful in my documentation.

Finally, thank you all my friends here at UIUC, especially the ones in the Vietnamese Student Community, who make my first time ever studying abroad an extremely special and unforgettable experience.

Table of Contents

List of Tables

List of Figures

Chapter 1

Introduction

String theory is one of the leading candidates for a consistent quantum gravity theory. It is more than just a successful incorporation of the two pillars of theoretical Physics: Quantum Mechanics and General Relativity. In addition, it reveals profound physical implication and relates different regimes of Physics that look very unrelated from the outset; either between the short and the long, through T-duality, or the weak and the strong, through S-duality. Remarkably, it also lays out a framework for another impressive, distinctive type of duality which relates theories in different dimensionalities, the string/gauge duality. Simply speaking, the string/gauge duality conjectures a correspondence between String theory (or supergravity as its low energy limit) in a certain background geometry and a gauge theory living on the geometry's boundary. In essence, any bit of information in the "bulk" can be encoded in the "boundary" and vice versa. Hence the name holography.

Needless to say, holography is one of the most interesting recent development in String theory. It has a profound consequences, touching various aspect of modern Physics such as confinement and chiral symmetry breaking, Quark-Gluon plasma, fluid dynamics, quantum Hall effect, superconductivity, etc. A detailed introduction of the conjecture is out of the scope of this thesis. However, the basic idea can be sketched as follows.

In String theory, there are solitonic objects called D-branes. A Dp-brane is a p spatial dimension (infinitely) extended object where open strings can end on. For example, D0-brane is geometrically the same as a usual point particle. In the low energy limit, theories in the world volume of a stack of N_c coincident D-branes are $p+1$-dimensional supersymmetric gauge theories with the gauge group $U(N_c)$. As being solitonic objects in String theory, D-branes are realized in supergravity (which is the low energy limit of String theory) as black hole solutions. It is these black hole solutions that play a central role. The string-gauge conjecture then says that [1] [2] in the large N_c limit String theory on the near horizon regime of these black hole solutions is dual to the D-brane's world volume theories on the boundary of the black hole geometry. The temperature of the field theory is the Hawking's temperature of the black holes. Now in certain limit of the parameters, stringy loop effect is very suppressed and stringy excitations are very massive, leaving

us with only classical supergravity on one side of the duality (the String theory side). On the other side, in exactly the same limit, the corresponding gauge theories are strongly coupled. The duality hence relates classical computations in supergravity to fully non-perturbative observables in gauge theories. In the special case where the temperature is zero and the gauge theory is the conformal $N = 4$ super Yang-Mills, as for the extremal D3-branes, the near horizon regime of the geometry produced by D3-branes is AdS_5

$$ds^2 = \frac{L^2}{z^2}\Big(- dt^2 + d\vec{x}^2 + dz^2\Big) \tag{1.1}$$

(multiplied by an internal 5-sphere S^5). Hence the name AdS/CFT. Here L is the radius of AdS. The boundary of this geometry is at $z = 0$. It is for this case that the conjecture has been tested extensively. Various quantities in the gauge theory such as the central charge, Wilson loops, correlation functions and renormalization group flow (when the theory is slightly deformed) can be computed from the supergravity side. In literature, the black hole geometry is called the "bulk" geometry, while the D-branes world volume theories are referred as the "boundary" field theories.

The conjecture is recently extended by Melvin-twisting the D3-branes's geometry [3, 4, 5]. At zero temperature, the near horizon geometry is the so-called Schrödinger geometry

$$ds^2 = \frac{L^2}{z^2}\left(-\frac{\beta^2}{z^2}dt^2 + 2dtd\xi + d\vec{x}^2 + dz^2\right) \tag{1.2}$$

(also multiplied by an S^5), which possesses the non-relativistic conformal isometries for any L and β. Although it is not yet clear what is the boundary of this geometry, it is widely believed that the dual theory exists and is some non-relativistic conformal field theory sitting at $z = 0$. The nature of this correspondence, which we shall call Sch/nrCFT or non-relativistic holography, is unfortunately largely unknown compared to its relativistic counterpart. In this thesis we will develop a very first yet important step toward the understanding of the non-relativistic holography by studying various aspects of probe scalars and fermions in the bulk geometry.

So far we have been talking about a so-called top-down approach of holography, in which a string embedding of the bulk geometry (and other possible fields) is prerequisite. There is, however, a bottom-up approach. The idea is that AdS/CFT or Sch/nrCFT, after being stripped off the fancy and complicated decorations of supersymmetry and various limits taken, leave us with a hope for a more general sense of holography, in which gravity itself is actually describable as a field theory in one dimension lower. This hope bases on the fact that gravity possesses no local conserved quantities, due to general covariance. Conserved quantities are always quasi-local and are entirely encoded in the boundary of the region being computed.

Black holes thermodynamics is a well-known example. The bottom-up approach hence does not require (or, more reasonably put, does not yet worry about) a string embedding of the interested model from the outset. As long as it contains gravity, it is very possible that there is a holographic dual. In fact, non-relativistic holography was first proposed in this approach [6, 7].

Phenomenologically, holographic models in which the boundary theories possess some desired properties can be constructed using either of the two approaches. In the top-down approach, apart from the D-brane backgrounds of String theory, probe D-branes can be added [8] to include flavor degrees of freedom. The desire is to realize QCD-like properties such as confinement, asymptotic freedom, chiral symmetry breaking, meson spectroscopy, etc. in the boundary [9, 10, 11, 12, 13, 14, 15]. We will elaborate this direction in details in chapter 2, where a system of background Dq-branes intersecting with probe Dp and anti Dp-branes are constructed and studied. In the bottom-up approach, QCD-like holographic models are extensively investigated [16, 17, 18, 19, 20]. Parity symmetry breaking in the boundary can also be realized, as discussed in chapter 3, by considering torsional gravity [21]. Recently, condensed matter oriented models such as superconductivity, superfluidity, quantum Hall effect, Lifshitz-like theories, etc, are successfully constructed [22, 23, 24, 25, 26, 27].

In the heart of holography is the idea laid out by Witten [28] which relates the path integral with specified boundary conditions in the bulk to the partition function with sources inserted at the boundary

$$Z_{bulk}[\phi_I^{(0)}] = \langle e^{S_{bd}+\phi_I^{(0)}\hat{O}_I}\rangle. \tag{1.3}$$

Here S_{bd} is the un-deformed action of the boundary theory, $\phi_I^{(0)}$ is the boundary value for a generic field ϕ_I (with possibly an extra index I) and $\hat{O}_I$ its dual operator in the boundary. For example, if ϕ_I is a gauge field or the metric, $\hat{O}_I$ should be some boundary conserved current or the stress-energy tensor, respectively. The scaling dimension of $\hat{O}_I$ is determined uniquely from the space-time dimensionality and the characteristics of ϕ_I (spin and mass). The time-ordered 2-point function of $\hat{O}_I$ can be computed directly from (1.3)

$$\langle T\ \hat{O}_I\hat{O}'_J\rangle = \frac{\delta^2 Z_{bulk}[\phi_I^{(0)}]}{\delta\phi_I^{(0)}\delta\phi_J^{(0)'}} \tag{1.4}$$

The application of (1.3), however, is not as straightforward as it looks. In general, we need to worry about various conceptual problems: the boundary condition, variational principle and renormalization.

To illustrate the idea, consider a non-back reacting scalar field on AdS_{d+1} background (1.1). (In the top-down approach, this corresponds to working on the extremal D3-branes background, taking the near

horizon limit and truncating the linearized bulk theory to a sector that involves only a scalar field)

$$S = -\frac{1}{2}\int \sqrt{-g}d^dxdt\Big(\partial_\mu\phi\partial^\mu\phi + m^2\phi^2\Big). \tag{1.5}$$

Solving the equation of motion, we get

$$\phi = \phi^{(0)}(zk)^{d/2}K_\nu(kz) + \psi^{(0)}(zk)^{d/2}I_\nu(kz), \tag{1.6}$$

where $\nu = \sqrt{\frac{d^2}{4}+m^2}$, $k = \sqrt{\vec{k}^2}$ and $\phi^{(0)}$, $\psi^{(0)}$ are arbitrary functions of the transverse momentum. Now as K_ν dictates the near boundary expansion of ϕ, $\phi^{(0)}$ will determine the $z = 0$ boundary condition for the scalar field. However, as is obvious fixing $\phi^{(0)}$ does not completely fix the on-shell solution. Another boundary condition is required. Different such boundary conditions in the bulk are thus interpreted as corresponding to different causal processes in the boundary theory. For example, the authors of [29] believed that requiring $\phi \sim e^{ikz}$ as $z \to \infty$ (namely, setting $\psi = 0$ in (1.6)) allowed us to compute the retarded 2-point function of the dual operator. A more systematic, yet sophisticated, treatment of the boundary condition problem for relativistic holography was discussed in [30, 31]. There a unique procedure of gluing together segments of bulk geometries corresponding to a given time-contour in the boundary theory is postulated and proved to yield the expected results for various 2-point functions. In chapter 4, we will elaborate the method and extend it to the non-relativistic holography in the simple case of scalar fields.

The variational principle and renormalization problem are closely related. The former involves ensuring the proper Dirichlet boundary condition in the bulk, while the latter requires the bulk partition function $Z_{bulk}[\phi_I^{(0)}]$ to be finite. In practice, the classical (super)gravity limit is usually taken so that the partition function can be identified with the exponential of on-shell action $e^{iS^{os}_{bulk}[\phi_I^{(0)}]}$. The variational principle and renormalization thus amount to adding appropriate counter terms to the bulk action such that the total action's variation vanishes when fixing $\phi^{(0)}$ and its on-shell value is finite. These issues have been discussed extensively in different contexts [**?**, 33, 34, 35, 36]. In the case of the scalar field at hands, the counter terms are found to be

$$S_{ct} = \int_{z=\epsilon} d^dxdt\sqrt{-\gamma}\Big(\frac{d-\Delta}{2}\phi^2 + \frac{1}{2(\Delta-d-2)}\phi\Box_\gamma\phi + \dots\Big), \tag{1.7}$$

where $\sqrt{-\gamma} = z^{-d}$ is the d-dimensional induced metric determinant, $\Box_\gamma = z^2\vec{k}^2$ and $\Delta = \frac{d}{2}+\nu$ the scaling dimension of the dual operator. The dots represent higher derivative terms. For special cases where ν is an integer, logarithmic counter terms $\sim \log\epsilon$ may appear. Chapter 5 and 6 will be devoted to develop a de-

tailed treatment of variational principle and renormalization for fermions and vector fields on the Schrödinger space-time.

This thesis attempts to discuss holography both at the phenomenological and conceptual level. Chapter 2 introduces a generalization of a so-called Sakai-Sugimito model [13, 14], in which a transversely intersecting system of Dq-Dp-$\overline{\text{D}p}$-branes is constructed in the bulk. In the boundary, confinement, chiral phase transitions and their relation are carefully studied for various values of q and p. The next chapter intends to break parity symmetry in the boundary theory by including torsion in 3+1 bulk gravity [21]. Torsonal gravity is realized by adding a topological Nieh-Yan term (with space-time dependent coefficient) into the Einstein-Hilbert action with negative cosmological constant. In Euclidean signature, an exact solitonic solution is found, resembling in many ways the Abrikosov vortex solution in superconductivity. The dual theory is suggested to behave qualitatively as the 2+1 Gross-Neveu theory coupled to a U(1) gauge field, sitting on its parity breaking vacuum. Chapter 4 extends the Skenderis-van Rees realtime formalism for the boundary condition problem to non-relativistic holography, starting with a scalar field on Schrödinger space-time [37]. The boundary 2-point functions so obtained are accurate, including the $i\epsilon$ insertion, which confirms the method. In the same background, we then move on to study probe fermions and vector fields [38, 39] in chapter 5 and 6, respectively. Representation theory is carefully worked out, showing significant difference from the relativistic cases. The variational principle and renormalization problem are deliberately tackled and solved. The time-ordered 2-point functions are also computed for different values of the parameters.

Chapter 2

Transversely Intersecting D-branes at Finite Temperature and Chiral Phase Transition

2.1 Introduction, summary and conclusions

A very interesting holographic model of QCD which realizes dynamical breaking of non-Abelian chiral symmetry in a nice geometrical way is the Sakai-Sugimoto model [13]. In this model, one starts with N_c D4-branes extended in $(x^0x^1x^2x^3x^4)$-directions with x^4 being a circle of radius R. The low energy theory on the branes is a $(4+1)$-dimensional $SU(N_c)$ SYM with sixteen supercharges. To break supersymmetry, anti-periodic boundary condition for fermions around the x^4-circle must be chosen. To this system, $N_{\rm f}$ D8 and $N_{\rm f}$ $\overline{\rm D}8$-branes are added such that they intersect the D4-branes at two $(3+1)$-dimensional subspaces $\mathbb{R}^{3,1}$, and are separated in the compact x^4-direction by a coordinate distance of $\ell_0 = \pi R$. In other words, the D8 and $\overline{\rm D}8$-branes are located asymptotically at the antipodal points on the circle. The massless degrees of freedom of the system are the gauge bosons coming from $4-4$ strings and chiral fermions coming from 4-8 strings. (Before compactifying x^4, there are also massless adjoint scalars and fermions coming from the $4-4$ strings. These modes become massive upon compactifying x^4 and choosing anti-periodic boundary condition for the adjoint fermions; fermions get masses at tree level whereas scalars get masses due to loop effects.) The fermions localized at the intersection of D4 and D8-branes have (by definition) left-handed chirality and the fermions at the intersection of D4 and $\overline{\rm D}8$-branes are right-handed. The $U(N_{\rm f}) \times U(N_{\rm f})$ gauge symmetry of the D8 and $\overline{\rm D}8$-branes in this model is interpreted as the chiral symmetry of the fermions living at the intersections. At weak effective four-dimensional 't Hooft coupling λ_4 the low energy theory contains QCD but this is not the limit amenable to analysis by the gauge-gravity duality. At strong-coupling ($\lambda_4 \gg 1$), however, the theory is not QCD but can be analyzed using the gauge-gravity duality [40, 41, 42, 43], and it has been suggested that it is in the same universality class as QCD. In lack of any rigorous proof for this universality, the best one can do is to check whether this model at large N_c and large four-dimensional 't Hooft coupling exhibits the key features of QCD; namely, confinement and spontaneous chiral symmetry breaking. In fact, it apparently does [13]. By considering $N_{\rm f}$ D8 and $N_{\rm f}$ $\overline{\rm D}8$-branes as probe "flavor" branes in the near-horizon geometry of N_c "color" D4-branes and analyzing the Dirac-Born-Infeld (DBI) action

of the flavor branes in the background, one observes that at some radial point in the bulk the preferred configuration of the flavor branes is that of smoothly-connected D8 and $\overline{\text{D}}8$-branes. This geometrical picture is interpreted as dynamical breaking of $U(N_{\text{f}}) \times U(N_{\text{f}})$ chiral symmetry (where the branes are asymptotically separated) down to a single $U(N_{\text{f}})$ (where the branes connect). The model also shows confinement [44, 45].

Although choosing $\ell_0 = \pi R$ makes calculations a bit simpler, there is no particular reason to consider the flavor branes to be asymptotically located at the antipodal points of x^4. In fact, the $\ell_0 \ll \pi R$ limit of the Sakai-Sugimoto model is very interesting in its own right. By analyzing the $\ell_0 \ll \pi R$ limit, or equivalently the $R \to \infty$ limit, it was realized in [46] that the theory at the intersections can be analyzed both at weak and strong effective four-dimensional 't Hooft coupling λ_4. At weak-coupling the model can be analyzed using field theoretic methods and in fact is a non-local version of Nambu-Jona-Lasinio (NJL) model [47]. At strong-coupling it can be analyzed by studying the DBI action of the flavor branes in the near-horizon geometry of the color branes and exhibits chiral symmetry breaking via a smooth fusion of the flavor branes at some (radial) point in the bulk. A nice feature of this model is that the scale of chiral symmetry breaking is different from that of confinement [46], and one can completely turn off confinement by taking the $R \to \infty$ limit. Therefore the $\ell_0 \ll \pi R$ limit of the Sakai-Sugimoto model provides a clean holographic model of just chiral symmetry breaking without complications due to confinement.

The finite-temperature analysis (at large N_c and large 't Hooft coupling λ_4) of the Sakai-Sugimoto model as well as the holographic NJL model [46], was carried out in [48, 49]. Putting the flavor branes as probes ($N_{\text{f}} \ll N_c$) in the near-horizon geometry of N_c non-extremal D4-branes and analyzing the DBI action of the flavor branes, one obtains [48, 49] that at low temperatures (compared to ℓ_0^{-1}) the energetically-favorable solution is that of smoothly-connected D8 and $\overline{\text{D}}8$-branes which, like its zero-temperature counterpart, is a realization of chiral symmetry breaking. At high enough temperatures, on the other hand, the preferred (in the path integral sense) configuration is that of disjoint D8 and $\overline{\text{D}}8$-branes, hence chiral symmetry is restored. Also, when x^4 is compact and $\ell_0 < \pi R$, there exists an intermediate phase where the dual gauge theory is deconfined while chiral symmetry is broken [48].

It is certainly interesting to explore whether the holographic realization of chiral symmetry breaking and restoration is specific to a particular model such as the aforementioned ones, or generic in the sense that other intersecting brane models will realize it, too. To search for genericness (or non-genericness) of chiral symmetry breaking in intersecting brane models, a system of Dq-Dp-$\overline{\text{D}p}$-branes was considered at zero temperature in [50] where the color Dq-branes are stretched in non-compact $(x^0 x^1 \dots x^q)$-directions. The flavor Dp and $\overline{\text{D}p}$-branes intersect the color branes at two $(r+1)$-dimensional subspaces $\mathbb{R}^{r,1}$. Without flavor branes, the low energy theory on the color branes and whether it can be decoupled from gravity (or

other non-field theoretic degrees of freedom) with an appropriate scaling limit was analyzed in [51]. The low energy theory on the Dq-branes is asymptotically free for $q < 3$, conformal for $q = 3$, and infrared free for $q > 3$. While for $q \leq 5$, there always exists a scaling limit for which the open string modes can be decoupled from the closed string modes, there exists no such limit for $q = 6$. With the flavor branes present, an analysis was carried out in [50] where the behavior of the model for both small and large effective 't Hooft coupling $\lambda_{\rm eff} \sim \lambda_{q+1}\ell_0^{3-q}$ (ℓ_0 is the asymptotic coordinate distance between Dp and $\overline{\rm D}p$-branes, and λ_{q+1} is the 't Hooft coupling of the $(q+1)$-dimensional theory on the Dq-branes.) was considered. Taking the $N_c \to \infty$ limit while keeping $\lambda_{\rm eff}$ fixed and large, amounts, in the probe approximation, to putting the flavor branes in the near-horizon geometry of N_c color branes. (See [50, 51] for the validity of the supergravity analysis in these models.) Determining the shape of the flavor branes (relevant for chiral symmetry breaking) by analyzing their DBI action in the background geometry, it was observed that [50] for $q \leq 4$ there always exists a smoothly-connected brane solution which is energetically favorable. For a subclass of these general intersecting brane models, namely those for which $q+p-r = 9$, the above-mentioned connected solutions can be identified with the $U(N_{\rm f}) \times U(N_{\rm f})$ chiral symmetry being spontaneously broken. Following [50] we will call the brane models for which $q+p-r = 9$ as transversely-intersecting brane models and their intersections as transverse intersections. For $q = 5$, there exists no connected solution except when ℓ_0 takes a particular value. For this particular value of ℓ_0 which is around the scale of non-locality of the low energy theory on the D5-branes (which is a little string theory; see [52] for a review of little string theories), there is a continuum of connected solutions whose turning points can be anywhere in the radial coordinate of the bulk geometry. All such solutions are equally energetically favorable. For $q = 6$, there is a connected solution but is not the preferred one. The more energetically favorable solution, in this case, is that of disjoint branes. Due to the lacking of an appropriate decoupling limit for $q = 6$, it is not clear whether one can realize such a solution as a phase for which chiral symmetry is unbroken.

Summary and conclusions The purpose of this chapter is to investigate some aspects of non-compact transversely-intersecting D-brane models at finite temperature, in particular the number of solutions, their behavior, and whether or not such solutions can be identified with a chirally broken (or restored) phase of the dual gauge theory living at the intersections [14]. The main reason for us to consider transverse intersections is that in the probe approximation the generalization of the Abelian $U(1) \times U(1)$ chiral symmetry to the non-Abelian case is straightforward: one just replaces $N_{\rm f} = 1$ with general $N_{\rm f}$, and multiplies the flavor DBI action by $N_{\rm f}$. This is *not* the case in other holographic models of chiral symmetry breaking and restoration[1].

[1] For non-transverse intersections, namely $q + p - r \neq 9$, one can identify a symmetry in the common transverse direction as a chiral symmetry for the fermions of the intersections [53]. In some cases the generalization to low-rank non-Abelian chiral symmetry is possible [54], but such generalizations are not generic.

Note that the Sakai-Sugimoto model [13], its non-compact version [46], and the D2-D8-$\overline{\text{D8}}$ model analyzed in [55] which holographically realizes a non-local version of the Gross-Neveu model [56] are examples of transverse intersections.

This chapter is organized as follows. In section two we first review the general set up of the transversely-intersecting Dq-Dp-$\overline{\text{D}p}$-branes, then consider the system at finite temperature at large N_c and large effective 't Hooft coupling λ_{eff}. There are two saddle point contributions (thermal and black brane) to the bulk Euclidean path integral, and each can potentially be used as a background geometry dual to the color theory. Comparing the free energies of the two saddle points, we determine which one is dominant (has lower free energy) for various q's. For $q \neq 5$, the dominant saddle point is the black brane geometry, whereas for $q = 5$, the thermal geometry is typically dominant. In section three we present the solutions to the equation of motion for the DBI action of the flavor branes placed in the near horizon geometry of black Dq-branes. By a combination of analytical and numerical techniques, we show that, unlike the zero-temperature case, for ℓ_0/β less than a critical value, there exist generically two branches of smoothly-connected solutions (and of course, a solution with disjoint branes) for $q \leq 4$. (β is the circumference of the asymptotic Euclidean time circle, and is equal to the inverse of the dual gauge theory temperature T.) Note that some of these branches were previously missed in the literature. One branch which we will call the "long" connected solution gets very close to the horizon of the black Dq-branes whereas the other one named "short" connected solution stays farther away from it. Beyond the critical value, the flavor branes are "screened" and cannot exist as a connected solution. The situation is, however, different for $q = 5, 6$. For $q = 5$ and $T < (2\pi R_{5+1})^{-1}$, where R_{5+1} denotes the characteristic radius of the D5-brane geometry, the flavor branes must be placed in the near horizon geometry of thermal D5-branes. Like the zero temperature case, we find that there exists an infinite number of connected solutions when ℓ_0 is around the non-locality scale of the low energy theory on the D5-branes. This scale is set by the (inverse) hagedorn temperature of D5-brane little string theory. There are no connected solution for other values of ℓ_0, though. For $T = (2\pi R_{5+1})^{-1}$ the flavor branes should be considered in the near horizon geometry of black D5-branes. In this case there always exists one connected solution, as well as a disjoint solution, for small ℓ_0 (compared to $(2\pi R_{5+1})^{-1}$). In fact, at this particular temperature there is one connected solution for ℓ_0's much less than R_{5+1}. The number of solutions for ℓ_0 beyond the non-locality scale ($\sim R_{5+1}$) depends on the dimension of the intersections. For four-dimensional intersections, there are two connected solutions up to a critical value whereas for two-dimensional intersections there is no connected solution. Of course, for both two- and four-dimensional intersection there is always a solution representing disjoint branes. Having determined the flavor brane solutions in the background of thermal and black D5-branes, it is not clear whether or how these

solutions represent a chirally-broken or restored phase in the dual theory, mainly because in the geometry of D5 − branes, there are modes (non-field theoretic) which cannot totally be decoupled from the dual field theory degrees of freedom. Lastly, for $q = 6$, independent of what value ℓ_0/β takes, there always exist one connected solution (and a disjoint solution).

In section four, we map out different phases of the dual gauge theories and determine whether or not there is a chiral symmetry breaking-restoration phase transition. We do this by comparing the regularized free energies of the various branches of the solutions found in section three. For $q \leq 4$ the short solution is preferred to both long and disjoint solutions at small enough temperatures (compared to ℓ_0^{-1}), hence chiral symmetry is broken. At high temperatures, however, chiral symmetry gets restored and this phase transition is first order. For $q = 5$ and $T < (2\pi R_{5+1})^{-1}$, the infinite number of connected solutions are all equally energetically favorable, and each one of them is preferred over the disjoint solution. For $T = (2\pi R_{5+1})^{-1}$, we find that for small enough $\ell_0/(2\pi R_{5+1})$ the disjoint solution is preferred. For larger values of ℓ_0, there is no connected solution so the disjoint solution is the vacuum. As we alluded to earlier, it is not clear to us that the preferred solutions of the flavor branes in the background of color D5-branes can be associated with different phases of the dual theory. For $q = 6$, although we find that the disjoint solution is always preferred and there is no phase transition, there is no clear way to associate this solution with unbroken chiral symmetry in the dual field theory. This is because the is no decoupling limit that one can take to separate the gravitational degrees of freedom of those of the dual theory.

Section five is devoted to a brief analysis of the number of solutions and their energies for transversely-intersecting Dq-Dp-$\overline{\text{D}p}$-branes with compact x^q. In section six we speculate how the order parameter for chiral symmetry breaking can be realized in finite-temperature transversely-intersecting D-branes by including the thermal dynamics of an open string tachyon stretched between the flavor branes, and how it may depend on temperature. Finally, in the appendix we present detailed calculations for the free energies of the near horizon geometries of color Dq-branes (with the topology of either $\text{S}^1 \times \text{S}^1$ or $\text{S}^1 \times \mathbb{R}$ in the $t - x^q$ submanifold) to determine the dominant background geometry (either thermal or black brane) at low and high temperatures.

2.2 Transverse intersections at finite temperature

We start this section by reviewing first the general setup for transverse intersections of Dq-Dp-$\overline{\text{D}p}$-branes and identifying the massless degrees of freedom at intersections. We consider the system at finite temperature in the large N_c and large 't Hooft coupling limits. Since there is more than one background, we determine the one with the lowest free energy and consider that as the background dual to the color sector of the dual

theory at finite temperature. We then write the equation of motion for the flavor branes. This section is followed in the next section by an analysis of the solutions to the equation of motion as a function of the dimensions of the intersections r, as well as q. (For transverse intersections p, the spacial dimension of the flavor branes, is determined once r and q are given.)

2.2.1 General setup

Consider a system of intersecting Dq-Dp-$\overline{\text{D}p}$-branes in flat non-compact ten-dimensional Minkowski space where N_c Dq-branes are stretched in $(x^0x^1\dots x^q)$-directions, and each stack of $N_{\rm f}$ Dp and $N_{\rm f}$ $\overline{\text{D}p}$-branes are extended in $(x^0x^1\dots x^r)$- and $(x^{q+1}\dots x^9)$-directions. The Dp- and $\overline{\text{D}p}$-branes are separated in the x^q-direction by a coordinate distance ℓ_0 and intersect the Dq-branes at two $(r+1)$-dimensional intersections

	x^0	x^1	$\dots$	x^r	$\dots$	x^q	$\dots\dots$	x^9
Dq	$\times$	$\times$	$\dots$	$\times$	$\dots$	$\times$	$\dots\dots$	.
Dp	$\times$	$\times$	$\dots$	$\times$	$\dots$	.	$\dots\dots$	$\times$
$\overline{\text{D}p}$	$\times$	$\times$	$\dots$	$\times$	$\dots$	.	$\dots\dots$	$\times$.

(2.1)

Using T-duality one can determine the massless degrees of freedom localized at the intersection. It turns out that for transverse intersections, $q+p-r=9$, the massless modes which come from the Ramond sector in the $p-q$ strings are Weyl fermions. These fermions are in the fundamentals of $U(N_c)$ and $U(N_{\rm f})$. The massless modes at the other intersection are also Weyl fermions which transform in the fundamentals of $U(N_c)$ and $U(N_{\rm f})$ of the $\overline{\text{D}p}$-branes.

One way to put the above system at finite temperature (at large N_c, large effective 't Hooft coupling $\lambda_{\rm eff}$, and in the probe approximation $N_{\rm f}\ll N_c$) is to start with the geometry of black Dq-branes as background. The Euclidean metric for this geometry is

$$ds^2=\left(\frac{u}{R_{q+1}}\right)^{\frac{7-q}{2}}\left(f(u)dt^2+d\vec{x}^2\right)+\left(\frac{u}{R_{q+1}}\right)^{-\frac{7-q}{2}}\left(\frac{du^2}{f(u)}+u^2d\Omega_{8-q}^2\right), \tag{2.2}$$

with

$$f(u)=1-\left(\frac{u_T}{u}\right)^{7-q}, \tag{2.3}$$

where in the metric $d\Omega_{8-q}^2$ is the line element of a $(8-q)$-sphere with a radius equal to unity, and R_{q+1},

which denotes the characteristic radius of the geometry, is given by

$$R_{q+1}^{7-q} = (2\sqrt{\pi})^{5-q}\Gamma\Big(\frac{7-q}{2}\Big)g_s N_c l_s^{7-q} = 2^{7-2q}(\sqrt{\pi})^{9-3q}\Gamma\Big(\frac{7-q}{2}\Big)g_{q+1}^2 N_c l_s^{10-2q}, \tag{2.4}$$

where g_s is the string coupling. The Euclidean time is periodically identified: $t \sim t + \beta$, where β is equal to the inverse of the temperature T of the black branes. In (2.3) the horizon radius u_T is related to β as

$$T = \beta^{-1} = \frac{7-q}{4\pi}\Big(\frac{u_T}{R_{q+1}}\Big)^{\frac{7-q}{2}}\frac{1}{u_T}. \tag{2.5}$$

The relationship between u_T and β comes about in order to avoid a conical singularity in the metric at $u = u_T$. Note that for black D5-branes β is independent of u_T, and equals $2\pi R_{5+1}$.

Also, the dilaton ϕ and the q-form RR-flux F_q are given by

$$e^{\phi} = g_s\left(\frac{u}{R_{q+1}}\right)^{\frac{1}{4}(q-3)(7-q)}, \qquad F_q = \frac{2\pi N_c}{V_{8-q}}\epsilon_{8-q}, \tag{2.6}$$

where V_{8-q} and ϵ_{8-q} are the volume and the volume form of the unit $(8-q)$-sphere, respectively.

There is, however, another background with the same asymptotics as (2.2) which may potentially compete with the aforementioned background. The metric for this (thermal) geometry is

$$ds^2 = \left(\frac{u}{R_{q+1}}\right)^{\frac{7-q}{2}}\Big(dt^2 + d\vec{x}^2\Big) + \left(\frac{u}{R_{q+1}}\right)^{-\frac{7-q}{2}}\Big(du^2 + u^2 d\Omega_{8-q}^2\Big), \tag{2.7}$$

with the Euclidean time t being periodically identified with a period $\beta = T^{-1}$. Unlike the black brane geometries (2.2), β could take arbitrary values in the thermal geometries (2.7). The dilaton and the q-form RR-flux are the same as (2.6).

In the appendix we have calculated the free energies of both thermal and black brane geometries. Except for $q = 5$, the difference in free energies ΔS of the two geometries subject to the same asymptotics is given by

$$\Delta S = S_{\text{thermal}} - S_{\text{black brane}} = \frac{9-q}{g_s^2}V_9 u_T^{7-q}, \tag{2.8}$$

where V_9 is the volume of space transverse to the radial coordinate u: $V_9 = \text{Vol}(\text{S}^{8-q})\text{Vol}(\mathbb{R}^q)\text{Vol}(\text{S}^1_\beta)$. The volume V_9 is measured in string unit l_s where for simplicity we set $l_s = 1$. The difference in free energies (2.8) shows that the thermal background is less energetically favorable compared to the the black brane background (2.2). Thus, there is no Hawking-Page type transition between the two geometries which

holographically indicates that there is no confinement-deconfinement phase transition in the dual theory. The situation is different for $q = 5$. Semi-classically, once the characteristic radius R_{5+1} is given, the black D5-brane geometry will have a fixed temperature $T = (2\pi R_{5+1})^{-1}$. At this specific temperature, there are two saddle points contributing to the (type IIB) supergravity path integral: thermal and black D5-brane geometries. The difference in free energies of the two saddle points is (see the appendix for more details)

$$S_{\text{thermal D5}} - S_{\text{black D5-brane}} = \frac{8\pi}{g_s^2}\text{Vol}(\text{S}^3)\text{Vol}(\mathbb{R}^5)R_{5+1}u_T^2, \qquad \text{at} \qquad \beta = 2\pi R_{5+1}, \tag{2.9}$$

showing that the black brane geometry is the saddle point with lower free energy. However, at temperatures other than $(2\pi R_{5+1})^{-1}$, the thermal geometry is the only saddle point, although due to the hagedorn temperature of the D5-brane theory, one should only consider temperatures less than $(2\pi R_{5+1})^{-1}$. Thus, for $T < (2\pi R_{5+1})^{-1}$ we use the thermal D5-brane geometry as background.

2.2.2 Flavor Dp-$\overline{\text{D}p}$-branes in black Dq-brane geometries

We are interested in the dynamics of the flavor Dp and $\overline{\text{D}p}$-branes in the background of the black Dq-brane geometries. As we alluded to earlier, for $q = 5$ the thermal geometry of N_c D5-branes (once the limit of the near horizon geometry is taken) is the background that one should use for the dual finite temperature field theory for $T < (2\pi R_{5+1})^{-1}$. We also analyze the dynamics of the flavor branes in the background of the black D5-branes in which case it is understood that the dual theory is at a fixed temperature $T = (2\pi R_{5+1})^{-1}$. We are interested in the static shape of the flavor branes as a function of the radial coordinate u. Therefore we choose the embedding

$$\begin{array}{ccccccc} t = \sigma^0, & & x^1 = \sigma^1, & \cdots & x^r = \sigma^r, & & x^q = \sigma^q, \\ u = u(\sigma^q), & & x^{q+2} = \sigma^{q+1}, & \cdots & x^8 = \sigma^{p-1}, & & x^9 = \sigma^p, \end{array} \tag{2.10}$$

subject to the boundary condition

$$u(\pm\frac{\ell_0}{2}) = \infty, \tag{2.11}$$

where $\{\sigma^0, \cdots, \sigma^p\}$ are the worldvolume coordinates of the flavor branes. This boundary condition simply states that the asymptotic coordinate distance between the Dp and $\overline{\text{D}p}$-branes is ℓ_0. Ultimately the stability of such an assumption lies in the large N_c limit.

From now on, we set $N_{\text{f}} = 1$. As it becomes apparent in what follows, the generalization to $N_{\text{f}} \ll N_c$ is straightforward. The dynamics of a Dp-brane (and a $\overline{\text{D}p}$-brane) is determined by its DBI plus Chern-Simons

action. Solving the equations of motion for the gauge field, one can safely set the gauge field equal to zero and just work with the DBI part of the action. After all, it is this part of the full action which is relevant for our purpose of determining the shape of the Dp and $\overline{\text{D}p}$-branes. Therefore, with gauge field(s) set equal to zero, the dynamics is captured by the DBI action

$$S_{\text{DBI}} = \mu_p \int d^{p+1}\sigma \; e^{-\phi}\sqrt{\det(g_{ab})}, \tag{2.12}$$

where μ_p is a constant, and $g_{ab} = G_{MN}\partial_a x^M \partial_b x^N$ is the induced metric on the worldvolume of the Dp-brane. For a Dp-brane forming a curve $u = u(x^q)$, the DBI action (2.12) reads

$$S_{\text{DBI}} = \beta\, C(q,r) \int d^r x \; dx^q \; u^{\frac{\gamma}{2}} \Big[f(u) + \Big(\frac{u}{R_{q+1}}\Big)^{2\delta} u'^2 \Big]^{\frac{1}{2}}, \tag{2.13}$$

where

$$\begin{aligned} C(q,r) &= \frac{\mu_p}{g_s}\, \text{Vol}(\text{S}^{8-q}) {R_{q+1}}^{\frac{1}{4}(q-7)(r-3)}, \\ \gamma &= 2 + \frac{1}{2}(7-q)(r+1), \\ \delta &= \frac{1}{2}(q-7), \end{aligned} \tag{2.14}$$

and $u' = du/dx^q$. For a Dp-brane forming a curve $u(x^q)$ in the thermal D5-brane geometry the DBI action is obtained by setting $f(u) = 1$ in (2.13). The integrand in (2.13) does not explicitly depend on x^q, therefore $\mathcal{L} - u'\partial\mathcal{L}/\partial u'$ must be conserved (with respect to x^q). A first integral of the equation of motion is then obtained

$$u^{\frac{\gamma}{2}} f(u) \Big[f(u) + \Big(\frac{u}{R_{q+1}}\Big)^{2\delta} u'^2 \Big]^{-\frac{1}{2}} = u_0^{\frac{\gamma}{2}}, \tag{2.15}$$

where u_0 parametrizes the solutions. We now analyze the solutions of (2.15).

2.3 Multiple branches of solutions

The simplest solution of the equation of motion in (2.15), namely $u_0 = 0$, corresponds to $x^q =$ constant. In order to satisfy the boundary condition (2.11), one obtains $x^q = \pm\ell_0/2$. So, the $u_0 = 0$ solution corresponds to disjoint Dp and $\overline{\text{D}p}$-branes descending all the way down to the horizon at $u = u_T$. Also, note that the existence of this solution is independent of β.

For $u_0 \neq 0$, solving for $u^{'}$ yields

$$u^{'2} = \frac{1}{{u_0}^{\gamma}}\Big(\frac{u}{R_{q+1}}\Big)^{-2\delta} f(u)\,\Big({u^{\gamma}f(u) - {u_0}^{\gamma}}\Big). \tag{2.16}$$

Since the left hand side of (2.16) is non-negative, the right hand side of (2.16) must also be non-negative resulting in $u \geq \max\{u_T, u_*\}$, where u_* is a possible turning point. Therefore, for allowed solutions one must have $u \geq u_* > u_T$.

The possible turning points are determined by analyzing the zeros of the right hand side of (2.16). Setting $f(u_*) = 0$ will not result in a valid turning point. So, the other possibilities come from solving $u_*^{\gamma} f(u_*) - u_0^{\gamma} = 0$, which we will rewrite as follows

$$u_*^{\gamma} - u_*^{\sigma} u_T^{-2\delta} - u_0^{\gamma} = 0, \tag{2.17}$$

where

$$\sigma = \gamma + 2\delta = 2 + \frac{1}{2}(7-q)(r-1). \tag{2.18}$$

Note that since $r \neq 0$ (and in fact, for the cases of interest, it is either 1 or 3), σ is always a positive integer which, combined with the fact that $\delta < 0$, implies that $\sigma < \gamma$.

We use (2.16) to relate the integration constant u_*, or equivalently u_0, to the parameters of the theory, namely the (inverse) temperature β and the asymptotic distance between the Dp and $\overline{\text{D}p}$-branes ℓ_0. First, rearrange (2.16) to get

$$\begin{aligned} x^q(u) &= R^{-\delta} u_0^{\frac{\gamma}{2}} \int_{u_*}^{u} \Big(u^{-2\delta} - u_T^{-2\delta}\Big)^{-\frac{1}{2}} \Big(u^{\gamma} - u^{\sigma} {u_T}^{-2\delta} - u_0^{\gamma}\Big)^{-\frac{1}{2}} du \\ &= R^{-\delta}(u_*^{\gamma} - u_*^{\sigma} u_T^{-2\delta})^{\frac{1}{2}} \int_{u_*}^{u} \Big(u^{-2\delta} - u_T^{-2\delta}\Big)^{-\frac{1}{2}} \times \\ &\quad \Big(u^{\gamma} - u^{\sigma} {u_T}^{-2\delta} - (u_*^{\gamma} - u_*^{\sigma} u_T^{-2\delta})\Big)^{-\frac{1}{2}} du, \end{aligned} \tag{2.19}$$

where in the second line we used (2.17) to trade u_0 for u_*. Changing to a new (dimensionless) variable $z = u/u_T$, (2.19) becomes

$$x^q(z) = -\frac{\delta}{2\pi}\beta(z_*^{\gamma} - z_*^{\sigma})^{\frac{1}{2}} \int_{z_*}^{z} \Big(\tilde{z}^{-2\delta} - 1\Big)^{-\frac{1}{2}} \Big(\tilde{z}^{\gamma} - \tilde{z}^{\sigma} - (z_*^{\gamma} - z_*^{\sigma})\Big)^{-\frac{1}{2}} d\tilde{z}, \tag{2.20}$$

where $z_* \in (1, \infty)$. Taking the $z \to \infty$ limit, we can relate z_* to β and ℓ_0

$$\frac{\ell_0}{\beta} = -\frac{\delta}{\pi} (z_*^\gamma - z_*^\sigma)^{\frac{1}{2}} \int_{z_*}^\infty \left(z^{-2\delta} - 1\right)^{-\frac{1}{2}} \left(z^\gamma - z^\sigma - (z_*^\gamma - z_*^\sigma)\right)^{-\frac{1}{2}} dz. \tag{2.21}$$

As we mentioned earlier, the solutions to the equation of motion are parametrized by possible value(s) of the turning point z_*. For a fixed ℓ_0/β, it is the number of z_* which determines the number of (connected) solutions. Thus, one has to analyze ℓ_0/β as a function of z_* to determine the number of solutions for a fixed ℓ_0/β.

2.3.1 Analytical analysis

There are regions of z_* for which ℓ_0/β as a function of z_* can be given analytically. These are the $z_* \to 1^+$ and $z_* \gg 1$ regions. For any z_*, the integral in (2.21) can be evaluated numerically. The numerical results will be presented shortly after the analytical analysis for the two limiting cases is given.

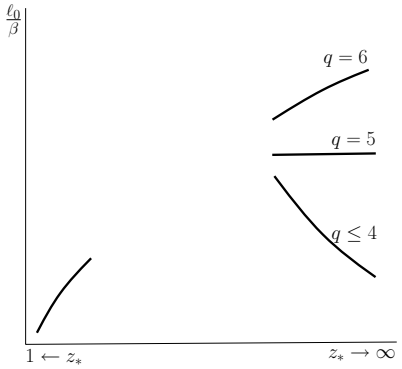

Figure 2.1: Behavior of ℓ_0/β versus z_* in two regions of $z_* \to 1$ and $z_* \gg 1$ for various q's. Except for $q = 5$, these plots illustrate the number of connected Dp-branes at low and high temperatures placed in the background of black Dq-branes. For $q = 5$, it is understood that β is fixed; $\beta = 2\pi R_{5+1}$, and different solutions is obtained by varying ℓ_0.

First consider the $z_* \to 1^+$ limit. Taking $z_* = 1 + \epsilon$ where $0 < \epsilon \ll 1$, (2.21) is approximated by

$$\frac{\ell_0}{\beta} \sim -\frac{\delta}{\pi} \sqrt{-2\delta\epsilon} \int_{1+\epsilon}^\infty (z^{-2\delta} - 1)^{-\frac{1}{2}} (z^\gamma - z^\sigma + 2\delta\epsilon)^{-\frac{1}{2}} dz. \tag{2.22}$$

Ignoring some numerical prefactors, the behavior of (2.22), is approximated by $\sqrt{\epsilon} \int^\infty z^{\delta - \frac{\gamma}{2}} dz$ for large values of z. Since $\delta - \frac{\gamma}{2} < -2$ for all q and r of interest, one has $\sqrt{\epsilon} \int^\infty z^{\delta - \frac{\gamma}{2}} dz \sim \sqrt{\epsilon}$. On the other hand, when z approaches z_* such that $z - z_* > 0$, we define $z = z_* + x$ with $0 < x \ll 1$, and expand out the

integrand of (2.22) around x. We get

$$\begin{aligned}\frac{\ell_0}{\beta} &\sim -\frac{\delta}{\pi\sqrt{-2\delta}}\sqrt{\epsilon}\int_0 (x(x+\epsilon))^{-\frac{1}{2}}dx \\ &\sim -\frac{1}{\pi}\sqrt{-2\delta}\sqrt{\epsilon}\log\sqrt{\epsilon},\end{aligned} \tag{2.23}$$

indicating that the leading behavior of ℓ_0/β in the $z_* \to 1$ limit is $-\sqrt{\epsilon}\log\sqrt{\epsilon}$.

For the $z_* \gg 1$ region, we can approximate (2.21) by (recall $\delta < 0$ and $\sigma < \gamma$)

$$\begin{aligned}\frac{\ell_0}{\beta} &\sim -\frac{\delta}{\pi}\, z_*^{\frac{\gamma}{2}}\int_{z_*}^{\infty} z^{\delta}\Big(z^{\gamma}-z_*^{\gamma}\Big)^{-\frac{1}{2}}dz+\cdots \\ &= -\frac{\delta}{\pi}z_*^{1+\delta}\int_1^{\infty} y^{\delta}\Big(y^{\gamma}-1\Big)^{-\frac{1}{2}}dy+\cdots \\ &= -\frac{\delta}{\gamma\sqrt{\pi}}\frac{\Gamma\Big[\frac{\gamma-2(1+\delta)}{2\gamma}\Big]}{\Gamma\Big[\frac{\gamma-(1+\delta)}{\gamma}\Big]}\, z_*^{1+\delta}+\cdots,\end{aligned} \tag{2.24}$$

where $\cdots$ represents terms subleading in z_*, and in the second line in (2.24) we have changed the variable from z to $y = z/z_*$. Thus, aside from a numerical factor, the $z_* \to \infty$ limit of (2.21) reads

$$\frac{\ell_0}{\beta} \sim z_*^{1+\delta}. \tag{2.25}$$

This expression is identical to the one derived for the zero temperature case in [50]. This resemblance is not accidental because the large z_* limit corresponds to having a turning point very far away from the horizon of the background geometry. The results obtained for this limit should then match those derived for the zero temperature case. An interesting feature of (2.25) is that for the black D5-branes $\ell_0/(2\pi R_{5+1})$ is independent of z_* and approaches a constant value of $1/(r+3)$. This value has been argued in [50] to be around the scale of non-locality of the low energy effective theory on D5-branes. The analysis for the dynamics of the flavor branes placed in the thermal D5-brane geometry is the same as the analysis when they are placed in the zero temperature D5-brane geometry. The zero temperature analysis has already been done in [50] where it was found that there exist an infinite number of connected solutions for one specific value of $\ell_0 = 2\pi R_{5+1}/(r+1)$, and none for other ℓ_0's.

Analyzing (2.21) for the two regions of $z_* \to 1^+$ and $z_* \gg 1$, the minimum crude conclusion that one can draw is that for small enough ℓ_0/β there exist two connected solutions (one closer to the horizon which we will name "long" connected solution, and the other farther away from it named "short" connected solution) for $q \leq 4$ and only one curved solution for $q = 6$. For $q = 5$ and for $T < (2\pi R_{5+1})^{-1}$, there exists an infinite

number of connected solutions for just $\ell_0 = 2\pi R_{5+1}/(r+1)$ and none for others. On the other hand, for $T = (2\pi R_{5+1})^{-1}$, there is only one connected solution given that $\ell_0 \ll 2\pi R_{5+1}$. The analysis for the two z_* regions has been summarized in Figure 2.1.

2.3.2 Numerical analysis for the number of solutions

For generic values of ℓ_0/β, the allowed number of solutions can be determined by numerically integrating (2.21) and plotting ℓ_0/β versus z_*. The results for various intersections and Dq-branes are shown in Figure 2. Although we have plotted ℓ_0/β versus z_* for $z_* \in (1, 50)$, the qualitative behavior of the plots stays the same if one considered larger values of z_*. As we will describe below, the number of curved solutions depends on what configuration is being considered. Note that regardless of the configuration, there always exists a disjoint solution. In what follows in the rest of this subsection, when we say there exist one or two solutions for a particular system we have connected solutions in mind.

$(3+1)$-dimensional intersections In this case there are three allowed D-brane configurations which are transversely intersecting. These are the D4-D8-$\overline{\text{D}}$8, D5-D7-$\overline{\text{D}}$7 and D6-D6-$\overline{\text{D}}$6 configurations shown on the top row in Figure 2.2.

For the D4-D8-$\overline{\text{D}}$8 configuration (shown on the upper left corner in Figure 2), there is a critical value of $(\ell_0/\beta)_{\text{cr}} \approx 0.17$ beyond which there exists no connected solution for the flavor branes. Below this critical value there are two connected solutions which we earlier called the "short" and the "long" connected solutions. The existence of these two types of solutions and the critical value of 0.17 were already noted by the authors of [49] in the their analysis of the holographic NJL model at finite temperature. We will see in the next section that the short solution is always more energetically favorable to the long one. Since there also exists a disjoint solution, determining the chirally-broken or chirally-symmetric phase of the dual field theory (which is a non-local version of the NJL model [46]) is just a matter of comparing the free energies of the disjoint and short connected solution. This will be done in the next section.

The analysis for the D5-D7-$\overline{\text{D}}$7 and D6-D6-$\overline{\text{D}}$6 cases are, however, more subtle, and the holographic interpretation of the solutions is less transparent for reasons to be mentioned below. For the D5-D7-$\overline{\text{D}}$7 configuration at temperature $T = (2\pi R_{5+1})^{-1}$, there are two critical values of $(\ell_0/(2\pi R_{5+1}))_{\text{cr}} \approx 0.168$ and 0.175. For $\ell_0/(2\pi R_{5+1}) < 0.168$ there is always one connected solution, for $0.168 < \ell_0/(2\pi R_{5+1}) < 0.175$ there are two, and for $\ell_0/(2\pi R_{5+1}) > 0.175$ there exists none. Comparing these results to the ones obtained for the zero-temperature D5-D7-$\overline{\text{D}}$7 configuration, one observes that while at zero temperature [50], there are either an infinite number of solutions or none, at $T = (2\pi R_{5+1})^{-1}$ there are different numbers of solutions

(one, two, or none) depending on what values ℓ_0 take; see Figures 2 and 3. For D5-D7-$\overline{\text{D}}$7 configuration at temperatures $T < (2\pi R_{5+1})^{-1}$, the situation is the same as the zero temperature case. There exist connected solutions only for a specific value of $\ell_0 = \pi R_{5+1}/3$. Indeed, there are an infinite number of such solutions; see Figure 3.

For D6-D6-$\overline{\text{D}}$6 configuration, the situation is simpler. For any ℓ_0/β there always exists one and only one connected solution. As we will see in the next section all these connected solutions are less energetically favorable compared to disjoint solutions. The observation that for color D6-branes at finite temperature there is always one connected solution, hence no "screening length", is in accord with the fact that the near horizon geometry of D6-branes cannot be decoupled from the gravitational modes of the bulk geometry [51].

$(1+1)$-dimensional intersections In this case, there are five allowed configurations (shown on the second and third rows in Figure 2), namely D2-D8-$\overline{\text{D}}$8, D3-D7-$\overline{\text{D}}$7, D4-D6-$\overline{\text{D}}$6, D5-D5-$\overline{\text{D}}$5 and D6-D4-$\overline{\text{D}}$4. Configurations with $q \leq 4$ show similar behavior. For $q \leq 4$ there always exists a critical $(\ell_0/\beta)_{\text{cr}}$ beyond which connected solutions cease to exist. The critical value obtained from Figure 2 is $(\ell_0/\beta)_{\text{cr}} \approx 0.225, 0.223, 0.227$ for color D2, D3 and D4-branes, respectively. Below these critical values there are two solutions, the short and long solutions[2].

For the D5-D5-$\overline{\text{D}}$5 system at $T = (2\pi R_{5+1})^{-1}$, below a critical value of $(\ell_0/(2\pi R_{5+1}))_{\text{cr}} \approx 0.251$ there is always one solution whereas above this value connected solutions do not exist. Note the difference (depicted in Figure 3) of this case with the D5-D7-$\overline{\text{D}}$7 system: for the D5-D5-$\overline{\text{D}}$5 configuration, there is no range of $\ell_0/(2\pi R_{5+1})$ for which there exist the short and long solutions. Like the D5-D7-$\overline{\text{D}}$7 configuration, for the D5-D5-$\overline{\text{D}}$5 system at $T < (2\pi R_{5+1})^{-1}$, there is an infinite number of connected solutions when $2\ell_0 = \pi R_{5+1}$ and none for other ℓ_0's.

For the D6-D4-$\overline{\text{D}}$4 configuration, there is always one connected solution for arbitrary values of ℓ_0/β. Notice that the behavior of the flavor branes in the geometry of color D5 and D6-branes with $(1+1)$-dimensional intersections is qualitatively the same as their behavior with $(3+1)$-dimensional intersections.

2.4 Energy of the configurations

As we saw in the previous section there are typically more than one solution for a given ℓ_0/β. In fact, just to recap, for ℓ_0/β less than a critical value there are generically three branches of solutions for $q \leq 4$; one disjoint and two connected solutions. There are also an infinite number of solutions for $q = 5$ at

[2]The authors of [55] studied the D2-D8-$\overline{\text{D}}$8 system at finite temperature but missed the existence of the long connected solution.

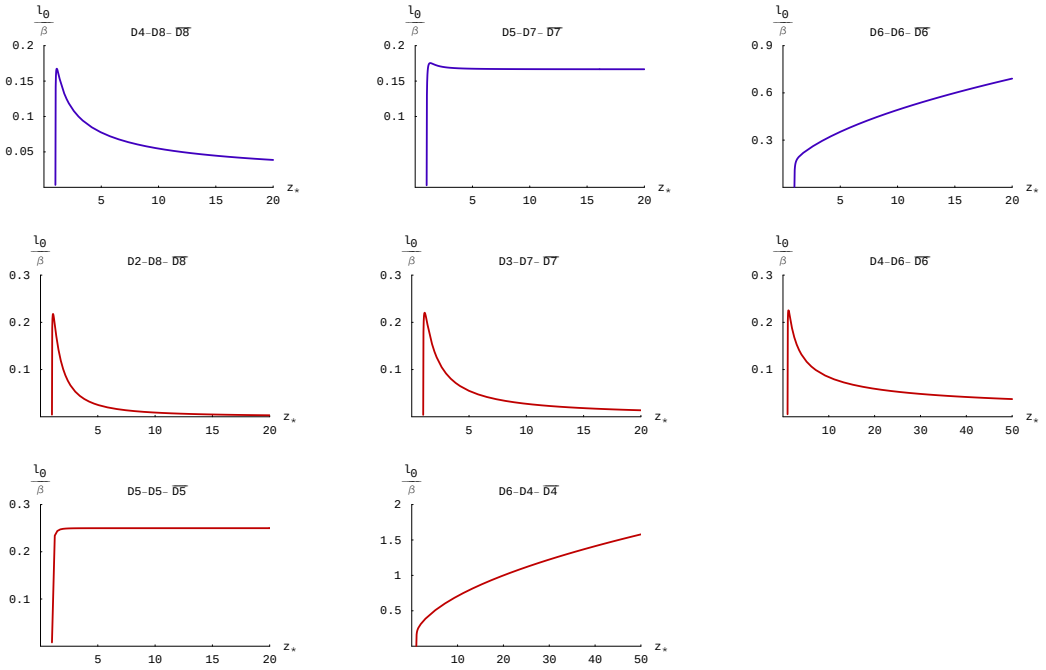

Figure 2.2: Behavior of ℓ_0/β versus z_* obtained numerically for generic values z_* for various q's and intersections of interest, i.e. $r = 1$ and $r = 3$. The blue plots show the behavior for $3 + 1$ intersections whereas the red plots show the behavior for $1 + 1$ intersections. These plots show the number of connected Dp-branes (for all temperatures) placed in the background of black Dq-branes. For $q = 5$, the temperature T is fixed: $T = (2\pi R_{5+1})^{-1}$. Except for $q = 5, 6$, such solutions can potentially be realized as different phases of the holographic dual theories.

$T < (2\pi R_{5+1})^{-1}$ as long as $\ell_0 = 2\pi R_{5+1}/(r+3)$. There are two branches of solutions for $q = 6$ for any ℓ_0/β; one disjoint and one connected solution. Since there are various configurations for a particular value of ℓ_0/β, one needs to compare their on-shell actions to determine which configuration is more energetically favorable. In this section we analyze the energy of these configurations by a combination of analytical and numerical techniques. The energy of these configurations by themselves is infinite. We regulate the energies of connected configurations by subtracting from them the energy of disjoint configurations

$$\tilde{E} = \lim_{\Lambda\to\infty}\left\{\int_{z_*}^{\Lambda} dz\ z^{\frac{\sigma}{2}}\left(1-\frac{z_*^{\gamma}-z_*^{\sigma}}{z^{\gamma}-z^{\sigma}}\right)^{-\frac{1}{2}} - \int_{1}^{\Lambda} dz\ z^{\frac{\sigma}{2}}\right\}, \tag{2.26}$$

where Λ is a cutoff and the difference in energy E is related to $\tilde{E}$ as

$$E = -\frac{\delta\beta^2}{\pi}C(q,r)\ u_T^{\frac{\gamma}{2}}\int d^r x\ \tilde{E}. \tag{2.27}$$

2.4.1 Analytical analysis

The integral in (2.26) is complicated and as far as we know cannot be integrated analytically for generic values of z_*. However, like the integral in (2.21), there are two regions of $z_* \to 1$ and $z_* \gg 1$ for which we can integrate $\tilde{E}(z_*)$ analytically. In the $z_* \to 1$ limit, it can be shown that $\tilde{E}$ is positive for all q and r. Indeed, let's rewrite (2.26) as follows

$$\begin{aligned}\tilde{E}_\Lambda &= \int_{z_*}^{\Lambda} dz\ z^{\frac{\sigma}{2}}\Big[\Big(1-\frac{z_*^\gamma - z_*^\sigma}{z^\gamma - z^\sigma}\Big)^{-\frac{1}{2}} - 1\Big] - \int_1^{z_*} dz\ z^{\frac{\sigma}{2}} \\ &= \Big(\int_{z_*}^{z_*'} dz\ z^{\frac{\sigma}{2}}\Big[\Big(1-\frac{z_*^\gamma - z_*^\sigma}{z^\gamma - z^\sigma}\Big)^{-\frac{1}{2}} - 1\Big] - \int_1^{z_*} dz\ z^{\frac{\sigma}{2}}\Big) \\ &\qquad + \int_{z_*'}^{\Lambda} dz\ z^{\frac{\sigma}{2}}\Big[\Big(1-\frac{z_*^\gamma - z_*^\sigma}{z^\gamma - z^\sigma}\Big)^{-\frac{1}{2}} - 1\Big]. \end{aligned} \tag{2.28}$$

The last integral in (2.28) is positive for any z_*'. If $z_* = 1+\epsilon$, we can choose $z_*' = 1+3\epsilon$ and the difference in the bracket is estimated to be

$$\epsilon(\sqrt{6}-2) + \epsilon\Big(\log(\sqrt{2}+\sqrt{3}) - 1\Big) + o(\epsilon^2), \tag{2.29}$$

which is also positive.

Approximating (2.26) in the $z_* \gg 1$ region yields

$$\begin{aligned}\tilde{E}_\Lambda &\sim \int_{z_*}^{\Lambda} dz\ z^{\delta+\gamma}\Big(z^\gamma - z_*^\gamma\Big)^{-\frac{1}{2}} - \int_1^{\Lambda} dz\ z^{\frac{\sigma}{2}}, \\ &= \Big\{\int_{z_*}^{\Lambda} dz\ z^{\delta+\gamma}\Big(z^\gamma - z_*^\gamma\Big)^{-\frac{1}{2}} - \int_0^{\Lambda} dz\ z^{\frac{\sigma}{2}}\Big\} + \frac{2}{\sigma+2}. \end{aligned} \tag{2.30}$$

Note that in the large z_* limit, $z_* \simeq z_0$ where $z_0 = u_0/u_T$. As a result, from (2.30) we see that the energy of the connected configurations approaches their zero temperature value obtained in [50]. This is expected since in this regime the connected flavor branes are very far away from the horizon hence receive little effect from it. The disjoint configuration, on the other hand, always keeps in touch with the horizon and gets a finite temperature contribution $-\frac{2}{\sigma+2}$. The term in the curly bracket of (2.30) is already computed in [50] in terms of Beta functions, giving an energy difference of

$$\begin{aligned}\tilde{E} &= \lim_{\Lambda\to\infty}\tilde{E}_\Lambda \\ &= \frac{1}{\gamma} z_*^{\frac{\gamma}{2}+\delta+1} B\Big[-\frac{1}{2} - \frac{\delta+1}{\gamma}, \frac{1}{2}\Big] + \frac{2}{\sigma+2}. \end{aligned} \tag{2.31}$$

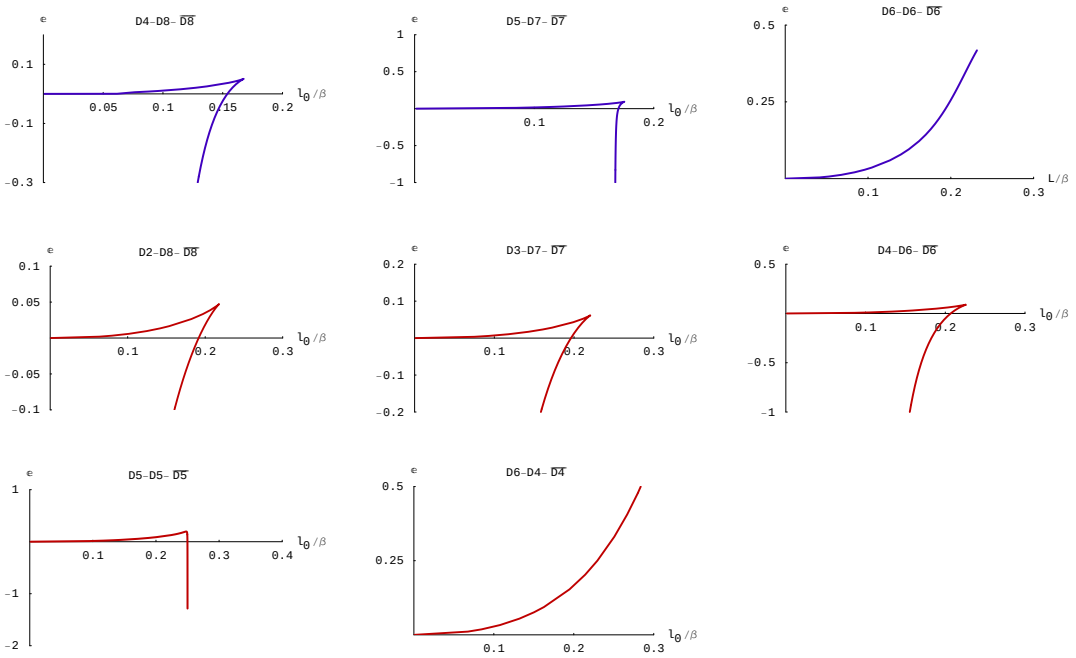

Figure 2.3: Behavior of $\tilde{E}$ versus ℓ_0/β obtained numerically for various q's and intersections of interest, i.e. $r = 1$ and $r = 3$. The blue plots show the behavior for $3+1$ intersections whereas the red plots show the behavior for $1+1$ intersections. The plots for the color D5-branes are for a fixed (inverse) temperature of $\beta = 2\pi R_{5+1}$.

Since $z_* \gg 1$, the last term is irrelevant in determining the sign of $\tilde{E}$. We see immediately that $\tilde{E} > 0$ for $q \geq 6$ and $\tilde{E} < 0$ for $q \leq 4$. For $q = 5$, the Beta function vanishes, and a more careful investigation must be made to determine the sign of $\tilde{E}$. It turns out that in going from (2.26) to (2.30), we have over-estimated the energy for the joined brane configurations: there is a correction with leading behavior $\sim -z_*^{(r-1)/2}$ for large z_*. Thus, for $q = 5$ we have $\tilde{E} < 0$ for $r > 1$, while the analytic analysis is not reliable for $r = 1$. The analytic results for the two aforementioned limits of z_* are summarized in Figure 4.

2.4.2 Numerical results and phase transitions

For generic value of z_* the integral in (2.26) can be numerically integrated and one can plot $\tilde{E}$ versus z_*. Instead we will numerically eliminate z_* between (2.21) and (2.26) and plot $\tilde{E}$ versus ℓ_0/β. The reason for doing so is that one can easily observe the transitions, say from a connected configuration to a disjoint configuration, in terms of both ℓ_0 and β. The numerical results are shown in Figure 5. In the following we will analyze these graphs and determine the phases of the vacuum as one varies ℓ_0/β.

$(3+1)$-dimensional intersections As mentioned in the previous section, for $3+1$-dimensional intersections we have three configurations. Consider first the D4-D8-$\overline{\text{D}}$8 system. For $\ell_0/\beta < (\ell_0/\beta)^{\text{e}}_{\text{cr}} \approx 0.154$ the

short solution is more energetically favorable compared to both the disjoint and the long solutions. This corresponds to the chiral symmetry being broken. (Here $(\ell_0/\beta)^{\rm e}_{\rm cr}$ is a critical value read off the energy diagrams in Figure 5. It is different from $(\ell_0/\beta)_{\rm cr}$ obtained from the plots of Figure 2.) Above this value (up to $\ell_0/\beta \approx 0.17$) both short and long curved solutions have more energy compared to the disjoint solution, indicating that the disjoint solution is the vacuum, hence chiral symmetry is restored and the phase transition is of first order. Thus the chiral symmetry breaking-restoration phase transition occurs at $(\ell_0/\beta)^{\rm e}_{\rm cr} \approx 0.154$.

For the D5-D7-$\overline{\rm D}$7 system at $T = (2\pi R_{5+1})^{-1}$ the behavior is surprising and to some extent more involved. On the D5-D7-$\overline{\rm D}$7 plot in Figure 5 there are two special points with $(\ell_0)^{\rm e}_{\rm cr} \approx 0.168$ and 0.17 (in units of $2\pi R_{5+1}$). For $\ell_0/(2\pi R_{5+1}) < 0.168$ the disjoint solution is more energetically favorable, hence chiral symmetry in the dual theory is intact given that such a solution can represent a valid phase of the dual theory. For $0.168 < \ell_0/(2\pi R_{5+1}) < 0.17$ there are three kinds of solutions, disjoint, short and long. It turns out that the short solution has less energy than the other two indicating that chiral symmetry is broken. For $\ell_0/(2\pi R_{5+1}) > 0.17$ the disjoint solution becomes more energetically favorable, hence potentially chiral symmetry gets restored. For temperatures less than $(2\pi R_{5+1})^{-1}$, the situation is the same as the zero temperature case: there are an infinite number of connected solutions when $3\ell_0 = \pi R_{5+1}$, each equally energetically favored, and each of them more favored over the disjoint solution. The existence of such solutions may be rooted in the fact that the low energy theory on the color D5-branes is a non-local field theory, a little string theory. Due to the fact that in the case of background D5-brane geometry the dual field theory degrees of freedom cannot be totally decoupled from non-field theoretic degrees of freedom, it is not clear to us whether such solutions can represent a chirally-broken phase of the dual gauge theory despite the fact that, geometrically, they are smoothly connected.

For the D6-D6-$\overline{\rm D}$6 system, the disjoint solution is always favorable, although it is not clear whether one can give a holographic interpretation that the "dual" field theory is in a chirally-symmetric phase. This is because there exists no decoupling limit suitable for holography in the case of background D6-branes.

$(1+1)$-dimensional intersections For (1+1)-dimensional intersections, there are five allowed configurations. Among these the models based on background Dq-branes with $q \leq 4$ exhibit similar behaviors to their counterparts with (3+1)-dimensional intersection. That is to say for sufficiently low temperatures (compared to $1/\ell_0$) chiral symmetry is broken while above a critical temperature it gets restored. The critical values at which this (first order) phase transition occurs are $(\ell_0/\beta)^{\rm e}_{\rm cr} \approx 0.191$, 0.196 and 0.206 for color D2, D3 and D4-branes, respectively.

The model with color D5-branes again shows some surprises. Because of the mixing between the field

theoretic and non-field theoretic degrees of freedom in holography involving background D5-branes, we have no evidence that different behaviors of the flavor branes represent, via holographic point of view, either chirally-symmetric or chirally-broken phases of the dual field theory. Nevertheless, one finds the following results. At $T = (2\pi R_{5+1})^{-1}$ and for small enough ℓ_0 ($\ell_0 < (\ell_0)^{\rm e}_{\rm cr} \approx 0.2498 \times 2\pi R_{5+1}$) the disjoint solution is preferred. Increasing ℓ_0 up to $\ell_0/(2\pi R_{5+1}) < 0.251$ will result in a phase where the connected solution is favorable. This phase appears in our plot because we put a cutoff of $\Lambda = 5$ to regulate the energy integral. Increasing the cutoff will decrease the range of ℓ_0 for which this phase exists. It is plausible that in the $\Lambda \to \infty$ limit this phase disappears although our numerics does not allow us to check this explicitly. Sticking for now with the cutoff we chose, if one increases ℓ_0 further, there will be another phase transition to a phase where the disjoint solution becomes favored. Due to space limitations, the resolution of the D5-D5-$\overline{\rm D}5$ plot in Figure 5 does not allow one to see all these phases. For temperatures less than $(2\pi R_{5+1})^{-1}$, like the zero temperature case, there are an infinite number of connected solutions for $\ell_0 = \pi R_{5+1}/2$, each equally energetically favored, and none for other ℓ_0's. Each of these connected solutions is more favored over the disjoint solution. For the D6-D4-$\overline{\rm D}4$ system, there is no phase transition and it is always the disjoint solution which is energetically favorable.

2.5 Transverse intersections at finite temperature with compact x^q

An interesting property of the models we are studying here is that when x^q is compact the scale of chiral symmetry breaking is generically different from the scale of confinement which results in additional phases. For example, for the Sakai-Sugimoto model at finite temperature, it was shown [48] that there exists an intermediate phase where the system is deconfined while chiral symmetry is broken.

At finite temperature and x^q direction being compact (with a radius of R_c), there are three geometries where the topology of the $t - x^q$ submanifold is $\mathrm{S}^1 \times \mathrm{S}^1$. One is a geometry which has the metric

$$ds^2 = \left(\frac{u}{R_{q+1}}\right)^{\frac{7-q}{2}} \left(dt^2 + d\vec{x}^2 + g(u)(dx^q)^2\right) + \left(\frac{u}{R_{q+1}}\right)^{-\frac{7-q}{2}} \left(\frac{du^2}{g(u)} + u^2 d\Omega_{8-q}{}^2\right), \tag{2.32}$$

with

$$g(u) = 1 - \left(\frac{u_{\rm KK}}{u}\right)^{7-q}. \tag{2.33}$$

We will call this geometry the thermal geometry. Although the Euclidean time period β is arbitrary in

this geometry, the x^q-circle cannot have arbitrary periodicity. In order for this geometry to be smooth at $u = u_{\rm KK}$ in the $x^q - u$ submanifold, one has to have

$$\Delta x^q = \beta_c = \frac{4\pi}{7-q}\left(\frac{R_{q+1}}{u_{\rm KK}}\right)^{\frac{7-q}{2}} u_{\rm KK}, \tag{2.34}$$

where we have defined $\beta_c = 2\pi R_c$. Although we do not specify the q-dependence of β_c and R_c, one should keep in mind that they depend on $u_{\rm KK}$ and R_{q+1} differently through (2.34) depending on what value for q is given. There is another geometry whose metric takes the form

$$ds^2 = \left(\frac{u}{R_{q+1}}\right)^{\frac{7-q}{2}}\left(dt^2 + d\vec{x}^2 + (dx^q)^2\right) + \left(\frac{u}{R_{q+1}}\right)^{-\frac{7-q}{2}}\left(du^2 + u^2 d\Omega_{8-q}{}^2\right). \tag{2.35}$$

There is also the black brane geometry which is basically the same as (2.2) but with x^q compact, and has the (Euclidean) metric

$$ds^2 = \left(\frac{u}{R_{q+1}}\right)^{\frac{7-q}{2}}\left(f(u)dt^2 + d\vec{x}^2 + (dx^q)^2\right) + \left(\frac{u}{R_{q+1}}\right)^{-\frac{7-q}{2}}\left(\frac{du^2}{f(u)} + u^2 d\Omega_{8-q}{}^2\right), \tag{2.36}$$

where

$$f(u) = 1 - \left(\frac{u_T}{u}\right)^{7-q}. \tag{2.37}$$

In this geometry the x^q-circle has arbitrary periodicity whereas β is fixed by

$$\beta = \frac{4\pi}{7-q}\left(\frac{R_{q+1}}{u_T}\right)^{\frac{7-q}{2}} u_T. \tag{2.38}$$

For all three geometries, the dilaton ϕ, and the q-form RR-flux F_q are given in (2.6); see the appendix for more details. Also, R_{q+1} is given in (2.4).

The three geometries whose line elements are given in (2.32), (2.35) and (2.36) are saddle points of either type IIA or type IIB Euclidean path integral. For a given temperature, one needs to compare their (regularized) free energies to determine which solution dominates the path integral. We have calculated the free energies of these solutions in the appendix. For $q \leq 4$, both the thermal and the black brane geometries have less free energy compared to the geometry in (2.35), and this result is independent of temperature. So, to determine the lowest energy saddle point we need to compare the free energies of (2.32) and (2.36). The

difference in their free energies is given by

$$S_{\text{thermal}} - S_{\text{black brane}} = \frac{9-q}{g_s^2} V_9 \left(\frac{4\pi}{7-q} R_{q+1}^{\frac{1}{2}(7-q)} \right)^{2\frac{7-q}{5-q}} \left(\beta^{2\frac{q-7}{5-q}} - \beta_c^{2\frac{q-7}{5-q}} \right), \tag{2.39}$$

where $V_9 = \beta\beta_c \text{Vol}(\text{S}^{8-q})\text{Vol}(\mathbb{R}^{q-1})$ where we set $l_s = 1$. Thus the thermal geometry (2.32) dominates when $\beta > 2\pi R_c$ whereas for $\beta < 2\pi R_c$ it is the black brane geometry (2.36) which gives the dominant contribution to the Euclidean path integral. This phase transition which happens at $\beta = \beta_c$ is the holographic dual of confinement-deconfinement phase transition in the corresponding dual gauge theories [44].

For $q = 6$, again, both the thermal and black brane geometries have less free energy compared to the geometry in (2.35). The difference in free energies for the geometries in (2.32) and (2.36) is given by

$$S_{\text{thermal D6}} - S_{\text{black D6-brane}} = \frac{3V_9}{16\pi^2 g_s^2 R_{6+1}} (\beta^2 - \beta_c^2), \tag{2.40}$$

where $V_9 = \beta\beta_c \text{Vol}(\text{S}^2)\text{Vol}(\mathbb{R}^5)$. So, (2.40) indicates a phase transition at $\beta = 2\pi R_c$. Unlike the $q \leq 4$ cases, for $q = 6$ the thermal geometry (2.32) dominates for $\beta < 2\pi R_c$ whereas for $\beta > 2\pi R_c$ the black brane geometry (2.36) dominates.

For $q = 5$, one needs to consider more possiblities. For $\beta = 2\pi R_{5+1}$, there are two cases: either $\beta_c = 2\pi R_{5+1}$ or $\beta_c \neq 2\pi R_{5+1}$. For $\beta_c = 2\pi R_{5+1}$, both (2.32) and (2.36) are more favored over the geometry whose metric is given in (2.35). The difference in free energies of (2.32) and (2.36) is

$$S_{\text{thermal D5}} - S_{\text{black D5-brane}} = \frac{4}{g_s^2} V_9 (u_T^2 - u_{\text{KK}}^2), \qquad \text{at} \qquad \beta_c = 2\pi R_{5+1}. \tag{2.41}$$

where $V_9 = \beta\beta_c \text{Vol}(\text{S}^3)\text{Vol}(\mathbb{R}^4)$. For $\beta_c \neq 2\pi R_{5+1}$, on the other hand, the two saddle points with the same asymptotics are the black brane geometry and the geometry in (2.35). In this case, the black brane geometry is the dominant one

$$\Delta S = \frac{4}{g_s^2} V_9 u_T^2 > 0. \tag{2.42}$$

There are also two possibilities when $\beta \neq 2\pi R_{5+1}$. If $\beta_c \neq 2\pi R_{5+1}$, the only saddle point consistent with the asymptotics is (2.35) which determines the vacuum. If, on the other hand, $\beta_c = 2\pi R_{5+1}$, there are two geometries with the same asymptotics, thermal and the one given in (2.35). The thermal geometry is

dominant because

$$\Delta S = -\frac{4}{g_s^2} V_9 u_{\rm KK}^2 < 0. \tag{2.43}$$

With x^q being compact, the flavor branes are now sitting at two points separated by a distance ℓ_0 on the x^q-circle. Note that there is no reason for the flavors branes to be located at the antipodal points on the circle. As before, we consider the transverse intersections of the flavor and the color branes, and choose the same embeddings and boundary conditions for the flavor branes as we did in (2.10) and (2.11) except that now $\ell_0 \leq \pi R_c$. In what follows, we will focus on $q \leq 4$ cases and consider both low and high temperature phases of the background. In particular, we would like to know whether there always exists a range of temperature above the deconfinement temperature where chiral symmetry is broken.

2.5.1 Behavior at high and low temperatures

For temperatures above the deconfinement temperature β_c the profile of the flavor branes takes essentially the same form as it did when x^q was non-compact, hence, indicating the existence of short and long (smoothly) connected solutions. Note that when x^q is compact, for a fixed ℓ_0, there is now a lower bound on ℓ_0/β set by the deconfinement temperature. For completeness, we have plotted ℓ_0/β versus z_* (z_* being the radial position at which the brane and anti-brane smoothly join) in Figure 6. The lower dotted line in each plot represents the deconfinement temperature. As an example, we chose it to be at $\beta_c = 10\ell_0$. The upper dotted line shows chiral symmetry breaking-restoration phase transition which comes from comparing the energies of connected and disjoint solutions. One can show, using energy considerations, that below the upper dotted line chiral symmetry is broken in a deconfined phase via short connected solution while it is restored above the line (where we have deconfinement with chiral symmetry restoration).

In the low temperature regime where the system is in a confined phase, the DBI action for the flavor branes in the thermal background (2.32) now reads (with gauge fields set equal to zero)

$$S_{\rm DBI} = \beta\, C(q,r) \int d^r x\; dx^q\; u^{\frac{\gamma}{2}} \Big[g(u) + \frac{1}{g(u)} \Big(\frac{u}{R_{q+1}} \Big)^{2\delta} u'^2 \Big]^{\frac{1}{2}}, \tag{2.44}$$

where $C(q,r)$, γ and δ have all been defined in (2.14). The equation of motion for the profile is now

$$u^{\frac{\gamma}{2}} g(u) \Big[g(u) + \frac{1}{g(u)} \Big(\frac{u}{R_{q+1}} \Big)^{2\delta} u'^2 \Big]^{-\frac{1}{2}} = w_0^{\frac{\gamma}{2}}, \tag{2.45}$$

with w_0 parameterizing the solutions. There exists a solution with $w_0 = 0$ representing disjoint Dp and

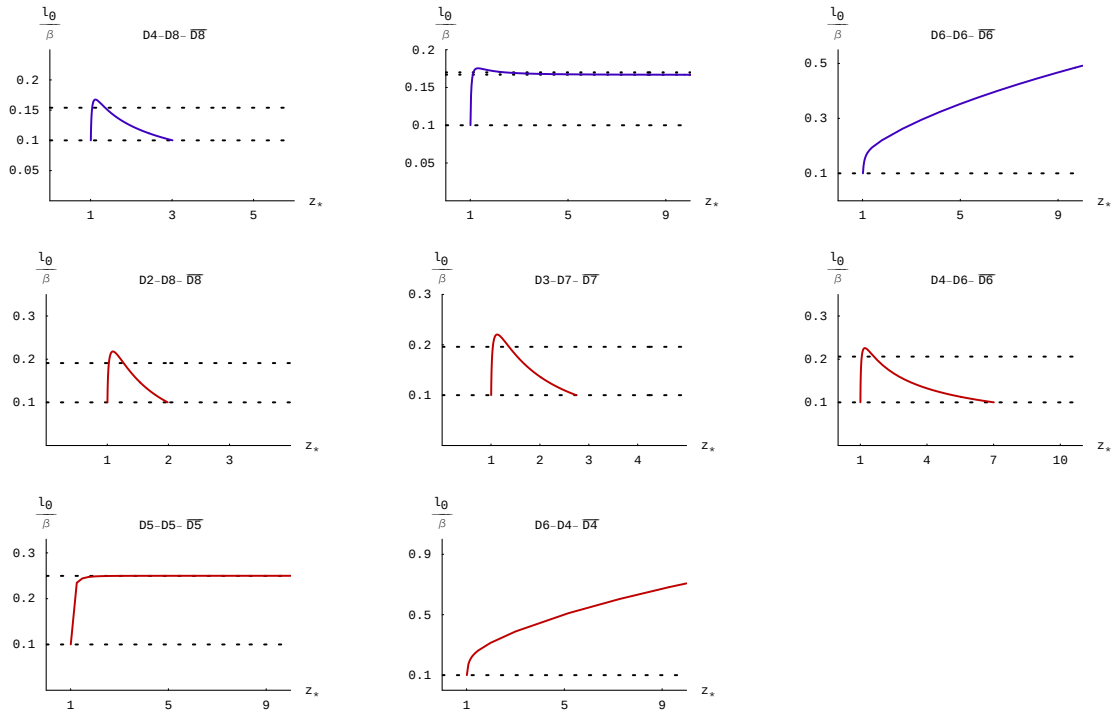

Figure 2.4: Behavior of ℓ_0/β versus z_* above the deconfinement temperature for $q = 2, 3, 4$. The lower dotted line represents a transition to the confined phase whereas the upper dotted line represents chiral symmetry breaking-restoration phase transition.

$\overline{Dp}$-branes descending down to $u = u_{\rm KK}$. For $w_0 \neq 0$, solving (2.45) for $u^{'}$ yields

$$u^{'2} = \frac{1}{{w_0}^{\gamma}}\Big(\frac{u}{R_{q+1}}\Big)^{-2\delta} g(u)^2 \Big(u^{\gamma} g(u) - {w_0}^{\gamma}\Big). \tag{2.46}$$

Denoting the possible turning point(s) by w_*, analysis of (2.46) shows that $u \geq w_* > u_{\rm KK}$, with w_* satisfying

$$w_*^{\gamma} - w_*^{\sigma} u_{\rm KK}^{-2\delta} - w_0^{\gamma} = 0, \tag{2.47}$$

where σ has been defined as before. Integrating (2.46) gives

$$x^q(y) = -\frac{\delta}{2\pi}\beta_c (y_*^{\gamma} - y_*^{\sigma})^{\frac{1}{2}} \int_{y_*}^{y} \Big(\tilde{y}^{-2\delta} - 1\Big)^{-1} \Big(\tilde{y}^{\gamma} - \tilde{y}^{\sigma} - (y_*^{\gamma} - y_*^{\sigma})\Big)^{-\frac{1}{2}} d\tilde{y}, \tag{2.48}$$

where we have defined $y = (u/u_{\rm KK}) \in (1, \infty)$, and $y_* = w_*/u_{\rm KK}$. Using (2.48) we can relate y_* to ℓ_0

$$\frac{\ell_0}{\beta_c} = -\frac{\delta}{\pi}\ (y_*^{\gamma} - y_*^{\sigma})^{\frac{1}{2}} \int_{y_*}^{\infty} \Big(y^{-2\delta} - 1\Big)^{-1} \Big(y^{\gamma} - y^{\sigma} - (y_*^{\gamma} - y_*^{\sigma})\Big)^{-\frac{1}{2}} dy. \tag{2.49}$$

The analysis of ℓ_0/β_c as a function of y_* determines the number of solutions. ℓ_0/β_c versus y_* has been

numerically plotted in Figure 7 for intersections of interest and for $q = 2, 3, 4$. As it is seen from Figure 7, there is always one smoothly connected solution (as well as a disjoint solution). The red and blue plots represent smoothly connected solutions for (1+1)-dimensional and (3+1)-dimensional intersections, respectively.

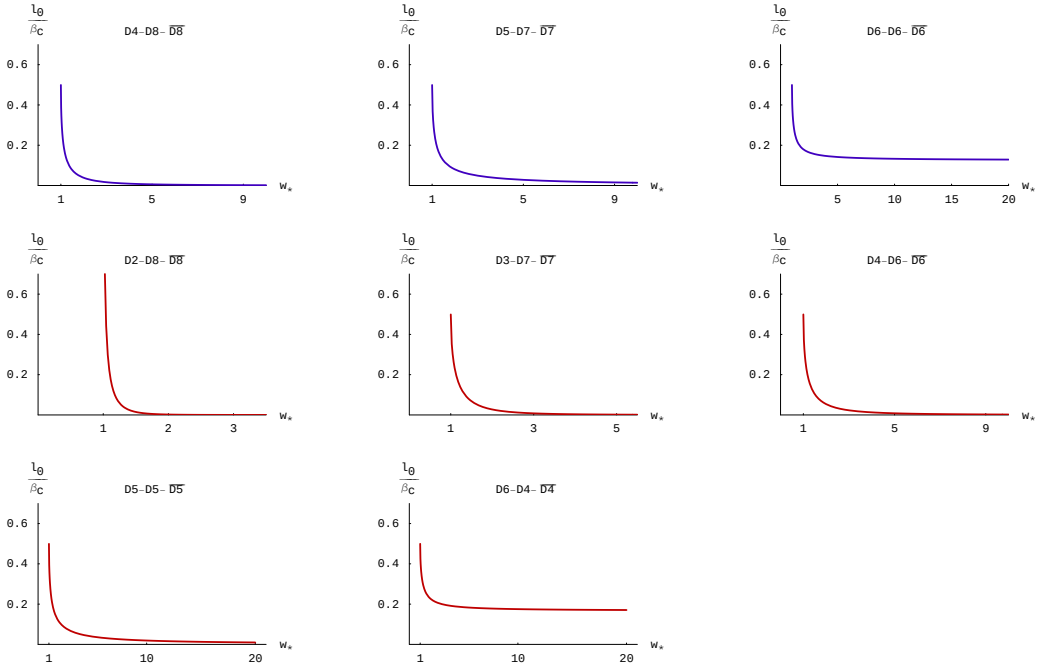

Figure 2.5: Behavior of ℓ_0/β_c versus w_* for $q = 2, 3, 4$.

For the energy of the connected solutions, one obtains

$$E = -\frac{\delta\beta}{\pi}\beta_c C(q,r)\ u_{\rm KK}^{\frac{\gamma}{2}} \int dx^r\ \tilde{E}, \tag{2.50}$$

where

$$\tilde{E} = \lim_{\Lambda\to\infty}\left\{\int_{y_*}^{\Lambda} dy\ y^{\frac{\sigma}{2}}\left(1-y^{2\delta}\right)^{-\frac{1}{2}}\left(1-\frac{y_*^\gamma - y_*^\sigma}{y^\gamma - y^\sigma}\right)^{-\frac{1}{2}} - \int_1^{\Lambda} dy\ \left(1-y^{2\delta}\right)^{-\frac{1}{2}} y^{\frac{\sigma}{2}}\right\}, \tag{2.51}$$

and Λ is a cutoff. Like the previous sections, one can numerically eliminate y_* between (2.49) and (2.51) and plot $\tilde{E}$ versus ℓ_0/β_c. Although we have not shown the plots here, one can check (numerically) that the smoothly connected solutions are always more energetically favorable compared to the disjoint solutions.

The plots in Figure 7 not only show the existence of a unique smoothly coonected solution (for the confined phase) but also indicate a big difference for the behavior of the flavor branes below and above

the confinement-deconfinement phase transition. For example consider the plot for D3- D7-$\overline{\text{D}}$7 system. Each point on the plot represents a unique curved solution for which increasing the temperature (up to the deconfinement temperature β_c) will have no effect on the shape of the U-shaped flavor branes. That is to say that changing the temperature will not cause the flavor D7-$\overline{\text{D}}$7-branes to join either closer to $u_{\rm KK}$ or farther away from it. Once ℓ_0 and β_c are specified, the shape of the brane stays the same independent of the variation of the temperature up to the deconfinement temperature. The behavior just mentioned is significantly different from the behavior of the flavor branes at high temperatures (where they are in black brane backgrounds). For a fixed ℓ_0, each point on the plot of D3-D7-$\overline{\text{D}}$7 system in Figure 7 represents one (or two) smoothly connected solution(s) for only a specific temperature. Varying the temperature will now change the shape of the connected flavor branes and force them to go either closer to the horizon or stay farther away from it.

There is another difference which is worthy of mentioning here. At the temperature for which the confinement-deconfinement phase transition occurs, namely at $\beta = \beta_c$, $u_{\rm KK} = u_T$. For a fixed ℓ_0, flavor branes at temperatures above β_c join at a radial point closer to $u_{\rm KK} = u_T$ than the same flavor branes placed at temperatures below β_c.

2.6 Discussion

In this chapter, we analyzed some aspects of transversely-intersecting Dq-Dp-$\overline{\text{D}p}$-branes at finite temperature. In particular, we mapped out different vacuum configurations which can holographically be identified with chiral symmetry breaking (or restoration) phase of their holographic dual theories. Although we showed that generically the long connected solutions are less energetically favorable compared to the short connected solutions we did not discuss their stability against small perturbations. Presumably a stability analysis along the lines of [57] can be done to show that the long connected solution is unstable against small perturbations. The analysis presented here can be generalized in various directions. For example, one can add a chemical potential to the setup and look for new phases as was done in some specific models in [58, 59, 60, 61], or consider the sysytem at background electric and magnetic fields [62, 63, 64] and study the conductivity of the system or the effect of the magnetic field on the chiral symmetry-restoration temperature. We hope to come back to these interesting issues in future.

Also, our analysis was entirely based on the DBI action for the flavor Dp-$\overline{\text{D}p}$-branes. In transversely-intersecting D-branes, working with just the DBI (plus the Chern-Simons part of the) action misses, from holographic perspectives, an important part of the physics, namely the vev of the fermion bilinear as an

order parameter for chiral symmetry breaking. To determine the fermion bilinear from the holographic point of view there should be a mode propagating in the bulk geometry such that asymptotically its normalizable mode can be identified with the vev of the fermion bilinear. The DBI plus the Chern-Simons action cannot give rise to the mass of the localized chiral fermions either. Note that for transverse intersections one cannot write an explicit mass term for the fermions of the intersections because there is no transverse space common to both the color and the flavor branes. So it is not possible to stretch an open string between the color and flavor branes in the transverse directions. Therefore, the fermion mass must be generated dynamically. It has been argued in [46] that including the dynamics of an open string stretched between the flavor branes into the analysis will address the question of how one can compute fermion mass and bilinear vev in these holographic models. More concretely, the scalar mode of this open string which transforms as bifundamental of $U(N_{\rm f}) \times U(N_{\rm f})$ has the right quantum numbers to be potentially holographically dual to the fermion mass and condensation.

Recently, the authors of [65, 66, 67] shed light on this issue by starting with the so-called tachyon-DBI action [68] claimed to correctly incorporate the role of the open string scalar mode, the tachyon, in a system of separated Dp-$\overline{\rm D}p$-branes. In fact, it was shown in [66, 67] that for the Sakai-Sugimoto model at zero temperature, the open string tachyon will asymptotically have a normalizable as well as a non-normalizable mode. They identified the normalizable mode with the vev of the fermion bilinear (order parameter for chiral symmetry breaking) and the non-normalizable mode with the fermion mass. It is not hard to generalize the calculations of [66, 67] to include all transversely-intersecting Dq-Dp-$\overline{\rm D}p$ systems at zero temperature where one finds that there always exist both normalizable and non-normalizable modes for the asymptotic behavior of the tachyon, and in the bulk of the geometry the tachyon condenses roughly at the same radial point where the flavor branes smoothly join [69]. The calculation of the fermion mass and condensate for transversely-intersecting Dq-Dp-$\overline{\rm D}p$ systems at finite temperature requires not only considering the tachyon-DBI action of [68] in the black brane background of (2.2) but also calculating the tachyon potential as a function of the temperature. In the case of a coincident brane and anti-brane in flat background, a partial result for such a calculation was given in [70] (see also [71]). Some attempts in generalizing the results of [70, 71] for separated brane-anti-branes (at least in the case of separated D8-$\overline{\rm D}8$ in flat space) has recently started in [72]. For our purpose of extracting information about fermion mass and condensate, knowing the dependence of the tachyon potential for separated flavor Dp-$\overline{\rm D}p$-branes seems crucial. Ignoring the temperature dependence on tachyon potential at zeroth order yields unsatisfactory results: It gives rise to the same results as one would have obtained in the zero temperature case [69]. We know that this is not the right behavior because at zero temperature there is no chiral phase transition.

Chapter 3

Torsion and the Gravity Dual of Parity Breaking in AdS_4/CFT_3 Holography

AdS_4/CFT_3 is currently emerging as a novel paradigm of holography that has qualitatively different properties from the more familiar AdS_5/CFT_4 correspondence. Particularly intriguing is the recent accumulation of evidence that AdS_4/CFT_3 can be used to describe a plethora of phenomena in 2+1 dimensional condensed matter systems, such as quantum criticality [73, 74], Quantum Hall transitions [75, 76, 77, 78], superconductivity [79, 80, 81, 82, 83], supefluidity [84, 85] and spontaneous symmetry breaking [86, 87, 88]. Furthermore, AdS_4/CFT_3 is the appropriate setup to study the holographic consequences of generalized electric-magnetic duality of gravity and higher-spin gauge fields [89, 90, 91, 92, 93].

In the absence of an explicit AdS_4/CFT_3 correspondence example,[1] various toy models have been used to study its general qualitative aspects. One of the aims of the present work it to provide yet another model that can be used to unveil some salient and intriguing properties of AdS_4/CFT_3 holography. However, this is not our only aim. We also wish to study here the relevance of torsion to four dimensional gravity from a holographic point of view. The study of torsion is an interesting subject in itself that poses formal and phenomenological challenges.[2] In the context of a string theory description of gravity, torsion is omnipresent through antisymmetric tensor fields. AdS_4/CFT_3 provides the basic setup where four dimensional torsion can be holographically investigated.

We consider a simple toy model where torsion is introduced via the topological Nieh-Yan class [21]. In particular, we consider the modification of the Einstein-Hilbert action with a negative cosmological constant by the Nieh-Yan class, the latter having a spacetime-dependent coefficient. In the context of the 3+1-split formalism for gravity [89] we point out that the torsional degrees of freedom are carried by the 'gravitational magnetic field.' In pure gravity the magnetic field is fully determined by the frame field, and torsion vanishes. In our model, the spacetime dependence of the Nieh-Yan coefficient makes some of the components of the magnetic field dynamical and as a consequence torsional degrees of freedom enter the theory. Our toy model is simple enough such that only one of the torsional degrees of freedom becomes dynamical. This degree

[1] The recently suggested field theoretic models for M2 branes [94, 95, 96, 97, 98, 99] are important steps towards the understanding of the boundary side of AdS_4/CFT_3.

[2] See [100, 101, 102] for recent reviews and [103, 104] for other recent works.

of freedom can be either carried by a pseudoscalar, in which case our model is equivalent to a massless pseudoscalar coupled to gravity, or by a two-form gauge potential. In the latter case our model becomes equivalent to a Kalb-Ramond field coupled to gravity.

Next, we find an exact solution of the equations of motion in Euclidean signature. Our metric ansatz is that of a domain wall (in the bulk). The solution, the *torsion vortex*, has two distinct asymptotically AdS_4 regimes along the "radial" coordinate. The pseudoscalar has a kink profile and it is finite at both of the asymptotic regimes. Our torsion vortex can be viewed as a generalization of the axionic wormhole solution of [105] in the case of non-zero cosmological constant. See also [106] for recent work on AdS wormholes. Having in mind the holographic interpretation of our model we focus mainly on the case where the torsional degree of freedom is carried by a pseudoscalar field. Following standard holographic recipes we find that the torsion vortex is the gravity dual of a three dimensional system that possesses two distinct parity breaking vacua. The two vacua are distinguished by the relative sign of the pseudoscalar order parameter. Our bulk picture suggests that the transition from one vacuum to the other can be done by a marginal deformation of the theory. In Appendix B we suggest that the above qualitative properties can be realized in the boundary by the three dimensional Gross-Neveu model coupled to U(1) gauge fields.

Finally, we point out that the bulk physics of our vortex solution bears some resemblance to the Abrikosov vortex of superconducting systems. There is a natural mapping of the parameters of the torsion vortex to those of the Abrikosov vortex. We show that the gravitational parameter that is interpreted as an order parameter satisfies a ϕ^4-like equation and this motivates us to suggest that the cosmological constant is related to the "critical temperature" as $\Lambda \sim T - T_c$. We end with a discussion of multi-vortex configurations and vortex condensation. The outcome of this analysis is that H-flux supports bubbles of flat spacetime.

The chapter is organized as follows. In Section 2 we discuss the relevance of torsional degrees of freedom in gravity and their relation with the gravitational magnetic field. In Section 3 we present our toy model and its various equivalent manifestations and discuss its 3+1-split formalism of [89]. In Section 4 we present the explicit torsion vortex solution of our model. In Section 5 we discuss the holography of the torsion vortex. Section 6 contains the bulk physics of the vortex and its relationship to the Abrikosov vortex. It also contains the discussion of multi-vortices and vortex condensation. Technical details and the discussion of the three-dimensional Gross-Neveu model coupled to U(1) gauge fields are contained in the Appendices.

3.1 Torsional degrees of freedom in gravity

3.1.1 Preliminaries

In this chapter we will consider a four dimensional spacetime with a negative cosmological constant. The Einstein-Hilbert action may be written as[3]

$$I_{EH} = \int_M \left(\epsilon_{abcd} e^a \wedge e^b \wedge R^{cd} - \frac{1}{6}\Lambda \epsilon_{abcd} e^a \wedge e^b \wedge e^c \wedge e^d \right) , \tag{3.1}$$

where e^a denote the one-form frame fields, while $\omega^a{}_b$ are the connection one-forms with curvature $R^a{}_b = d\omega^a{}_b + \omega^a{}_c \wedge \omega^c{}_b$. As is well-known the variation of (3.1) gives the Einstein equations and also the zero torsion constraint $T^a = de^a + \omega^a{}_b \wedge e^b = 0$. By virtue of the latter this action can be written entirely in terms of metric variables.

There are also a number of other terms that one may consider. These are all of potential interest to holography because being total derivatives they may induce interesting boundary effects. We may parameterize these terms as follows (writing all possible $SO(3,1)$-invariant 4-forms constructed from $e^a, R^a{}_b, T^a$):

$$I_{top} = n \int_M C_{NY} + 2\gamma^{-1} \int_M C_{Im} + p \int_M P_4 + q \int_M E_4 \, , \tag{3.2}$$

where $C_{NY} = T^a \wedge T_a - R_{ab} \wedge e^a \wedge e^b = d(T^a \wedge e_a)$ is the Nieh-Yan form, γ is often referred to as the Immirzi parameter with $C_{Im} = R^a{}_b \wedge e^b \wedge e_a$, $P_4 = -\frac{1}{8\pi^2} R^a{}_b \wedge R^b{}_a = -\frac{1}{8\pi^2} d(\omega^a{}_b \wedge R^b{}_a - \frac{1}{3}\omega^a{}_b \wedge \omega^b{}_c \wedge \omega^c{}_a)$ is the Pontryagin form and $E_4 = -\frac{1}{32\pi^2}\epsilon_{abcd} R^{ab} \wedge R^{cd}$ is the Euler form. We note that $P_4 + \frac{\sigma_\perp a^2}{4\pi^2} C_{NY}$ and $C_{NY} - C_{Im}$ are actually $SO(3,2)$ invariants [101]. These terms become of more interest, even in gravity, if we allow the coefficients to become fields. Although we will not consider this problem here in full generality, we will consider a particular example. We note that there is older literature, principally by d'Auria and Regge [107] that also considered some such cases (usually in asymptotically Minkowski geometries). In the course of the chapter, we will review what is known from those older works. The purpose of our work, amongst other things, is to bring this up to date, and in particular focus on aspects of holography.

3.1.2 Torsion and the magnetic field of gravity

Our simple model involves only the Nieh-Yan (NY) term. It is interesting to discuss the physics of this topological invariant before we embark on detailed calculations. We will see below that the NY term in

[3] We use $I_{EH} = -16\pi G_4 S_{EH}$ where S_{EH} is the usually normalized gravitational action. To fix notation we note that the Einstein equations that follow from S_{EH} are $G_{\mu\nu} + \Lambda g_{\mu\nu} = 0$. We will also write $\Lambda = -3\sigma_\perp / L^2$.

gravity plays a role similar to that of the θ-angle in gauge theories.

To see this, we explain below the relationship between the gravitational magnetic field B^α and torsion. Consider the 3+1 split[4] of the Einstein-Hilbert action (1) with the addition of the usual gravitational Gibbons-Hawking boundary term I_{GH} [89, 91, 92]

$$\begin{aligned} I_{EH}+I_{GH} = & \int dt \wedge \left(\dot{\tilde{e}}^\alpha \wedge (-4\sigma_\perp \epsilon_{\alpha\beta\gamma}\tilde{e}^\beta \wedge K^\gamma)\right. \\ & +2\sigma_\perp N \left\{ 2\tilde{d}\left(B^\alpha \wedge \tilde{e}_\alpha\right) + 2B^\alpha \wedge \tilde{T}_\alpha + \epsilon_{\alpha\beta\gamma}\left(\sigma B^\alpha \wedge B^\beta - K^\alpha \wedge K^\beta - \frac{\sigma_\perp \Lambda}{3}\tilde{e}^\alpha \wedge \tilde{e}^\beta\right) \wedge \tilde{e}^\gamma \right\} \\ & \left. -4\sigma_\perp N^\alpha \epsilon_{\alpha\beta\gamma}(\tilde{D}K)^\beta \wedge \tilde{e}^\gamma + 4Q^\alpha (K_\beta \wedge \tilde{e}^\beta)\wedge \tilde{e}_\alpha + 4q^0{}_\alpha \left\{ \epsilon^\alpha{}_{\beta\gamma}\tilde{T}^\beta \wedge \tilde{e}^\gamma \right\} \right) . \end{aligned} \tag{3.3}$$

In the 3+1 split formalism the dynamical variables in (3.3) are the "spatial"[5] one-forms $\tilde{e}^\alpha$, K^α and B^α. The first two are canonically conjugate variables. The magnetic field B^α carries the torsional degrees of freedom as it can be seen for example if we write the definition of the non-trivial 'spatial' torsion as

$$\tilde{T}^\alpha = \tilde{d}\tilde{e}^\alpha - \sigma \epsilon^{\alpha\beta\gamma} B_\beta \wedge \tilde{e}_\gamma \, . \tag{3.4}$$

It is easily seen that the radial component of torsion T^0 is determined by $\tilde{e}^\alpha$ and K^α. Notice that (3.4) implies that the tensor $B_{\alpha\beta}$ is odd under 'spatial' parity, hence the trace $B^\alpha_{\ \alpha}$ is a pseudoscalar. Although a priori the torsional degrees of freedom are not connected with the pair of conjugate variables $\tilde{e}^\alpha$ and K^α, they are not dynamical as there is no kinetic term for B^α. Rather, they enter (3.3) algebraically and as such they yield the algebraic zero torsion condition by virtue of which the magnetic field is related to the frame field. Indeed, as discussed in Ref. [89], the $q^0_{\ \alpha}$ constraint sets to zero the antisymmetric part of B^α in deDonder gauge, such that the first term in the second line of (3.3) vanishes. Then, the variation of (3.3) with respect to B^α yields $\tilde{T}^\alpha = 0$, leaving as true dynamical variables $\tilde{e}^\alpha$ and K^α. This is the gravitational analogue of the electromagnetic case where the magnetic field is related to the gauge potential via the Bianchi identity.

Consider now adding to the Einstein-Hilbert action the Nieh-Yan class C_{NY} with a constant coefficient θ. Over a compact manifold, the NY class is a topological invariant and takes integer values[6] [101]. Having in mind holography, we are interested here in manifolds with boundary. In particular, the $3+1$ split has been set up so that the boundary is a constant-t slice. The NY term reduces to a boundary contribution.

[4] In appendix **??** we present a brief review of the 3+1 split formalism where the definitions of the various relevant quantities appear and notation is explained. We note here that σ is the overall signature of the spacetime, while $\sigma_\perp$ is the signature of the radial direction and σ_3 the signature of the boundary.

[5] By spatial, we will mean orthogonal to the "radial" coordinate t. In the case of AdS_4, this radial coordinate is spacelike, and thus $\sigma_\perp = +1$.

[6] More precisely, $C_{NY}/(2\pi L)^2$ is integral, as it is equal to the difference of two Pontryagin forms.

The explicit calculation yields

$$\mathcal{I}_{NY} \equiv -2\sigma_\perp \theta \int C_{NY} = 2\sigma_\perp \theta \int dt \wedge \left[2\epsilon_{\alpha\beta\gamma} \dot{\tilde{e}}^\alpha \wedge \tilde{e}^\beta \wedge B^\gamma + \epsilon_{\alpha\beta\gamma} \dot{B}^\alpha \wedge \tilde{e}^\beta \wedge \tilde{e}^\gamma \right] . \tag{3.5}$$

Adding (3.5) to (3.3) we obtain

$$\begin{aligned} I_{EH} + I_{GH} + \mathcal{I}_{NY} \quad = \quad & \int dt \wedge \Big(\dot{\tilde{e}}^\alpha \wedge (-4\sigma_\perp \epsilon_{\alpha\beta\gamma} \tilde{e}^\beta \wedge [K^\gamma - \theta B^\gamma]) + 2\sigma_\perp \theta \epsilon_{\alpha\beta\gamma} \dot{B}^\alpha \wedge \tilde{e}^\beta \wedge \tilde{e}^\gamma \\ & + \text{constraint terms} \Big) . \end{aligned} \tag{3.6}$$

Notice that the $\mathcal{I}_{NY}$ term has two effects. One is to modify the canonical momentum variable $K^\alpha \mapsto K^\alpha - \theta B^\alpha$. This is analogous to the effect of the θ-angle in the canonical description of electromagnetism [108]. The other is to provide a kinetic term for the singlet component of the magnetic field (one easily verifies that only $B^\alpha{}_\alpha$ contributes in the second term in the first line of (3.6)). This second effect has no analogue in electromagnetism. Taking the variation of (3.6) with respect to B^α, one finds that the zero torsion condition still holds. This is expected of course since the $\mathcal{I}_{NY}$ term is purely a boundary term. As a consequence, the true dynamical variables remain $\tilde{e}^\alpha$ and K^α. However, the holography is slightly modified. The variation of (3.6) gives on-shell

$$\delta \left(I_{EH} + I_{GH} + \mathcal{I}_{NY} \right)_{on\ shell} = \int_{\partial \mathcal{M}} \delta \tilde{e}^\alpha \wedge \left(-4\sigma_\perp \epsilon_{\alpha\beta\gamma} \tilde{e}^\beta \wedge [K^\gamma - \theta B^\gamma] \right)_{on\ shell} . \tag{3.7}$$

After the appropriate subtraction of divergences [91, 92], (3.7) yields a modified boundary energy momentum tensor. The modification is due to the term $4\sigma_\perp \theta \epsilon_{\alpha\beta\gamma} \tilde{e}^\beta \wedge B^\gamma$ which is parity odd and corresponds to the unique symmetric, conserved and traceless tensor of rank two and scaling dimension three that can be constructed from the three-dimensional metric [109]. It is the exact analogue of the topological spin-1 current constructed from the three dimensional gauge potential.

The form of the action (3.6) unveils an intriguing possibility. The above holographic interpretation was based on the zero torsion condition that connects B^α to the frame field. However, to get the zero torsion condition from (3.6) we needed to integrate by parts the last term in the first line. Hence, if θ were t-dependent, the torsion would no longer be zero and the trace B^α_α would become a proper dynamical degree of freedom independent of $\tilde{e}^\alpha$. In such a case the holographic interpretation of (3.6) would change. The new bulk degree of freedom would couple to a new pseudoscalar boundary operator. As a consequence, we have the possibility to probe additional aspects of the boundary physics and describe new 2+1 dimensional phenomena. That we do in the next section.

3.2 The Nieh-Yan models

3.2.1 General aspects

In the previous section we sketched a mechanism by which torsional degrees of freedom become dynamical. In particular, we have argued that the addition of the Nieh-Yan class with a space-time dependent coefficient in the Einstein-Hilbert action makes dynamical a pseudoscalar degree of freedom connected to the trace of the gravitational magnetic field. Adding boundary terms to the bulk action corresponds to a canonical transformation. Consequently, by adding boundary terms we can change the canonical interpretation and the variational principle. Consider first the action

$$I'_{NY} = I_{EH}[e,\omega] + I_{GH}[e,\omega] + 2\int_M F(x) C_{NY}\,, \tag{3.8}$$

where F is a pseudoscalar 'axion' field with no kinetic term. If $F \equiv -\sigma_\perp \theta$ were a constant, this theory would be equivalent to that studied in the last section. With $F = F(x)$, we have additional terms in the action involving gradients of F. If we perform the $3+1$ split on this action, we will find that $\tilde{e}^\alpha$ and B^α are canonical coordinates, and their conjugate momenta will depend on F.

The action as given may be supplemented by additional boundary terms. Such boundary terms are analogous to the Gibbons-Hawking term in gravity, but here involve the torsional degrees of freedom. In particular, we can replace I'_{NY} by

$$I_{NY} = I_{EH}[e,\omega] + I_{GH}[e,\omega] - 2\int_M dF \wedge T_a \wedge e^a\,. \tag{3.9}$$

This action is such that $\tilde{e}^\alpha$ and F are canonical coordinates with appropriate boundary conditions, while B^α appears in the momentum conjugate to F. To investigate this theory, we note that the variation of the action takes the form

$$\begin{aligned}\delta I_{NY} = {} & 2\int_M \delta e^d \wedge \left[\epsilon_{abcd} e^b \wedge \left(R^{cd} - \frac{1}{3}\Lambda e^c \wedge e^d\right) + 2dF \wedge T_d\right] \\ & +2\int_M \delta\omega^{ab} \wedge \left[\epsilon_{abcd} T^c \wedge e^d + dF \wedge e_b \wedge e_a\right] + 2\int_M \delta F\; C_{NY} \\ & +2\int_M d[\delta e^a \wedge \left(\epsilon_{abcd} e^b \wedge \omega^{cd} - dF \wedge e_a\right) - T_a \wedge e^a \delta F]\,.\end{aligned} \tag{3.10}$$

A non-trivial configuration of F would source a particular component of the torsion. Indeed the classical

equations of motion can be manipulated to yield in the bulk

$$T^a \wedge e_a = 3 *_4 dF \,, \tag{3.11}$$

where $*_4$ denotes the Hodge-$*$ operation. However, as d'Auria and Regge [107] showed, this classical system is equivalent to a pseudoscalar coupled to torsionless gravity.

$$I_{PS} = I_{EH}[e, \mathring{\omega}] + I_{GH}[e, \mathring{\omega}] - 3 \int_M dF \wedge *_4 dF \,. \tag{3.12}$$

This comes about as follows. We write the connection as $\omega = \mathring{\omega} + \Omega$, where $\mathring{\omega}$ is torsionless, and insert the equation of motion (3.11). The latter becomes an equation[7] for Ω, and we obtain (3.12).

The holographic interpretation of a massless pseudoscalar field coupled to torsionless gravity is that it is dual to dimension $\Delta = 3, 0$ composite pseudoscalar operators in the boundary. The usual holographic dictionary then says that only the $\Delta = 3$ operator appears in the boundary theory since only this is above the unitarity bound of the three dimensional conformal group $SO(3,2)$. A scalar operator with dimension $\Delta = 0$ would simply correspond to a constant in the boundary. Hence, the sensible holographic interpretation of the massless bulk pseudoscalar is that its leading behaviour determines the marginal coupling of a $\Delta = 3$ operator; the expectation value of the operator itself is determined by the subleading behaviour of the bulk pseudoscalar.

Another equivalent formulation of this bulk theory is obtained by writing

$$*_4 dF = \frac{1}{3} H \,. \tag{3.13}$$

with H a 3-form field. This is the parameterization that would be most familiar from string theory, as the system simply corresponds to an antisymmetric 2-form field. In this formulation, we write

$$\begin{aligned} I_{KR} &= I_{EH}[e, \mathring{\omega}] + I_{GH}[e, \mathring{\omega}] + \frac{1}{3} \int_M H \wedge *_4 H + \sqrt{\frac{2}{3}} \int_M C \wedge d *_4 H \\ &= I_{EH}[e, \mathring{\omega}] + I_{GH}[e, \mathring{\omega}] - \frac{1}{2} \int_M dC \wedge *_4 dC + \int_M d(C \wedge *_4 dC) \,. \end{aligned} \tag{3.14}$$

In the first equation, C appears as a Lagrange multiplier for the 'Gauss constraint' and in the second expression, we have solved for the H equation of motion in the bulk, which is just $H = \sqrt{\frac{3}{2}} dC$.

[7] Explicitly this is $\Omega^a{}_b = \frac{\sigma}{4} \epsilon^{acd}{}_b \partial_c F e_d$.

3.2.2 The 3+1-split of the pseudoscalar Nieh-Yan model

To investigate the holographic aspects of our model it is most useful to use the 'radial quantization' in which we think of the radial coordinate as 'time' t. We have derived the radial 3+1 split in the first order formalism in [89], and this is summarized with explanations of notation in Appendix **??**. Here we update that calculation to include torsional terms. The Nieh-Yan deformation gives

$$\begin{aligned} -2\int dF\wedge T^a\wedge e_a &= 2\int dt\wedge\Big\{-\dot{F}\tilde{T}_\alpha\wedge\tilde{e}^\alpha-\dot{\tilde{e}}_\alpha\wedge\tilde{d}F\wedge\tilde{e}^\alpha+N[2\tilde{d}F\wedge K_\alpha\wedge\tilde{e}^\alpha] \\ &\quad +N^\alpha[2\tilde{d}F\wedge\tilde{T}_\alpha]+Q^\alpha[-\sigma\epsilon_{\alpha\beta\gamma}\tilde{d}F\wedge\tilde{e}^\beta\wedge\tilde{e}^\gamma]\Big\}. \end{aligned} \tag{3.15}$$

We see that the F field makes a contribution to the constraints, and has a conjugate momentum proportional to the scalar part of the torsion (the part transverse to the radial direction). The full bulk action becomes

$$\begin{aligned} I &= \int dt\wedge\Big(\dot{\tilde{e}}^\alpha\wedge(4\sigma_\perp\epsilon_{\alpha\beta\gamma}K^\gamma\wedge\tilde{e}^\beta-2\tilde{d}F\wedge\tilde{e}_\alpha)-2\dot{F}(\tilde{e}^\alpha\wedge\tilde{T}_\alpha) \\ &\quad +N\left\{2\epsilon_{\alpha\beta\gamma}\left({}^{(3)}R^{\alpha\beta}-\sigma_\perp K^\alpha\wedge K^\beta-\frac{\Lambda}{3}\tilde{e}^\alpha\wedge\tilde{e}^\beta\right)\wedge\tilde{e}^\gamma+4\tilde{d}F\wedge K_\alpha\wedge\tilde{e}^\alpha\right\} \\ &\quad +4N^\alpha\left\{-\sigma_\perp\epsilon_{\alpha\beta\gamma}(\tilde{D}K)^\beta\wedge\tilde{e}^\gamma+\tilde{d}F\wedge\tilde{T}_\alpha\right\} \\ &\quad +4Q^\alpha\left\{(K_\beta\wedge\tilde{e}^\beta)\wedge\tilde{e}_\alpha-\frac{1}{2}\sigma\epsilon_{\alpha\beta\gamma}\tilde{d}F\wedge\tilde{e}^\beta\wedge\tilde{e}^\gamma\right\} \\ &\quad +4q^0{}_\alpha\left\{\epsilon^\alpha{}_{\beta\gamma}\tilde{T}^\beta\wedge\tilde{e}^\gamma\right\}\Big). \end{aligned} \tag{3.16}$$

We notice that the Q-constraint term can be written in the form

$$4Q_\alpha\tilde{e}^\alpha\wedge\left(K_\beta\wedge\tilde{e}^\beta-\sigma*_3\tilde{d}F\right). \tag{3.17}$$

Because of this constraint (which relates the antisymmetric part of the extrinsic curvature to the vorticity of F), the momentum conjugate to $\tilde{e}^\alpha$ is symmetric, i.e.

$$\begin{aligned} \Pi_\alpha &= 4\sigma_\perp\epsilon_{\alpha\beta\gamma}K^\gamma\wedge\tilde{e}^\beta-2\tilde{d}F\wedge\tilde{e}_\alpha \\ &= 4\sigma_\perp\left(\epsilon_{\alpha\beta\gamma}K^\gamma\wedge\tilde{e}^\beta-\frac{1}{2}\sigma_3*_3(K_\beta\wedge\tilde{e}^\beta)\wedge\tilde{e}_\alpha\right). \end{aligned} \tag{3.18}$$

When written out in components, one finds that the antisymmetric part $K_{[\alpha\beta]}$ cancels

$$\Pi_\alpha=4\sigma_\perp(K_{(\beta\alpha)}-trK\ \eta_{\beta\alpha})\tilde{e}^\beta. \tag{3.19}$$

This result is consistent with the fact noted above, that the system may be equivalently described as a pseudoscalar field coupled to torsionless gravity. Moreover, if we take the deDonder gauge $d^\dagger \tilde{e}^\alpha = 0$, the torsion constraint implies that B is symmetric.

The $q^0{}_\alpha$ constraint yields $\tilde{T}^\beta_{\alpha\beta} = 0$. Out of the nine components of $\tilde{T}$, which transform as $\mathbf{5}+\mathbf{3}+\mathbf{1}$ under $SO(3)$ (or $SO(2,1)$), this sets the triplet to zero (the $\mathbf{5}$ also vanishes on an equation of motion). The momentum conjugate to F is given by

$$\Pi_F = -2\epsilon^{\alpha\beta\gamma}\tilde{T}_{\alpha\beta\gamma}\,. \tag{3.20}$$

This is the singlet part of the torsion, which has become dynamical in this description of the theory, in the sense that it is canonically conjugate to F.

3.3 The torsion vortex

We will now simplify the analysis by taking a coordinate basis, and looking for solutions of the form

$$\tilde{e}^\alpha = e^{A(t)}dx^\alpha, \qquad N = 1, \qquad N^\alpha = 0\,, \tag{3.21}$$

and we will further suppose that $F = F(t)$. In this case K^α and B^α reduce to one degree of freedom each as a result of the constraints

$$K_\alpha = k\tilde{e}_\alpha, \qquad B_\alpha = b\tilde{e}_\alpha\,, \tag{3.22}$$

and one finds $\Pi_A = -4\sigma_\perp k$ and $\Pi_F = 2\sigma b$. The action then takes the following relatively simple Hamiltonian form

$$I_{NY} \propto \int dt\, d^3x\; e^{3A(t)}\left[\dot{A}\Pi_A + \dot{F}\Pi_F - \left(\frac{1}{2}\sigma_3\Pi_F^2 + \frac{1}{8}\sigma_\perp\Pi_A^2 + \frac{2}{3}\Lambda\right)\right]. \tag{3.23}$$

and the equations of motion give

$$\dot{\Pi}_A = 3\dot{F}\Pi_F, \qquad \dot{\Pi}_F + 3\Pi_F\dot{A} = 0, \qquad \Pi_A = 4\sigma_\perp\dot{A}, \qquad \Pi_F = \sigma_3\dot{F} \quad , \tag{3.24}$$

$$\Pi_A^2 + 4\sigma\Pi_F^2 + \tfrac{16}{3}\sigma_\perp\Lambda = 0 \qquad . \tag{3.25}$$

These equations of motion could of course alternatively be obtained by considering the theory in the form (3.12). It is convenient to rescale $F(t) = \frac{1}{3}\Theta(t)$. Then the equations of motion can be put in the form

$$\ddot{A} + 3\dot{A}^2 - 3a^2 = 0, \qquad \ddot{A} = \frac{1}{12}\sigma\dot{\Theta}^2, \qquad \ddot{\Theta} + 3\dot{\Theta}\dot{A} = 0\,. \tag{3.26}$$

where we have set $\Lambda = -3\sigma_\perp a^2$ with $a = 1/L$. These are of the standard form of domain wall equations that have appeared numerous times in the AdS/CFT literature. However, there is a crucial difference. Notice that the first two of (3.26) imply

$$\dot{A}^2 + \frac{1}{36}\sigma\dot{\Theta}^2 - a^2 = 0\,. \tag{3.27}$$

For Euclidean signature ($\sigma = \sigma_3 = 1$) the second term in (3.27) has *positive* sign in contrast to most of the other holographic studies. This is due to the fact that in passing from Lorentzian to Euclidean signature the pseudoscalar kinetic term acquires the 'wrong sign' [110]. This property allows for a remarkable exact solution to the above system of non-linear equations in Euclidean signature, which we refer to as the *torsion vortex*. To obtain it we define

$$h(t) = \dot{A}(t)\,, \tag{3.28}$$

at which point we have

$$\dot{h} = \frac{1}{12}\dot{\Theta}^2, \quad \dot{h} + 3(h^2 - a^2) = 0\,. \tag{3.29}$$

The general solution is of the form

$$h(t) = a\tanh 3a(t - t_0) \tag{3.30}$$

and we then have

$$\Pi_F = \dot{F} = \pm 2\sqrt{a^2 - h^2(t)} = \pm 2a\ \mathrm{sech}\ 3a(t - t_0) \tag{3.31}$$

which gives

$$\Theta(t) = \Theta_0 \pm 4\arctan\left(e^{3a(t-t_0)}\right)\,. \tag{3.32}$$

The $\pm$ sign corresponds to kink/antikink and we will without loss of generality choose the $+$ sign. We may also solve for

$$e^{A(t)} = \alpha(2\cosh 3a(t - t_0))^{1/3} \tag{3.33}$$

The parameter α is an arbitrary positive integration constant that sets the overall scale of the spatial part of the metric. t_0 may be interpreted as the position of the vortex; when $t_0 = 0$ the torsion vortex sits in the middle between the two asymptotically AdS_4 regimes. Below, we will discuss the interesting holographic interpretation of the torsion vortex.

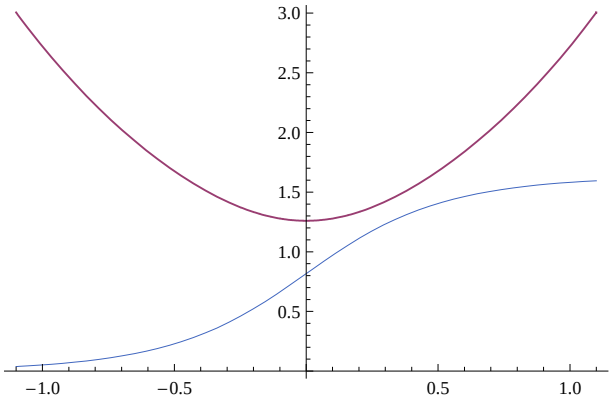

Figure 3.1: Plot of the torsion vortex solution vs. t. The blue dashed line is $e^{A(t)}$ while the red solid line is $\Theta(t)$. To make the plot, we have chosen $\Theta_0 = 0$.

Note the curvature and torsion of this solution:

$$R^{\alpha}{}_{\beta} = -\dot{F}\dot{A}\,\epsilon^{\alpha}{}_{\beta\gamma}dt \wedge e^{\gamma} - a^2 e^{\alpha} \wedge e_{\beta}\,, \tag{3.34}$$

$$R^{\alpha}{}_{0} = \left(\dot{h} + h^2\right) dt \wedge e^{\alpha} - \frac{1}{2}\dot{F}\dot{A}\,\epsilon^{\alpha}{}_{\beta\gamma}e^{\beta} \wedge e^{\gamma}\,, \tag{3.35}$$

$$T^{\alpha} = -\frac{1}{2}\dot{F}\,\epsilon^{\alpha}{}_{\beta\gamma}e^{\beta} \wedge e^{\gamma}\,, \tag{3.36}$$

$$T^{0} = 0\,. \tag{3.37}$$

These are non-singular for all $t \in (-\infty, \infty)$. The torsion vortex solution has divergent action, but this divergence is cancelled by boundary counterterms, the same counterterms which render the action of AdS_4 finite. To see this, the energy of the torsion vortex can be computed by evaluating the Euclidean action on the solution. Introducing a cutoff at $t = \pm L$, we find

$$I_{tv,on-shell} = 4a^2 \int \epsilon_{\alpha\beta\gamma}dx^{\alpha} \wedge dx^{\beta} \wedge dx^{\gamma} \int dt e^{3A(t)} \tag{3.38}$$

$$= (6\int \widehat{Vol}_3) \cdot \left(\frac{4}{3}a\alpha^3 e^{3aL} + \dots\right)\,, \tag{3.39}$$

where the ellipsis contains terms that vanish when the cutoff is removed. As in pure AdS_4, an appropriate counterterm is of the form [111, 112]

$$I_{c.t.} = -\frac{4a}{3}\int_{\partial M} \epsilon_{\alpha\beta\gamma}\tilde{e}^{\alpha} \wedge \tilde{e}^{\beta} \wedge \tilde{e}^{\gamma}\,. \tag{3.40}$$

In the present case, we have such a counterterm on *each* asymptotic boundary, and thus we find

$$I_{c.t.} = -2\frac{2a}{3}\alpha^3 e^{3aL} \cdot (6\int \widehat{Vol}_3)\,, \tag{3.41}$$

which exactly cancels the divergent energy of the torsion vortex.

Furthermore, we note that in the Kalb-Ramond representation, the solution has

$$H = \dot{\Theta} Vol_3 = \pm 6a\alpha^3 \widehat{Vol}_3 \equiv \hat{H}\widehat{Vol}_3\,, \tag{3.42}$$

where $\widehat{Vol}_3 = \frac{1}{6}\epsilon_{\alpha\beta\gamma}dx^\alpha \wedge dx^\beta \wedge dx^\gamma$. This corresponds to a 'topological quantum number' of the kink

$$\int *_4 H = \pm\Delta\Theta = \pm 2\pi. \tag{3.43}$$

3.4 The torsion vortex as the gravity dual of parity symmetry breaking

The holographic interpretation of the torsion vortex is also of interest. To study this, we set to zero without loss of generality the integration constant $\Theta_0 = 0$ and pick the plus sign in (3.31), (3.32). Next we need the asymptotic expansion of the vierbein which reads

$$\tilde{e}^\alpha = 2^{-1/3}\alpha e^{\pm a(t-t_0)}\left(1 + \frac{1}{3}e^{\mp 6a(t-t_0)} + \cdots\right)dx^\alpha \;\text{ for }\; t \to \pm\infty\,. \tag{3.44}$$

This shows that our solution is asymptotically anti-de Sitter for both $t \to \pm\infty$. The two asymptotic AdS spaces have the same cosmological constant. From this expansion we could read the expectation value of the renormalized boundary energy momentum tensor which would be given by the coefficient of the $e^{\pm 3at}$ term (see e.g. [91, 92]). Such a term is missing in (3.44), hence the expectation value of the boundary energy momentum tensor is zero.

It is not immediately apparent how to interpret these two asymptotic regimes. Are they truly distinct, or should they be identified in some way? We note that the pseudoscalar behaves in these asymptotic regimes as

$$\Theta(t) \;\to\; 4e^{-3a(t-t_0)} - \frac{4}{3}e^{-9a(t-t_0)} + \cdots \;\text{ for }\; t \to -\infty\,, \tag{3.45}$$

$$\Theta(t) \;\to\; 2\pi - 4e^{3a(t-t_0)} + \frac{4}{3}e^{9a(t-t_0)} + \cdots \;\text{ for }\; t \to +\infty\,. \tag{3.46}$$

From the above we confirm that $\Theta(t)$ is dual to a dimension $\Delta = 3$ boundary pseudoscalar that we denote $\mathcal{O}_3$. In each one of the asymptotically AdS regimes, the leading constant behavior of $\Theta(t)$ corresponds to the source (i.e., coupling constant) for $\mathcal{O}_3$ and the subleading term proportional to $e^{\mp 3a(t-t_0)}$ to the expectation value $\langle \mathcal{O}_3 \rangle$. The two asymptotic regimes are distinguished by the behavior of Θ. In fact, the essential difference is *parity*.

We can now describe the holography of our torsion vortex. In the $t \to -\infty$ boundary sits a three-dimensional CFT at a parity breaking vacuum state. The order parameter is the expectation value of the pseudoscalar which is $\langle \mathcal{O}_3 \rangle = 4$ in units of the AdS radius. The expectation value breaks of course the conformal invariance of the boundary theory. Then, the theory is deformed by the same pseudoscalar operator $g\mathcal{O}_3$ where g is a marginal coupling. The torsion vortex provides the holographic description of that deformation. A solution with two asymptotic regimes is difficult to interpret in terms of the usual holographic renormalization group. Note though that in this case, at $t \to +\infty$ the space becomes AdS with the *same* radius as at $t \to -\infty$. Hence, the two boundary theories have the same 'central charges'.[8]

We suggest that instead of interpreting the solution in terms of an RG flow, we should think of it as a transition between two inequivalent vacua of a single theory. This statement is supported by the behavior of $\Theta(t)$ in the two asymptotic regimes. For $t \to \infty$ the pseudoscalar asymptotes to the configuration (3.46). The interpretation is now that when the marginal coupling takes the fixed value $g_* = 2\pi$ we are back to the *same* CFT (i.e. having the same central charge) however in a distinct parity breaking vacuum such that $\langle \mathcal{O}_3 \rangle = -4$. In others words, the two asymptotic AdS regimes seem to describe two distinct parity breaking vacua of the same theory. The two vacua are distinguished by the expectation value of the parity breaking order parameter being $\langle \mathcal{O}_3 \rangle = \pm 4$. Quite remarkably, we also seem to find that starting in one of the two vacua, we can reach the other by a marginal deformation with a *fixed* value of the deformation parameter.

Since the marginal operator is of dimension $\Delta = 3$ and parity odd, we tentatively identify it with a Chern-Simons operator of a boundary gauge field. In this case the torsion vortex induces the T-transformation in the boundary CFT [113, 109]. In Appendix B we will argue that the three dimensional Gross-Neveu model coupled to abelian gauge fields exhibits a large-N vacuum structure that matches our holographic findings. Although our bulk model is extremely simple to provide details for its possible holographic dual, we regard this remarkable similarity as strong qualitative evidence that our torsion vortex is the gravity dual of the 'tunneling' between different parity breaking vacua in three dimensions. However, in a three-dimensional quantum field theory, we do not expect that tunneling can occur because of large volume effects,

[8] We use "central charge" in $d = 3$ for a quantity that counts the massless degrees of freedom at the fixed point. Such a quantity may be taken to be the coefficient in the two-point function of the energy momentum tensor or the coefficient of the free energy density. Recall that there is no conformal anomaly in $d = 3$.

and distinct vacua remain orthogonal. Thus, referring to the torsion vortex as a tunneling event should be taken figuratively. We leave to future work a more careful study of the boundary interpretation of the torsion vortex solution. An interpretation will depend on the precise topology of the boundary.[114]

3.5 Physics in the Bulk: The Superconductor Analogy

The bulk interpretation of the exact solution is also interesting. Because the pseudoscalar field undergoes $\Theta(t) \to \Theta(t) + 2\pi$ under t goes from $-\infty$ to $+\infty$, the exact solution corresponds to a topological kink. It satisfies

$$\int dt \dot{\Theta} = 2\pi$$

In Figure 2, we plot the solution.

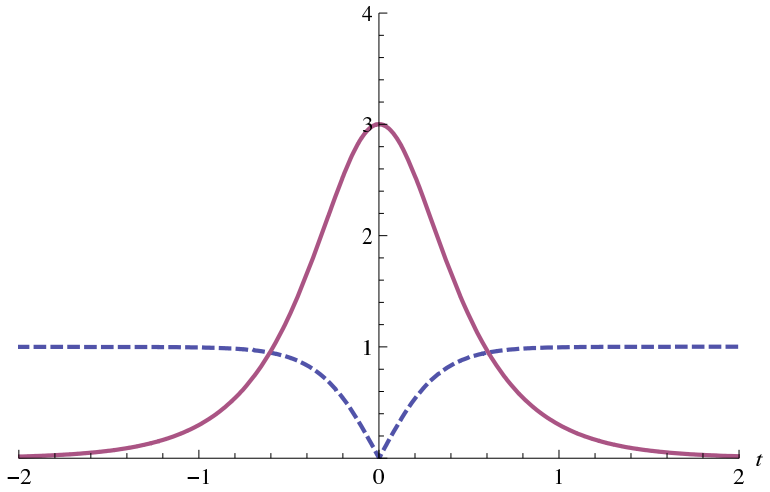

Figure 3.2: The blue dashed line is $|h(t)|$, resembling the order parameter of a superconductor, while the solid red line is Π_F, analogous to the magnetic induction of an Abrikosov vortex.

3.5.1 Gravity vortex as Abrikosov vortex

The gravity vortex solution (3.29-3.32) bears some resemblance to the Abrikosov vortex of superconducting systems. In this section, we will explore this and point out some possibly interesting features. The first thing to notice is that the plot in Figure **??** is identical to the profile of an Abrikosov vortex (see for example Figure 5.1 in Ref. [115].) The codimension differs,[9] but there is a correspondence between our radial t-direction and the radial direction in the Abrikosov vortex, and $|h|$ and Π_F correspond to the condensate and magnetic induction of the superconductor, respectively. Table 1 summarizes the correspondence. In this

[9]The difference in dimensionality of the core is what we expect, since it supports a 3-form field strength in contrast to a 2-form field strength in superconductivity.

Abrikosov vortex	Torsion vortex
order parameter Φ	order parameter $\|h\| = \|\dot{A}\|$
$T - T_c$	Λ
magnetic induction B	Π_F
magnetic field H	$\hat{H}$
$\mathbb{Z}$-quantized magnetic flux	$\mathbb{Z}_2$-quantized electric flux

Table 3.1: Abrikosov vortex v.s. Torsion vortex

correspondence, since the order parameter is $h = \dot{A}$, the superconducting phase (constant order parameter) corresponds to AdS_4, while the normal phase corresponds to flat space ($h = 0$). Far away from the core of the torsion vortex, the geometry is asymptotically AdS, but at the core the spatial slice (at $t \to t_0$) becomes flat. To see this, note that if we think of the system as a pseudoscalar coupled to torsionless gravity, the torsion vortex has $\mathring{\omega}^{\alpha}{}_{\beta} = 0$ and $\mathring{\omega}^{\alpha}{}_{0} = \dot{A}\tilde{e}^{\alpha}$, and so

$$\mathring{R}^{\alpha}{}_{\beta} = -h^2 \tilde{e}^{\alpha} \wedge \tilde{e}_{\beta}\,, \tag{3.47}$$

$$\mathring{R}^{\alpha}{}_{0} = (\dot{h} + h^2) dt \wedge \tilde{e}^{\alpha}\,, \tag{3.48}$$

$$\mathring{T}^{\alpha} = 0\,. \tag{3.49}$$

Thus, at the core, we find that the Riemann tensor has components

$$R^{\alpha}{}_{0\alpha 0} \to -3a^2\alpha\,, \tag{3.50}$$

$$R^{\alpha}{}_{\beta\alpha\beta} \to 0\,. \tag{3.51}$$

This behavior is in line with an Abrikosov vortex in which there is normal phase at the core and superconducting phase away from the core.

The analogue of the magnetic field is what we have called $\hat{H}$, proportional to the constant α^3. In the vortex, the magnetic induction, analogous to Π_F, has a penetration length $\lambda \sim 1/3a$, and the coherence length of the order parameter is $\xi \sim 1/6a$. The penetration and coherence length are obtained by looking at the exponential fall-off of these quantities in the core of the vortex, away from their values in the superconducting phase.

The torsion vortex also has a quantized flux $\int *_4 H = \Delta\Theta = 2\pi$. This flux is independent of any parameters of the solution and of any rescaling of fields in the theory. Thus, this is an analogue of the quantized magnetic flux in superconductivity.

Finally, note the following interesting feature. If we take a derivative of the second equation in (3.29), we arrive at

$$\ddot{h} - 6\Lambda h - 18h^3 = 0\,. \tag{3.52}$$

This looks like a Landau-Ginzburg equation of motion of an effective ϕ^4 theory. This leads us to interpret $\Lambda \sim T - T_c$. Of course, there is no real temperature in the case of the torsion vortex, but we note that this implies that the penetration and coherence lengths diverge as $T \to T_c$ with exponent $1/2$, as in superconductivity.

3.5.2 Multi-vortices and Vortex Condensation

In the last section, we noted that there is a strong analogue between the torsion vortex solution and superconductivity. It is intriguing to carry the analogy further and consider multi-vortex configurations. We have noted that at the core of the torsion vortex, the spatial sections are flat. Thus, one might imagine that if it was favourable for torsion vortices to condense, as vortices do in Type I superconductors, then finite regions of normal phase (corresponding to $\Lambda = 0$) would obtain. We will argue below that this can in fact occur, although the system appears not to be unstable.

To understand the physics involved, the first step is to consider a configuration of two vortices. In the superconductivity literature, this is a standard computation. One takes two vortices separated by a distance ℓ and computes the Euclidean action. More precisely, we will treat this here as follows. Denoting the torsion vortex schematically as $\Phi(t_0)$, we take a configuration

$$\begin{cases} \Phi(\ell/2), & t > 0 \\ \Phi(-\ell/2), & t < 0 \end{cases}\,. \tag{3.53}$$

We have taken a piecewise solution, because solutions of non-linear equations cannot be simply superimposed. The result is not quite a solution to the equations of motion of course, failing at the midpoint between the vortices. However, if we simply evaluate the Euclidean action, we find

$$S_E(\ell) = 4a\alpha^3 \sinh(3a\ell/2)\,. \tag{3.54}$$

Note that this is positive, so one might naively conclude that the vortices repel each other. However, recall that the vortex profile exists not in flat space-time, but in the metric given by (3.33), which rises asymptotically. As a result, as we move the vortices further apart, there is a corresponding rise in the metric

between the vortices. So, we should directly evaluate the force

$$F = -\frac{dS_E}{d\ell} = -6a\alpha^3 \cosh(3a\ell/2) < 0\,. \tag{3.55}$$

and thus we conclude that the vortices in fact *attract* each other. In the superconducting analogue, this implies that we have a *Type I superconductor*. In such a superconductor, the number of vortices is determined by the total magnetic flux, and the vortices tend to clump together forming (potentially) finite regions of normal phase within the superconductor.

We now describe the analogous situation in our gravitational system. We have noted that the constant $\hat{H}$ plays the role of the external magnetic induction, while H is the magnetic field, varying within the vortex, with $\Delta\Theta = \int *_4 H$. Following the superconducting analogue, if we put the system in a box of size $2L$ (that is we impose a cutoff on each AdS asymptotic) the flux conservation equation is of the form

$$\Delta\Theta = 2L\hat{H} \tag{3.56}$$

The vortices carry the flux in the superconductor, and so it is natural to ask what is the lowest energy configuration satisfying (3.56)? To analyze this, consider an array of n vortices in a region of size L_0. We take the vortices to be equally spaced, as one can show that deviating from such a configuration causes a rise in energy. For such a configuration, the flux quantization condition (3.56) gives a relation between n,L_0 and $\hat{H}$. Such a representative curve is shown in Fig 3.3a)

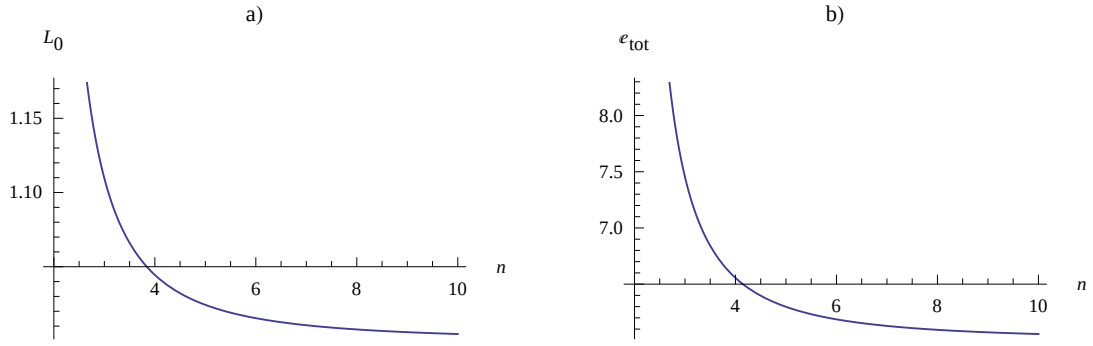

Figure 3.3: Size of normal state droplet a) and total energy b) vs. n for a multi-vortex.

If we solve this equation for L_0 as a function of n and $\hat{H}$, we can then compute the energy as a function of n. One obtains a curve as in Fig 3.3b). One notes that the energy is minimized for large n, and in that

case, the size L_0 asymptotes to a fixed value, which is found to be

$$L_0 = \frac{\hat{H}}{6a} \cdot 2L = \alpha^3 \cdot 2L \tag{3.57}$$

We conclude that the preferred configuration, given a fixed external flux, is a continuum of vortices arrayed over a finite size region. Within this droplet, the system is in the normal phase. We have noted that the vortex core is spatially flat, and so we surmise that within the droplet, the space-time is flat. The asymptotic value of energy in Fig 2.3b) is precisely minus that contributed by the cosmological constant. Again, the size of the droplet is set by the value of the external H-flux, and the boundary conditions are AdS. Note that for a fixed cutoff, there is a critical field (given by $\hat{H} = 6a$) for which the entire spacetime is flat.

3.6 Conclusions

In this chapter we have presented in detail a simple toy model, the Nieh-Yan model, where torsion enters through the spacetime dependence of the coupling constant of the Nieh-Yan topological invariant. Although we have discussed the model directly in terms of torsion, it can classically be put into equivalent forms as either a massless pseudoscalar or a Kalb-Ramond field coupled to gravity. The model has an interesting and non-trivial holographic interpretation. In particular, we have shown that it possesses an exact bulk solution in Euclidean signature, termed the torsion vortex, having two asymptotically AdS_4 regimes, while the pseudoscalar acquires a kink profile. We have argued then that the holographic interpretation of this torsion vortex is a three-dimensional CFT with two distinct parity breaking vacua. Moreover, our bulk solution may imply that the deformation by a classically marginal pseudoscalar with a fixed coupling constant induces a transition between the two parity breaking vacua separated by a domain wall, which would be at infinity in the boundary components.[114] Remarkably, this qualitative behaviour is seen already in the three-dimensional Gross-Neveu model coupled to $U(1)$ gauge fields. The economy of our bulk model does not allow a detailed identification of the bulk and boundary theories, nevertheless we believe that our results provide a strong base where an exact bulk/boundary dictionary for AdS_4/CFT_3 can be based. A further rather intriguing property of the torsion vortex is that it can be mapped into the standard Abrikosov vortex of superconductivity. Such a map identifies flat spacetime with a superconductor's normal phase, while AdS is identified with a superconducting phase. The cosmological constant would then measure the deviation from the 'critical temperature'. A phenomenon of vortex condensation is found, similar to the analogous case in type I superconductors.

The upshot of our results is that the torsional degrees of freedom of four dimensional gravity can provide

holographic descriptions for a number of interesting properties of three dimensional critical systems. It would be interesting to extend our analysis to more elaborate models where more torsional degrees of freedom become dynamical. It is also of interest to discuss whether our simple model can be embedded into M-theory.

Chapter 4

Real-Time Correlators and Non-Relativistic Holography

Correlation functions of operators in strongly coupled conformal field theories can often be computed using the AdS/CFT correspondence. Euclidean correlators have a long history[28, 116] while the rich analytic structure of various Lorentzian signature correlators, associated with the boundary condition problem in the bulk, can also be obtained. The earliest proposal for the latter was by Son and Starinets[29], and there have also been several elaborations of that method (see for example [117, 118]). Recently, Skenderis and van Rees[30, 31] showed how the complex time contour of an arbitrary correlation function can systematically be accounted for by gluing together manifolds of various signatures, carefully matching fields at the interfaces. This method was used to calculate scalar two-point functions in AdS space, and in asymptotically AdS spaces.

The extension of gauge-gravity duality ideas to a family of spacetimes of Galilean isometries and field theories with non-relativistic invariance [6, 7] has been of much interest in the recent literature. It is expected that such systems are of more direct relevance to condensed matter models. In particular, in the special case where the isometries enlarge to the full Schrödinger algebra, the correspondence was more controllable and extensively studied. The Schrödinger group itself has been of interest for many years as the full symmetry of the free Schrödinger wave equation (as well as a few systems with certain interactions). The reader will find discussions in the literature of the representation theory in many papers, particularly in low spatial dimensional cases [119, 120, 121, 122]. In the holography point of view, correlation functions have recently been computed using standard methods for scalars [6, 7, 123, 124] and for fermions [125]. String embedding of the $4+1$ Schrödinger geometry and extension to finite temperature and density was described in [3, 4, 5].

In this chapter, we reconsider *Lorentzian* correlators of non-relativistic systems by directly calculating them using the Skenderis and van Rees technique in various dimensional Schrödinger geometries [37]. We consider the time-ordered correlator and the Wightman function, as well as thermal correlators.

4.1 The Schrödinger Geometry and Scalar Fields

We consider the $d+3$ dimensional Lorentzian Schrödinger geometry[6, 7]

$$ds^2 = \frac{L^2}{z^2}\left(-\frac{\beta^2}{z^2}dt^2 + 2dtd\xi + d\vec{x}^2 + dz^2\right), \tag{4.1}$$

where $z \geq 0$ and β, L are length scales. The $\vec{x}$ are coordinates in d-dimensional space. Rather than giving a conformal class as in the relativistic (AdS) case, the quantity in parentheses is a metric of the Bargman type, in which the coordinate ξ is null. The Killing field $N = \partial_\xi$ generates the central extension of the Schrödinger algebra whose eigenvalue would be interpreted as 'mass' or 'particle number' in a weakly coupled non-relativistic particle theory. In the present context, fields propagating in the bulk are to be taken to be equivariant with respect to N

$$N\Psi = in\psi \tag{4.2}$$

and dual quasi-primary operators are labeled by both conformal dimension and n. The ξ-direction is taken to be compact so that the spectrum of dual operators is discrete.

This geometry has Schrödinger isometry with dynamical exponent equal to two. The Killing vectors are of the form

$$\begin{aligned}
N &= \partial_\xi && (4.3)\\
D &= z\partial_z + \vec{x}\cdot\vec{\partial} + 2t\partial_t && (4.4)\\
H &= \partial_t && (4.5)\\
C &= tz\partial_z + t\vec{x}\cdot\vec{\partial} + t^2\partial_t - \frac{1}{2}(\vec{x}^2 + z^2)\partial_\xi && (4.6)\\
M_{ij} &= x_i\partial_j - x_j\partial_i && (4.7)\\
\vec{K} &= -t\vec{\partial} + \vec{x}\partial_\xi && (4.8)\\
\vec{P} &= \vec{\partial} && (4.9)
\end{aligned}$$

N is central, and D, H, C form an $SL(2,\mathbb{R})$ algebra.

Consider a massive complex scalar propagating on the non-relativistic (Lorentzian) geometry with action

$$S = -\frac{1}{2}\int d^{d+3}x\sqrt{-g}\left(g^{\mu\nu}\partial_\mu\bar{\phi}\partial_\nu\phi + m_0^2/L^2|\phi|^2\right) \tag{4.10}$$

The usual interpretation is that the dual theory lives on $\mathbb{R}^{1,d}$ at $z = 0$ and is coordinatised by the $(t, \vec{x})$

coordinates–ξ is not geometric in the usual sense. The isometry $N : \xi \mapsto \xi + a$ is central and thus N is strictly conserved. Each operator of the boundary theory can be taken to have a fixed momentum ('particle number') conjugate to ξ. ξ is usually taken compact (with circumference R) so that the spectrum of possible momenta is discrete. In this case, the dimensionless ratio β/R is a parameter of the theory.

For example, the graviton mode coupling to the stress energy tensor of the boundary theory has particle number zero [3, 5]. Here, we will consider a complex scalar with definite but arbitrary particle number n. As we will see, it is very important that the scalar be complex. First, it carries a charge under N and so we should expect it to be complex. More importantly though, it is dual to an operator in a non-relativistic theory, and in such a theory there is a sort of polarization: a simple example of this occurs in free field theories, in which the elementary field creates a particle (and not anti-particle) state.

Now, in this chapter we consider correlators of various types. In this regard, as developed by Skenderis and van Rees[30, 31], we regard the metric (4.1) as defined formally for complex t, and a given correlator is constructed from a particular contour in the complex t plane. Here, we consider two such cases, in which the contour is constructed from horizontal (Lorentzian time) and vertical (Euclidean time) contour segments (see Fig. 4.1).

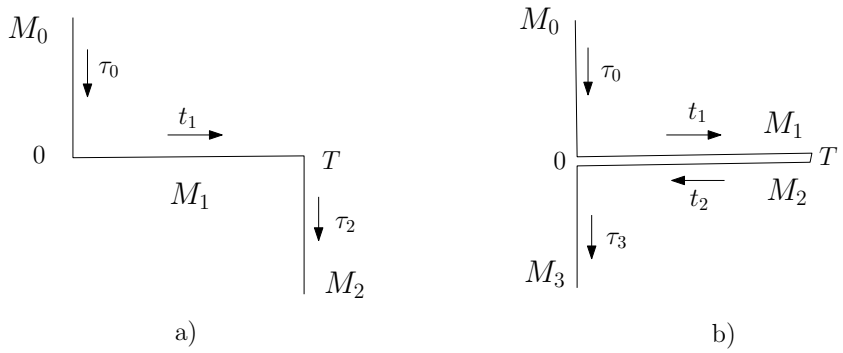

Figure 4.1: Contours corresponding to the time-ordered correlator and the Wightman function, respectively.

In the next two subsections, we consider scalar fields in Lorentzian time and in Euclidean time, respectively.

4.1.1 Lorentzian signature

Given the metric (4.1) for real time, the scalar equation of motion takes the form

$$z^2\partial_z^2\phi - (d+1)z\partial_z\phi + z^2(2\partial_t\partial_\xi + \partial_i^2\phi) + \beta^2\partial_\xi^2\phi - m_0^2\phi = 0. \tag{4.11}$$

We look for solutions of the form

$$\phi_{(n)} = e^{in\xi} e^{-i\omega t + i\vec{k}\cdot\vec{x}} f_{\omega,n,\vec{k}}(z), \qquad \bar{\phi}_{(n)} = e^{-in\xi} e^{i\omega t - i\vec{k}\cdot\vec{x}} \bar{f}_{\omega,n,\vec{k}}(z) \tag{4.12}$$

in which case f satisfies

$$z^2\partial_z^2 f - (d+1)z\partial_z f + z^2(2\omega n - \vec{k}^2)f - m^2 f = 0, \tag{4.13}$$

where $m^2 = m_0^2 + \beta^2 n^2$. The general solution of (4.13) can be written in terms of modified Bessel functions as

$$f_{n,\omega,\vec{k}}(z) \quad = \quad A(\omega,\vec{k}) z^{\frac{d}{2}+1} K_\nu(qz) + B(\omega,\vec{k}) z^{\frac{d}{2}+1} I_\nu(qz) \tag{4.14}$$

with $\nu = \sqrt{(\frac{d}{2}+1)^2 + m^2}$ and $q = \sqrt{q^2} = \sqrt{\vec{k}^2 - 2\omega n}$. K_ν and I_ν correspond to non-normalizable and normalizable modes, respectively. Their asymptotic behavior is as follows

$$z^{\frac{d}{2}+1} K_\nu(qz \to 0) \quad = \quad \Gamma(\nu) \frac{z^{\frac{d}{2}+1-\nu}}{2^{-\nu+1} q^\nu} + ... \tag{4.15}$$

$$z^{\frac{d}{2}+1} I_\nu(qz \to 0) \quad = \quad \frac{1}{\Gamma(\nu+1)} \frac{z^{\frac{d}{2}+1+\nu}}{2^\nu q^{-\nu}} + ... \tag{4.16}$$

$$z^{\frac{d}{2}+1} K_\nu(|qz| \to \infty) \quad = \quad \sqrt{\frac{\pi z^{d+1}}{2q}} e^{-qz} + ... \tag{4.17}$$

$$z^{\frac{d}{2}+1} I_\nu(|qz| \to \infty) \quad = \quad \sqrt{\frac{z^{d+1}}{2\pi q}} \Big[e^{qz}(1+...) + e^{-qz - i\pi(\nu+1/2)}(1+...) \Big]. \tag{4.18}$$

For $q^2 < 0$, both K_ν and I_ν are regular everywhere, while for $q^2 > 0$, I_ν diverges for large z and should be discarded. This situation is very similar to that of a scalar field propagating on AdS_{d+3}, where the solution can also be written in terms of modified Bessel functions. In fact this similarity is very useful and was employed in Ref. [124] to compute the non-relativistic bulk-to-boundary propagator. We note though that there is a small but important difference due to the non-relativistic nature of the boundary theory, that we will explain presently.

Without loss of generality, we take $n > 0$. To construct the most general solution (with fixed n), we must integrate over all values of $\omega, \vec{k}$. However, q has a branch point at $\omega = \vec{k}^2/2n$, and we must then say how to integrate over ω. Following [30], we do so by moving the branch point off of the real ω axis by defining $q_\epsilon = \sqrt{-2\omega n + \vec{k}^2 - i\epsilon}$, $\bar{q}_\epsilon = \sqrt{-2\omega n + \vec{k}^2 + i\epsilon}$. The branch cut is taken along the negative real axis. Clearly, we have made a choice here, but we will see later that this is the correct choice, for physical reasons. Notice that since $Re(q_\epsilon), Re(\bar{q}_\epsilon) > 0$, K_ν always decays exponentially as $|qz| \to \infty$. In contrast, the

large z behavior of I_ν tells us that $q, \bar{q}$ cannot have a real part. As a result, the $i\epsilon$ insertion should not be applied for the normalizable mode.[1]

With these comments, we arrive at the general solution to (4.13) in Lorentzian signature

$$\phi_{(n)}(t,\vec{x}) = e^{in\xi}\int \frac{d\omega}{2\pi}\frac{d^dk}{(2\pi)^d}\, e^{-i\omega t+i\vec{k}\cdot\vec{x}} z^{\frac{d}{2}+1}\left(A(\omega,\vec{k})K_\nu(q_\epsilon z)+\theta(-q^2)B(\omega,\vec{k})J_\nu(|q|z)\right) \tag{4.19}$$

where we have used $I_\nu(\sqrt{q^2}z) = I_\nu(-i|q|z) \sim J_\nu(|q|z)$.

4.1.2 Euclidean signature

Next, we consider a similar analysis in Euclidean signature. To do so, we Wick rotate the metric (4.1) to[123]

$$ds^2 = L^2\left(\beta^2\frac{d\tau^2}{z^4}+\frac{-2id\tau d\xi+d\vec{x}^2+dz^2}{z^2}\right) \tag{4.20}$$

Although this metric is complex and thus not physical, it is possible to trace carefully through the analysis, and this is what we need to do in any case for Euclidean signature.

The general solution is

$$\phi_{(n)}(\tau,\vec{x}) = e^{in\xi}\int \frac{d\omega_E}{2\pi}\frac{d^dk}{(2\pi)^d}\, e^{-i\omega_E\tau+i\vec{k}\cdot\vec{x}} z^{\frac{d}{2}+1}A(\omega_E,\vec{k})K_\nu(q_E z) \tag{4.21}$$

$$\bar{\phi}_{(n)}(\tau,\vec{x}) = e^{-in\xi}\int \frac{d\omega_E}{2\pi}\frac{d^dk}{(2\pi)^d}\, e^{i\omega_E\tau-i\vec{k}\cdot\vec{x}} z^{\frac{d}{2}+1}\bar{A}(\omega_E,\vec{k})K_\nu(\bar{q}_E z) \tag{4.22}$$

where now $q_E = \sqrt{q_E^2} = \sqrt{\vec{k}^2 - i2\omega_E n}$. Note that in this case, the branch point is at imaginary ω_E, and so no $i\epsilon$ insertion is necessary.

In contrast to the Lorentzian case, the Euclidean scalar does not have a normalizable mode. This is because q_E and $\bar{q}_E$ cannot be pure imaginary, so $I_\nu(q_E z)$ is never regular in the interior. It is important to note, however, that this statement applies to the case $\tau \in (-\infty, \infty)$. If τ is restricted, a normalizable mode can emerge. For example, if $\tau \in [0, \infty)$, we write $\omega_E = -i\omega$ for ϕ and $\omega_E = i\omega$ for $\bar{\phi}$ and the following mode is allowable

$$\phi \sim e^{in\xi}e^{-\omega\tau+i\vec{k}\cdot\vec{x}} z^{\frac{d}{2}+1}I_\nu(qz) \tag{4.23}$$

$$\bar{\phi} \sim e^{-in\xi}e^{-\omega\tau-i\vec{k}\cdot\vec{x}} z^{\frac{d}{2}+1}I_\nu(\bar{q}z) \tag{4.24}$$

[1] This fact was not clearly spelled out in Ref. [30] in the relativistic analogue, but we will see later that it is an important point.

as long as $\omega > 0$ and $-2\omega n + \vec{k}^2 < 0$, or equivalently $\omega > \vec{k}^2/2n$.

A similar result pertains in the finite temperature case where $\tau \in [0, \beta]$. Observe however that in contrast to the relativistic real-time formalism, there is no normalizable mode for the Euclidean segment if we restrict $\tau \in (-\infty, 0)$. This is because we would need both $\omega < 0$ and $-2\omega n + \vec{k}^2 < 0$, and these contradict each other. This will have important consequences. In particular we note that there is no normalizable mode in the segment M_0 of either contour in Fig. 4.1.

4.2 Non-Relativistic Holography and Correlators

4.2.1 Matching Conditions

To construct correlation functions, we must match solutions at the interfaces between contour segments. We will label field values on a contour segment M_n by a subscript, ϕ_n. Let us begin by considering the Lorentzian(M_1)-Lorentzian(M_2) interface in Fig. 4.1b, where $t_1 \in [0, T]$ and $t_2 \in [T, 2T]$ (where $T \to \infty$ is a large time). The total action (for these two segments) is

$$S = S_{M_1} + S_{M_2} = \int_0^T dt_1 \left(g^{\mu\nu}_{M_1} \partial_\mu \bar{\phi}_1 \partial_\nu \phi_1 + m_0^2 / L^2 \bar{\phi}_1 \phi_1 \right) - \int_T^{2T} dt_2 \left(g^{\mu\nu}_{M_1} \partial_\mu \bar{\phi}_2 \partial_\nu \phi_2 + m_0^2 / L^2 \bar{\phi}_2 \phi_2 \right) \quad (4.25)$$

The relative minus sign arises because M_1 and M_2 have opposite orientation. For the same reason, the metric in M_2 is

$$ds^2_{M_2} = L^2 \Big(-\beta^2 \frac{dt_2^2}{z^4} + \frac{-2dt_2 d\xi + d\vec{x}^2 + dz^2}{z^2} \Big), \quad (4.26)$$

which has an extra minus sign in the off-diagonal component.

Requiring continuity of the momentum conjugate to $\bar{\phi}$ at the intersection $t_1 = t_2 = T$, we get

$$\partial_\xi \phi_1 = \partial_\xi \phi_2. \quad (4.27)$$

Along with the continuity of ϕ, we conclude that the matching conditions at $t_1 = t_2 = T$ are

$$\phi_1(T) = \phi_2(T) \quad (4.28)$$

$$n_1 = n_2 \quad (4.29)$$

Thus, we do not need to impose first-order time derivative continuity of fields along the contour as in the

relativistic case — it is just replaced by particle number conservation. It turns out that (4.28,4.29) are also the matching conditions for Euclidean – Lorentzian interfaces.

4.2.2 Convergence and the Choice of Vacuum

The non-relativistic holographic correspondence is in general the same as its relativistic counterpart, where the path integral with specified boundary conditions in the bulk is identified with the partition function with sources inserted in the boundary theory. In the case of a complex bulk scalar, we must temporarily treat the sources $\phi_{(0)}$ and $\bar{\phi}_{(0)}$ as independent. The near boundary expansion of the fields are qualitatively the same as scalars on AdS_{d+3}

$$\phi_{(n)} = e^{in\xi}\Big\{\{z^{\Delta_-}\left(\phi_{(0)}+z^2\phi_{(2)}+o(z^4)\right)+z^{\Delta_+}\left(v_{(0)}+z^2v_{(2)}+o(z^4)\right)\Big\} \tag{4.30}$$

$$\bar{\phi}_{(n)} = e^{in\xi}\Big\{\{z^{\Delta_-}\left(\bar{\phi}_{(0)}+z^2\bar{\phi}_{(2)}+o(z^4)\right)+z^{\Delta_+}\left(\bar{v}_{(0)}+z^2\bar{v}_{(2)}+o(z^4)\right)\Big\}, \tag{4.31}$$

with $\Delta_\pm = 1+d/2\pm\nu$ and

$$\phi_{(2m)} = \frac{1}{2m(2\Delta_+-(d+2)-2m)}\Box_0\phi_{(2m-2)}, \tag{4.32}$$

where here $\Box_0 = 2in\partial_t+\partial_i^2$ is the non-relativistic Laplacian. As usual the holographic correspondence implies

$$e^{iS_C^{bulk}[\bar{\phi}_{(0)},\phi_{(0)}]} = \langle e^{i\int_C(\hat{\mathcal{O}}^\dagger\phi_{(0)}+\bar{\phi}_{(0)}\hat{\mathcal{O}})}\rangle, \tag{4.33}$$

where C denotes the contour. Although we have a very different geometry, it's easily seen that in each patch of the contour the bulk (either Euclidean or Lorentzian) on-shell action

$$S_{os} = \frac{1}{2}\int_\epsilon d^{d+1}xd\xi\sqrt{|g|}\;\bar{\phi}\;g^{zz}\;\partial_z\phi \tag{4.34}$$

is essentially the same as scalars on AdS_{d+3}. As a result, the renormalization procedure proceeds in the same way as AdS_{d+3}/CFT_{d+2}, which was carried out in much details in [**?**]. In specific, for Lorentzian signature the counter terms take the form,

$$S_{ct} = \int_\epsilon d^{d+1}xd\xi\sqrt{-\gamma}\Big(\frac{d+2-\Delta_+}{2}\bar{\phi}\phi+\frac{1}{2(\Delta_+-d-4)}\bar{\phi}\Box_\gamma\phi+\dots\Big), \tag{4.35}$$

where $\sqrt{-\gamma} = z^{-(d+2)}$ is the $(d+2)$-dimensional induced metric determinant and $\Box_\gamma = z^2(2in\partial_t+\partial_i^2)$ (we will set $L=1$ from now on). The dots represent higher derivative terms. For special cases where ν is an

integer, logarithmic counter terms $\sim \log \epsilon$ may appear [**?**]. It's important to note that S_{ct} preserves the Galilean subalgebra, since $[\Box_\gamma, K_i] = 0$. This is in parallel with relativistic holography where the Poincare subalgebra is preserved by the counter terms. In any case, $v_{(0)}$ will determine the v.e.v of the dual operator and its derivative with respect to the source $\phi_{(0)}$ gives us the 2-point functions.

There is, however, a subtlety of which we must be cognizant. Unlike relativistic field theories, in non-relativistic field theories an elementary field Ψ and its Hermitian conjugate $\Psi^\dagger$ play the role of creation and annihilation operators. There is a freedom to choose which is an annihilator, or equivalently a freedom to pick the vacuum. Once a convention is chosen, Ψ and $\Psi^\dagger$ are no longer on the same footing. This is also true for any operator $\hat{\mathcal{O}}$, $\hat{\mathcal{O}}^\dagger$, in which $\hat{\mathcal{O}}$ is constructed only from annihilators. This corresponds to the fact that there is only a single pole in the complex ω-plane in the non-relativistic case. Consequently, the time-ordered propagator will in fact have only a single temporal θ-function present. We expect to see this coming about in the analysis, but to see this properly, one has to be careful with the convergence of various integrals.

4.3 Correlation Functions

In both cases shown in Fig. 4.1, we have an initial vertical contour M_0. The correlation functions of interest are computed by including source(s) on horizontal component(s) of the contour. We first show that given such a contour component M_0, there is no normalizable mode (such a mode would be everywhere subleading in the $z \to 0$ expansion). This implies that any solution with a specific boundary condition is *unique*. Indeed, we argued in Section 4.1.2 that there is no non-trivial normalizable solution in M_0. So in the cases of interest (no sources on M_0), $\phi_0 = 0$ identically. The matching condition between ϕ_0 and ϕ_1 then requires that $\phi_1(t_1 = 0, \vec{x}, z) = 0$. The most general normalizable solution on M_1 is

$$\phi_1^{norm}(t_1, \vec{x}, z) = e^{in\xi} \int \frac{d\omega}{2\pi} \frac{d^d k}{(2\pi)^d} \; e^{-i\omega t_1 + i\vec{k}\cdot\vec{x}} z^{\frac{d}{2}+1} \theta(-q^2) B(\omega, \vec{k}) J_\nu(|q|z). \tag{4.36}$$

Multiply by $z^{-\frac{d}{2}} e^{-in\xi - i\vec{k}'\cdot\vec{x}} J_\nu(|q'|z)$ with $q'^2 = -2\omega' n + \vec{k}'^2 < 0$ and integrate over $\vec{x}$ and z. We then find

$$0 = \int \frac{d\omega}{2\pi} \frac{d^d k}{(2\pi)^d} d^d x \; e^{i\vec{x}\cdot(\vec{k}-\vec{k}')} B(\omega, \vec{k}) \theta(-q^2) \Big(\int_0^\infty dz \; z J_\nu(|q|z) J_\nu(|q'|z) \Big) \tag{4.37}$$

The z-integral is elementary, equals $\frac{1}{|q|}\delta(|q|-|q'|)$, and this becomes

$$\begin{aligned} 0 &= \int \frac{d\omega}{2\pi}\frac{d^dk}{(2\pi)^d}d^dx\, e^{i\vec{x}\cdot(\vec{k}-\vec{k}')}B(\omega,\vec{k})\theta(-q^2)\frac{1}{|q'|}\delta(|q|-|q'|) && (4.38)\\ &= \frac{1}{n}\int\frac{d\omega}{2\pi}B(\omega,\vec{k}')\theta(2\omega n-\vec{k}'^2)\delta(\omega-\omega') && (4.39)\\ &= \frac{1}{2\pi n}B(\omega',\vec{k}')\theta(-q'^2). && (4.40)\end{aligned}$$

Thus, if $\phi_1(t,\vec{x},z)=0$ at some time, there is no non-trivial normalizable mode. This reasoning in fact applies for all segments of both contours in Fig. 4.1.

4.3.1 Bulk-Boundary Propagator and Time-ordered Correlator

Given the absence of a normalizable mode, any solution with sources that we find for the two contours in Fig. 4.1 is unique. In this subsection, we consider contour Fig. 4.1a, with segments M_0 ($\tau_0\in(-\infty,0]$), M_1 ($t_1\in[0,T]$), M_2 ($\tau_2\in[0,\infty)$). We place a single δ-function source at $\vec{x}=0, t_1=\hat{t}_1$ on M_1. From our discussions above, ϕ_1 must be of the form

$$\phi_{1,(n)}(t_1,\vec{x},z)=\frac{2}{\Gamma(\nu)}e^{in\xi}z^{1+d/2}\int\frac{d\omega}{2\pi}\frac{d^dk}{(2\pi)^d}\, e^{-i\omega(t_1-\hat{t}_1)+i\vec{k}\cdot\vec{x}}\left(\frac{q_\epsilon}{2}\right)^\nu K_\nu(q_\epsilon z). \tag{4.41}$$

as this satisfies $z^{-\Delta_-}\phi_{1,(n)}(t_1,\vec{x},z)\big|_{z\to0}=e^{in\xi}\delta(t_1-\hat{t}_1)\delta(\vec{x})$, and any ambiguity corresponds to normalizable modes, which we have argued are zero. Since there are no sources on M_2, ϕ_2 takes the form

$$\phi_{2,(n)}=\frac{2\pi i}{\Gamma(\nu)}e^{in\xi}z^{1+d/2}\int\frac{d\omega}{2\pi}\frac{d^dk}{(2\pi)^d}\, e^{-\omega(\tau+iT-i\hat{t}_1)+i\vec{k}\cdot\vec{x}}\theta(-q^2)\left(\frac{|q|}{2}\right)^\nu J_\nu(|q|z). \tag{4.42}$$

which has been deduced from the matching condition $\phi_1(t_1=T)=\phi_2(\tau=0)$ as follows. For any time $t_1>\hat{t}_1$, we can re-expand ϕ_1 in terms of J_ν's. In particular, at $t_1=T$, we should have

$$\int\frac{d\omega}{2\pi}\frac{d^dk}{(2\pi)^d}\, e^{-i\omega(T-\hat{t}_1)+i\vec{k}\cdot\vec{x}}q_\epsilon^\nu zK_\nu(q_\epsilon z)=\int\frac{d\omega}{2\pi}\frac{d^dk}{(2\pi)^d}\, e^{-i\omega(T-\hat{t}_1)+i\vec{k}\cdot\vec{x}}C(\omega,\vec{k})\theta(-q^2)zJ_\nu(|q|z) \tag{4.43}$$

for some $C(\omega,\vec{k})$. To find this coefficient we use the same trick as in the last subsection: multiply both sides by $e^{i\omega'(T-\hat{t}_1)-i\vec{k}'\vec{x}}J_\nu(|q'|z)$ with $q'^2=-2\omega' n+\vec{k}'^2<0$ and integrate over $\vec{x},z$. The right-hand side gives

$\frac{1}{2\pi n}\theta(-q'^2)C(\omega',\vec{k}')$, while the left-hand side can be computed using the following identity

$$\int_0^\infty K_\mu(at)J_\nu(bt)t^{\mu+\nu+1}dt = \frac{(2a)^\mu(2b)^\nu\Gamma(\mu+\nu+1)}{(a^2+b^2)^{\mu+\nu+1}},$$
$$Re(\nu+1) > Re(\mu),\ Re(a) > |Im(b)| \tag{4.44}$$

to give $\frac{i}{2n}|q'|^\nu$.

The bulk-boundary propagator is essentially identified with ϕ_1 itself: if we simply strip off the $e^{in\xi}$ factor, we can write

$$K_{n,n'}(t,\vec{x},z) = \delta_{n,n'}K_{(n)}(t,\vec{x},z) \tag{4.45}$$
$$K_{(n)}(t,\vec{x},z;\hat{t}) = \frac{2z^{1+d/2}}{\Gamma(\nu)}\int\frac{d\omega}{2\pi}\frac{d^dk}{(2\pi)^d}\ e^{-i\omega(t-\hat{t})+i\vec{k}\cdot\vec{x}}\left(\frac{q_\epsilon}{2}\right)^\nu K_\nu(q_\epsilon z). \tag{4.46}$$

As shown in Ref. [124] for example, this is closely related to the bulk-boundary propagator in AdS_{d+3}. Alternatively, we may perform the integration directly, following the analogous treatment in Ref. [30]. To do so, it is convenient to convert the ω-integral to an integration over $p = q_\epsilon$, and the contour in the p-plane is as shown in Fig. 4.2. Here though there is just one branch point (at $\omega = \vec{k}^2/2n - i\epsilon$) and the $i\epsilon$ tells us

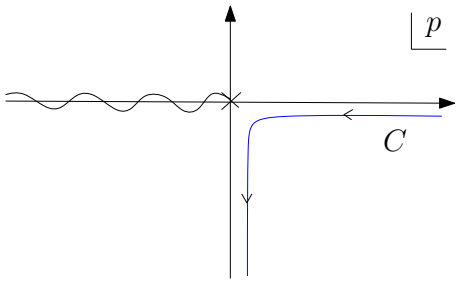

Figure 4.2: Contour of integration in the complex p-plane for the Lorentzian bulk-boundary propagator.

in which sense to traverse the cut. One arrives at

$$K_{(n)}(t,\vec{x},z;\hat{t}) = \theta(t_1-\hat{t}_1)\frac{1}{\pi^{d/2}\Gamma(\nu)}\left(\frac{n}{2i}\right)^{\Delta_+-1}\left(\frac{z}{t_1-\hat{t}_1}\right)^{\Delta_+}e^{in\frac{z^2+\vec{x}^2+i\epsilon}{2(t_1-\hat{t}_1)}} \tag{4.47}$$

where $\Delta_\pm = 1+d/2\pm\nu$.

The correlator is then identified with the z^{Δ_+} coefficient in the near boundary expansion of ϕ_1 (without the $e^{in\xi}$ factor)

$$\langle T\Big(\hat{\mathcal{O}}_{(n)}(\vec{x},t_1)\hat{\mathcal{O}}^\dagger_{(n)}(\vec{x}',t_1')\Big)\rangle = \frac{1}{\pi^{d/2}\Gamma(\nu)}\left(\frac{n}{2i}\right)^{\Delta_+-1}\frac{\theta(t_1-t_1')}{(t_1-t_1')^{\Delta_+}}e^{in\frac{(\vec{x}-\vec{x}')^2+i\epsilon}{2(t_1-t_1')}}. \tag{4.48}$$

4.3.2 Wightman function

The time-ordered correlator, as we have explained, contains a single temporal θ-function. It does not tell us about $\langle\hat{\mathcal{O}}(\vec{x},t_1)\hat{\mathcal{O}}^\dagger(\vec{x}',t_1')\rangle$ for $t_1' > t_1$. To find this 2-point function we work with the contour of Fig. 4.1b. Denote the segments by M_0 ($\tau_0 \in (-\infty,0]$), M_1 ($t_1 \in [0,T]$), M_2 ($t_2 \in [T,2T]$) and M_3 ($\tau_3 \in [0,\infty)$) as sketched in the figure. We place a δ-function source at $\vec{x}=0, t_1=\hat{t}_1$ on M_1 and nowhere else. The Wightman function is obtained then from ϕ_2, the field on M_2. Here $\phi_0=0$ and ϕ_1 remain the same as (4.41). Given experience from the last subsection, we can see immediately that ϕ_2 should be

$$\phi_{2,(n)} = \frac{2\pi i}{\Gamma(\nu)} e^{in\xi} z^{1+d/2} \int \frac{d\omega}{2\pi}\frac{d^dk}{(2\pi)^d}\; e^{-i\omega(2T-t_2-\hat{t}_1)+i\vec{k}\cdot\vec{x}} \left(\frac{|q|}{2}\right)^\nu \theta(-q^2) J_\nu(|q|z). \tag{4.49}$$

This has been determined by requiring the matching condition $\phi_1(t_1=T)=\phi_2(t_2=T)$. Notice the unusual $e^{+i\omega t_2+i\vec{k}\cdot\vec{x}}$ wave factor. It is related to the fact mentioned before that along this part of the contour, the metric has an extra minus sign in the $g_{t_2\xi}$ component.

It is now necessary to compute ϕ_2 in coordinate space. We make a change of variable $p=|q|=\sqrt{2\omega n-\vec{k}^2}$

$$\phi_2 = \frac{i}{n\Gamma(\nu)2^\nu} e^{in\xi} z^{1+d/2} \int_0^\infty dp\; e^{-ip^2(2T-t_2-\hat{t}_1)/2n} p^{\nu+1} J_\nu(pz) \int \frac{d^dk}{(2\pi)^d}\; e^{-ik^2(2T-t_2-\hat{t}_1)/2n} e^{i\vec{k}\cdot\vec{x}}. \tag{4.50}$$

We note that both integrals converge if $2T-t_2-\hat{t}_1 \to 2T-t_2-\hat{t}_1-i\epsilon$. The first integral is the standard integral involving Bessel functions, while the second one is just a Gaussian integral. The final result is

$$\phi_2 = e^{in\xi}\frac{1}{\pi^{d/2}\Gamma(\nu)}\left(\frac{n}{2i}\right)^{\Delta_+-1}\left(\frac{z}{\tilde{t}_2-\hat{t}_1-i\epsilon}\right)^{\Delta_+} e^{in\frac{z^2+\vec{x}^2}{2(\tilde{t}_2-\hat{t}_1-i\epsilon)}}. \tag{4.51}$$

where $\tilde{t}_2 = 2T-t_2$. Observe that ϕ_2 is closely related to the bulk-boundary propagator (4.47) except for the absence of the step function and a different $i\epsilon$ insertion, as expected.

The vacuum expectation value of $\hat{\mathcal{O}}(\tilde{t}_2,\vec{x})$ is

$$\langle\hat{\mathcal{O}}(\tilde{t}_2,\vec{x}) e^{i(\phi_{1(0)}\hat{\mathcal{O}}^\dagger+\bar{\phi}_{1(0)}\hat{\mathcal{O}})}\rangle = \frac{1}{\pi^{d/2}\Gamma(\nu)}\left(\frac{n}{2i}\right)^{\Delta_+-1}\int dt_1 d^dx' \frac{e^{in\frac{(\vec{x}-\vec{x}')^2}{2(\tilde{t}_2-t_1-i\epsilon)}}}{(\tilde{t}_2-t_1-i\epsilon)^{\Delta_+}}\phi_{1(0)}(t_1,\vec{x}'). \tag{4.52}$$

Taking a derivative with respect to $\phi_{1(0)}$ and setting the source to zero, we get the Wightman function

$$\langle\hat{\mathcal{O}}(\tilde{t}_2,\vec{x})\hat{\mathcal{O}}^\dagger(t_1,\vec{x}')\rangle = \frac{1}{\pi^{d/2}\Gamma(\nu)}\left(\frac{n}{2i}\right)^{\Delta_+-1}\frac{e^{in\frac{(\vec{x}-\vec{x}')^2}{2(\tilde{t}_2-t_1-i\epsilon)}}}{(\tilde{t}_2-t_1-i\epsilon)^{\Delta_+}} \tag{4.53}$$

Notice that $\hat{\mathcal{O}}^\dagger$ is always in the front of $\hat{\mathcal{O}}$ because t_1 is always the earlier contour time.

4.3.3 Thermal Correlator

Finally, we compute a thermal correlator by taking the time direction to be compact of period β.

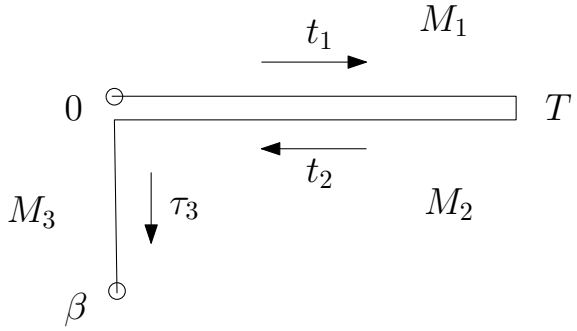

Figure 4.3: Thermal contour. Points with a circle are identified.

To compute the thermal time-ordered correlator and Wightman function, we consider the thermal contour shown in Fig. 4.3, where $t = 0$ and $t = -i\beta$ are identified. We place a δ-function source at $t_1 = \hat{t}_1, \vec{x} = 0$. Note that in contrast to the previous discussions, here there is no M_0 component of the contour. It is convenient in this context to write the general solution along M_1 in the form

$$\phi_1 = \frac{2e^{in\xi} z^{1+d/2}}{\Gamma(\nu)} \int \frac{d\omega}{2\pi} \frac{d^d k}{(2\pi)^d} \, e^{-i\omega(t_1-\hat{t}_1)+i\vec{k}\cdot\vec{x}} \Big(A(\omega,\vec{k}) \left(\frac{q_\epsilon}{2}\right)^\nu K_\nu(q_\epsilon z) + B(\omega,\vec{k}) \left(\frac{q_{-\epsilon}}{2}\right)^\nu K_\nu(q_{-\epsilon} z) \Big). \quad (4.54)$$

where $q_{-\epsilon} = \bar{q}_\epsilon = \sqrt{-2\omega n + \vec{k}^2 + i\epsilon}$. In order that this correspond to a δ-function source for $z \to 0$, we must have $A + B = 1$. (Furthermore, the case $B = -A$ corresponds to a normalizable mode.) Note that because of the condition on A, B, although A and B are not necessarily analytic functions, their sum is analytic. Thus for example, for any pole in A, there will be a corresponding pole in B with opposite residue. All of their poles will contribute opposite residues and cancel out each other in the limit $\epsilon \to 0$. In (4.54), the first term has support for $t_1 > \hat{t}_1$, while the second has support for $t_1 < \hat{t}_1$.

The matching condition at (M_1, M_2) and (M_2, M_3) intersections imply that

$$\phi_2 = \frac{2\pi i e^{in\xi} z^{1+d/2}}{\Gamma(\nu)} \int \frac{d\omega}{2\pi} \frac{d^d k}{(2\pi)^d} \, e^{-i\omega(2T-t_2-\hat{t}_1)+i\vec{k}\cdot\vec{x}} A(\omega,\vec{k}) \left(\frac{|q|}{2}\right)^\nu J_\nu(|q|z)\theta(-q^2) \quad (4.55)$$

$$\phi_3 = \frac{2\pi i e^{in\xi} z^{1+d/2}}{\Gamma(\nu)} \int \frac{d\omega}{2\pi} \frac{d^d k}{(2\pi)^d} \, e^{-\omega(\tau_3-i\hat{t}_1)+i\vec{k}\cdot\vec{x}} A(\omega,\vec{k}) \left(\frac{|q|}{2}\right)^\nu J_\nu(|q|z)\theta(-q^2) \quad (4.56)$$

The thermal condition $\phi_1(t_1 = 0) = \phi_3(\tau_3 = \beta)$ along with $A + B = 1$ then gives

$$A = \frac{1}{1 - e^{-\beta\omega}}, \qquad B = \frac{1}{1 - e^{+\beta\omega}}. \quad (4.57)$$

As usual, the time-ordered propagator is the coefficient of z^{Δ_+} in the small z expansion of ϕ_1 (without the $e^{in\xi}$ factor). Hence we get[2]

$$\langle T\Big(\hat{O}(x)\hat{O}^\dagger(x')\Big)\rangle \sim \int \frac{d\omega}{2\pi}\frac{d^dk}{(2\pi)^d}\; e^{-i\omega(t-t')+i\vec{k}\cdot(\vec{x}-\vec{x}')}\Big(\frac{(-2\omega n+\vec{k}^2-i\epsilon)^\nu}{1-e^{-\beta\omega}}+\frac{(-2\omega n+\vec{k}^2+i\epsilon)^\nu}{1-e^{\beta\omega}}\Big). \quad (4.58)$$

Note that this has the expected form for a thermal correlator[30]

$$\langle T\Big(\hat{O}(x)\hat{O}^\dagger(x')\Big)\rangle = -N(\omega)\Delta_A(\omega,\vec{k})+(1+N(\omega))\Delta_R(\omega,\vec{k}) \quad (4.59)$$

In the present notation, $N=-B$. We can also write this as the zero temperature result plus a finite temperature piece:

$$\langle T\Big(\hat{O}(x)\hat{O}^\dagger(x')\Big)\rangle \sim \int \frac{d\omega}{2\pi}\frac{d^dk}{(2\pi)^d}\; e^{-i\omega(t-t')+i\vec{k}\cdot(\vec{x}-\vec{x}')}\left[q_\epsilon^{2\nu}-\frac{1}{1-e^{\beta\omega}}(q_\epsilon^{2\nu}-q_{-\epsilon}^{2\nu})\right] \quad (4.60)$$

The Wightman function can also be read off from ϕ_2

$$\langle\hat{\mathcal{O}}(x)\hat{\mathcal{O}}^\dagger(x')\rangle \sim i\pi\int \frac{d\omega}{2\pi}\frac{d^dk}{(2\pi)^d}\; e^{-i\omega(t-t'-i\epsilon)+i\vec{k}(\vec{x}-\vec{x}')}\frac{(2\omega n-\vec{k}^2)^\nu}{1-e^{-\beta\omega}}\theta(2\omega n-\vec{k}^2) \quad (4.61)$$

[2]For integer ν, there is an extra logarithmic factor, namely $q_{\pm\epsilon}^{2\nu}$ is replaced by $q_{\pm\epsilon}^{2\nu}\ln q_{\pm\epsilon}^2$.

Chapter 5

Fermions and the Sch/nrCFT Correspondence

In the present chapter, we investigate fermionic operators in the vacuum Schrödinger geometries [38]. Although the problem of finite density is of most direct physical interest, the system poses some interesting problems even in the 'vacuum' geometry that possesses the full Schrödinger isometry. We believe that these issues should be sorted out before the finite temperature and density cases can be fully appreciated, and in fact it is possible to do so with complete precision as exact analytic solutions exist, as they do in the relativistic case [33, 34, 35, 36].

The system is, however, significantly different from its relativistic counterpart, as might be expected from the more rich representation theory. Nevertheless, we are able to show that a sensible Dirichlet problem exists for fermions. As in the relativistic case, the bulk on-shell action vanishes, and the on-shell action is determined entirely by boundary terms. These boundary terms are determined by the requirements of a sensible Dirichlet canonical structure and finiteness. In particular, we explain the structure of possible boundary terms (which are required to preserve the Galilean symmetry of the regulated boundary theory) and show that the on-shell action is finite with the inclusion of a finite number of local boundary counter terms.

5.1 Background

For convenience, let's rewrite the Schrödinger geometry

$$ds^2 = \frac{L^2}{z^2}\left(-\frac{\beta^2}{z^2}dt^2 + 2dtd\xi + d\vec{x}^2 + dz^2\right) \tag{5.1}$$

Although we are primarily interested in Euclidean correlator, we will be working on the Lorentzian geometry, as the former can be easily obtained by a Wick rotation. A convenient basis of orthonormalized ($\langle e^a, e^b\rangle = \eta^{ab}$) one-forms is

$$e^0 = \frac{L}{z}\left[\frac{z}{\beta}d\xi - \frac{\beta}{z}dt\right], \quad e^v = \frac{L}{\beta}d\xi, \quad e^r = \frac{L}{z}dz, \quad e^i = \frac{L}{z}dx^i \tag{5.2}$$

which are dual to the orthonormal basis vectors

$$e_0 = -\frac{z}{L}\frac{z}{\beta}\partial_t, \quad e_v = \frac{z}{L}\left[\frac{z}{\beta}\partial_t + \frac{\beta}{z}\partial_\xi\right], \quad e_r = \frac{z}{L}\partial_z, \quad e_i = \frac{z}{L}\partial_i \tag{5.3}$$

The Levi-Civita connection has non-zero components

$$\omega^0{}_r = \frac{1}{L}\left(e^v - 2e^0\right), \quad \omega^0{}_v = -\frac{1}{L}e^r, \quad \omega^v{}_r = -\frac{1}{L}e^0, \quad \omega^i{}_r = -\frac{1}{L}e^i \tag{5.4}$$

Correspondingly, the non-zero components of the Christoffel symbols are

$$\Gamma^z_{zz} = -\frac{1}{z} = \Gamma^\xi_{z\xi} = \Gamma^t_{zt} \tag{5.5}$$

$$\Gamma^i_{zj} = -\frac{1}{z}\delta^i_j, \quad \Gamma^z_{ij} = \frac{1}{z}\delta_{ij} \tag{5.6}$$

$$\Gamma^z_{t\xi} = \frac{1}{z}, \quad \Gamma^z_{tt} = -2\frac{\beta^2}{z^3}, \quad \Gamma^\xi_{zt} = \frac{\beta^2}{z^3} \tag{5.7}$$

5.1.1 Dirac Operator

The spin connection in the spinor representation is obtained by writing $\omega^a{}_b = \omega^A (T^A)^a{}_b$ and replacing the generators by those in the spinor representation. Since the local group is $SO(d+2,1)$, the index A can be thought of as an antisymmetric pair of vector indices. We will use a basis for the Clifford algebra

$$\{\gamma^a, \gamma^b\} = 2\eta^{ab} \tag{5.8}$$

where $a, b, ... = r, 0, v, i$. It is always possible to take a basis in which $\gamma^v\gamma^0$ and γ^r are *Hermitian*.[1] For example, a convenient basis is of the form

$$\gamma^0 = -i\sigma_2 \otimes 1, \quad \gamma^v = -\sigma_1 \otimes 1, \quad \gamma^i = \sigma_3 \otimes \tau^i, \quad \gamma^r = \sigma_3 \otimes \tau^r \tag{5.9}$$

where τ^i are a representation of $C\ell(d)$. We have $(T^{[ab]})^\alpha{}_\beta = -\frac{i}{4}([\gamma^a, \gamma^b])^\alpha{}_\beta$. Thus, the spin connection takes the form

$$\omega^\alpha{}_\beta \sim \omega^a{}_b([\gamma_a, \gamma^b])^\alpha{}_\beta. \tag{5.10}$$

[1] In particular, to be definite, we will take γ^0 to be anti-Hermitian and γ^v to be Hermitian.

The γ's are numerical matrices and their indices are those of the local frame, raised and lowered with η. The Dirac operator in general may be written

$$\not{D} = \gamma^c \left(e_c + \frac{1}{4} e_c^\mu \omega_\mu{}^a{}_b (\gamma_a \gamma^b) \right). \tag{5.11}$$

It will be convenient to split off the radial part

$$\not{D} = z \left[\gamma^r \partial_z + \gamma^i \partial_i \right] + \frac{z^2}{\beta} (\gamma^v - \gamma^0) \partial_t + \beta \gamma^v \partial_\xi - \frac{1}{2} \gamma^r \left[(d+2) 1 - \gamma_v \gamma_0 \right]. \tag{5.12}$$

The problem can be organized by defining projection operators

$$P_\pm = \frac{1 \pm \gamma^r}{2}, \quad Q_\pm = \frac{1 \pm \gamma^v \gamma^0}{2} \tag{5.13}$$

These commute with each other, so we can simultaneously diagonalize γ^r and $\gamma^v \gamma^0$. We note that these projection operators appear here naturally because *they commute with* $spin(d) \subset spin(d+2,1)$. Thus, we can be sure that full $spin(d)$ representations occur for each of the four projection sectors.

Noting then that we can rewrite

$$\gamma^v - \gamma^0 = -2 Q_+ \gamma^0 = -2 \gamma^0 Q_-, \quad \gamma^v = (Q_- - Q_+) \gamma^0 = \gamma^0 (Q_+ - Q_-) \tag{5.14}$$

the Dirac operator becomes

$$\not{D} = z \left[(P_+ - P_-) \partial_z + \gamma^i \partial_i \right] - 2 \frac{z^2}{\beta} \gamma^0 Q_- \partial_t + \beta \gamma^0 (Q_+ - Q_-) \partial_\xi - \frac{1}{2} (P_+ - P_-) \left[(d+2) 1 + (Q_+ - Q_-) \right] \tag{5.15}$$

Before proceeding with the solution of the Dirac equation, we will consider some details of the bulk representation of the Schrödinger algebra that will be important in interpreting the solutions.

5.1.2 The Schrödinger Algebra

In a local frame in the bulk, a field will carry a representation of $spin(d+2,1)$. Globally the geometry has isometries given by the Killing vectors given in the previous chapter

$$\begin{aligned} N &= \partial_\xi && (5.16)\\ D &= 2t\partial_t + \vec{x}\cdot\vec{\partial} + z\partial_z && (5.17)\\ H &= \partial_t && (5.18)\\ C &= t^2\partial_t + t\vec{x}\cdot\vec{\partial} - \frac{1}{2}\vec{x}^2\partial_\xi + tz\partial_z - \frac{1}{2}z^2\partial_\xi && (5.19)\\ M_{ij} &= x_i\partial_j - x_j\partial_i && (5.20)\\ \vec{K} &= -t\vec{\partial} + \vec{x}\partial_\xi && (5.21)\\ \vec{P} &= \vec{\partial} && (5.22) \end{aligned}$$

where we have written explicitly the bulk representation on functions. We note that M_{ij} generate $spin(d)$ and that $\{D, H, C\}$ together generate $sl(2,\mathbb{R})$. Since $sl(2,\mathbb{R}) \sim so(2,1)$, we recognize $spin(d) \oplus sl(2,\mathbb{R}) \subset spin(d+2,1)$. Thus the representation theory can be understood quite simply in terms of highest weight modules. It is traditional to take D diagonal with eigenvalues referred to generically as Δ, and since N is central, it can be diagonalized as well, and in fact there are super-selection sectors labelled by the eigenvalue of N

$$\Psi(z,t,\xi,\vec{x}) = e^{in\xi}\Psi(z,t,\vec{x}). \tag{5.23}$$

We refer to such functions as being equivariant.[2] Highest weight states of fixed n, Δ correspond directly to quasi-primary operators $\Psi(t=0,\vec{x}=0)$ in the boundary theory (at $z=0$).[3]

However, for a non-trivial representation, we expect that the generators are modified accordingly, and this structure is not complete. For example, we know (and we will verify below) that the $spin(d)$ generator should be replaced by

$$M_{ij} = x_i\partial_j - x_j\partial_i + \Sigma_{ij} \tag{5.24}$$

when acting on spinor fields. To see how this comes about, we can consider doing Schrödinger transformations

[2] According to [126], the bulk spacetime should be thought of as the total space of a fibre bundle over non-relativistic spacetime, with ξ the fibre coordinate. In this sense, eq. (5.23) is interpreted as meaning that the field is a section of the associated bundle of charge n. See also Refs.[127, 128].

[3] Here, by boundary we will simply mean the limit $z \to 0$. Further discussion may be found in a later section.

on the bulk spinor field. The spinor will transform by the Lie derivative[129]

$$\Psi \to \mathcal{L}_\xi \Psi = \nabla_\xi \Psi + \frac{1}{8}\langle \nabla_{e_a}\xi, e_b\rangle [\gamma^a, \gamma^b]\Psi \tag{5.25}$$

In this way, $\mathcal{L}_\xi$ commutes with the Dirac operator, at least as long as ξ is a Killing vector.

Let us warm up by evaluating the Lie derivative for the $spin(d)$ Killing vector

$$\xi_M = 2x_j \Theta^{ji}\partial_i \tag{5.26}$$

where Θ is antisymmetric. In this case, we compute

$$\begin{aligned} \nabla_{\xi_M}\Psi &= 2x_j\Theta^{ji}\partial_i\Psi - \frac{1}{z}x_j\Theta^{ji}\gamma_i\gamma^r\Psi & (5.27)\\ \langle \nabla_{e_a}\xi_M, e_b\rangle [\gamma^a,\gamma^b]\Psi &= 4\Theta_{ji}\left[\gamma^j\gamma^i + 2\frac{1}{z}x^j\gamma^i\gamma^r\right]\Psi & (5.28)\end{aligned}$$

This result does indeed correspond to (5.24). Now for ξ_K, we have

$$\xi_K = -t\vec{K}\cdot\vec{\partial} + (\vec{x}\cdot\vec{K})\partial_\xi \tag{5.29}$$

and we find

$$\mathcal{L}_K\Psi = (\vec{x}\cdot\vec{K})\partial_\xi\Psi - t\vec{K}\cdot\vec{\partial}\Psi + \frac{1}{2\beta}z(\gamma^0-\gamma^v)K_i\gamma^i\Psi \tag{5.30}$$

By similar computations, we conclude that the representation on spinors is

$$\begin{aligned} M_{ij} &= x_i\partial_j - x_j\partial_i + \frac{1}{4}[\gamma_i,\gamma_j] \equiv x_i\partial_j - x_j\partial_i + i\Sigma_{ij} & (5.31)\\ K_i &= -t\partial_i + x_i\partial_\xi + \frac{1}{2}\frac{z}{\beta}(\gamma^0-\gamma^v)\gamma_i \equiv -t\partial_i + x_i\partial_\xi + \kappa_i & (5.32)\\ C &= tz\partial_z + t\vec{x}\cdot\vec{\partial} + t^2\partial_t - \frac{1}{2}(\vec{x}^2+z^2)\partial_\xi + \hat{c} & (5.33)\end{aligned}$$

where $\hat{c} = +\frac{1}{2}\frac{z}{\beta}(\not{x} + z\gamma^r)(\gamma^0-\gamma^v)$. Notice that both κ_i and $\hat{c}$ are nilpotent. D, H, P_i are unmodified. The highest weight states of a Schrödinger multiplet are annihilated by both C and K_i, and so we see here that these conditions apparently do not act diagonally on $spin(d)$ components of the bulk Dirac spinor, but mix them at a generic point in the bulk. However, as we will see, the on-shell Dirac spinor is constructed from chiral spinors that are Q-chiral and as we show in detail in the appendix, $\hat{c}$ and κ are such that K_i and C act diagonally on these.

5.2 Solutions of the Dirac Equation

Now we write spinors as linear combinations of doubly chiral spinors

$$\Psi(z,t,\xi,\vec{x}) = e^{in\xi}\sum_{\varepsilon_r,\varepsilon_\ell}\int\frac{d\omega}{2\pi}\int\frac{d^dk}{(2\pi)^d}e^{i\vec{k}\cdot\vec{x}}e^{-i\omega t}\psi^{\varepsilon_r,\varepsilon_l}_{n,\omega,\vec{k}}(z) \tag{5.34}$$

where

$$\gamma^r\psi^{\varepsilon_r,\varepsilon_l}_{n,\omega,\vec{k}}(z) = \varepsilon_r\psi^{\varepsilon_r,\varepsilon_l}_{n,\omega,\vec{k}}(z) \tag{5.35}$$

$$\gamma^v\gamma^0\psi^{\varepsilon_r,\varepsilon_l}_{n,\omega,\vec{k}}(z) = \varepsilon_l\psi^{\varepsilon_r,\varepsilon_l}_{n,\omega,\vec{k}}(z) \tag{5.36}$$

and $\varepsilon_r,\varepsilon_l = \pm 1$. By projecting the Dirac equation with $P_\pm$ and $Q_\pm$, we find four equations (we drop the subscripts on ψ for brevity)

$$\left(z\partial_z - \frac{1}{2}(d+3) + m_0\right)\gamma^0\psi^{-,+} + iz\not{k}\gamma^0\psi^{+,+} + \frac{i}{\beta}(2\omega z^2 - n\beta^2)\psi^{+,-} = 0 \tag{5.37}$$

$$\left(z\partial_z - \frac{1}{2}(d+1) - m_0\right)\psi^{+,-} + iz\not{k}\psi^{-,-} + in\beta\gamma^0\psi^{-,+} = 0 \tag{5.38}$$

$$\left(z\partial_z - \frac{1}{2}(d+3) - m_0\right)\gamma^0\psi^{+,+} - iz\not{k}\gamma^0\psi^{-,+} - \frac{i}{\beta}(2\omega z^2 - n\beta^2)\psi^{-,-} = 0 \tag{5.39}$$

$$\left(z\partial_z - \frac{1}{2}(d+1) + m_0\right)\psi^{-,-} - iz\not{k}\psi^{+,-} - in\beta\gamma^0\psi^{+,+} = 0 \tag{5.40}$$

Note that we have used the notation $\not{k}$ to emphasize that this is the quantity in the trivial metric. The invariant is $\not{k} = \gamma^a e^i_a k_i$, and in the Schrödinger metric, this evaluates to $\not{k} = \frac{z}{L}\not{k}$. This accounts for the single powers of z accompanying $\not{k}$; this will be of additional importance later in the context of boundary renormalization.

It is not difficult to disentangle the Dirac equations, and we find in particular that

$$\left[z^2\partial_z^2 - (d+1)z\partial_z + \left(\frac{d}{2}+1\right)^2 - \mu^2_{\varepsilon_r} - q^2z^2\right]\psi^{\varepsilon_r,-} = 0 \tag{5.41}$$

where

$$\mu_{\varepsilon_r} = \sqrt{\left(\frac{1}{2} - \varepsilon_r m_0\right)^2 + n^2\beta^2} \tag{5.42}$$

and

$$q^2 = \vec{k}^2 - 2n\omega \tag{5.43}$$

In this paper, we consider only the case $n \neq 0$. We note that q^2 appears naturally, as it is the Fourier

transform of the Galilean-invariant Schrödinger operator $\mathcal{S} = i\partial_t - \frac{1}{2n}\vec{\nabla}^2$. In particular, we note that when acting on equivariants

$$[K_i, \mathcal{S}] = 0 \tag{5.44}$$

This fact will play a central role later in our discussion of renormalizability.

Thus we have

$$\psi^{\varepsilon_r,-}(\vec{k},\omega,z) = z^{1+d/2} K_{\mu_{\varepsilon_r}}(qz)\mathbf{u}_{\varepsilon_r}(\vec{k},\omega) \tag{5.45}$$

where $\mathbf{u}_\pm$ are independent doubly chiral $spin(d)$ spinors that satisfy

$$Q_+\mathbf{u}_\pm = 0, \qquad \gamma^r\mathbf{u}_\pm = \pm\mathbf{u}_\pm \tag{5.46}$$

Since we are interested in Euclidean correlator, we have dropped the solution proportional to $I_{\mu_{\varepsilon_r}}(qz)$ by requiring regularity at large z. Substituting these solutions back into the Dirac equations leads algebraically to the other components of the Dirac spinor

$$\psi^{\pm,+} \quad = \quad \pm\frac{i}{n\beta} z^{1+d/2}\gamma^0 \left[\left(qzK'_{\mu_\mp}(qz) + \left(\frac{1}{2} \pm m_0\right) K_{\mu_\mp}(qz)\right)\mathbf{u}_\mp(\vec{k},\omega) \mp izK_{\mu_\pm}(qz)\not{k}\mathbf{u}_\pm(\vec{k},\omega)\right]$$

The general on-shell field then is

$$\Psi = -z^{1+d/2}\sum_{\varepsilon_r}\left[\frac{i\varepsilon_r}{n\beta}\left(\frac{1}{2} - \varepsilon_r m_0 - i\varepsilon_r n\beta\gamma^0\right)K_{\mu_{\varepsilon_r}}(qz) + \frac{i\varepsilon_r}{n\beta}qzK'_{\mu_{\varepsilon_r}}(qz) + \frac{z}{n\beta}K_{\mu_{\varepsilon_r}}(qz)\not{k}\right]\gamma^0\mathbf{u}_{\varepsilon_r} \tag{5.47}$$

From this general solution, we see that the leading terms at the boundary are

$$\Psi \sim \sum_{\varepsilon_r} z^{\Delta^-_{\varepsilon_r}} \frac{\Gamma(\mu_{\varepsilon_r})}{2}\left(\frac{q}{2}\right)^{-\mu_{\varepsilon_r}} X^{\varepsilon_r}_{-(0)}\mathbf{u}_{\varepsilon_r} + \dots \tag{5.48}$$

where $X^{\varepsilon_r}_{-(0)} \equiv 1 - \frac{i\varepsilon_r}{n\beta}(\frac{1}{2} - \varepsilon_r m_0 - \mu_{\varepsilon_r})\gamma^0$ and where

$$\Delta^\pm_{\varepsilon_r} = 1 + \frac{d}{2} \pm \mu_{\varepsilon_r}, \tag{5.49}$$

We make several comments:

- For generic bulk mass, the two dimensions $\Delta^-_{\varepsilon_r}$ are irrationally related. Thus $\mathbf{u}_+$ and $\mathbf{u}_-$ must be taken as independent sources. The only counter-example (for $n \neq 0$) is if the bulk mass vanishes, in which case $\mu_+ = \mu_-$ and $\Delta^-_+ = \Delta^-_- \equiv \Delta^-$. Thus the massless case is special, in that the eigenvalues

of D are degenerate. One can show however that in either case, $\mathbf{u}_\pm$ transform separately under the Schrödinger algebra.

- More precisely, the coefficient of the leading singularity is of the form $X^{\varepsilon_r}_{-(0)}\mathbf{u}_{\varepsilon_r}$ and is not chiral. We note though that the $X^{\varepsilon_r}_{-(0)}$ are *constant* matrices and can be absorbed (by a basis change) into the definition of boundary operators.

- The dependence on $\not{k}$ is subleading in the near-boundary ($z \to 0$) expansion, and is associated with the *odd* powers of z.

- The general solution is obtained by specifying two $spin(d)$ spinors $\mathbf{u}_\pm$ that are Q-chiral ($Q_+\mathbf{u}_\pm = 0$). Thus the Dirac equation has eliminated half of the degrees of freedom, as expected.

- The Schrödinger covariance of this expression is not manifest as written. To see this, consider the symplectic 1-form

$$\alpha = -idx^\mu \otimes \partial_\mu \tag{5.50}$$

which when acting on plane waves gives

$$\alpha = -idz \otimes \partial_z + (nd\xi - \omega dt + \vec{k} \cdot d\vec{x}) \tag{5.51}$$

The scalar Lagrangian, for example, can be written

$$S_{scalar} \sim \int \sqrt{-g}\langle\alpha(\phi), \alpha(\phi)\rangle = -\int \sqrt{-g}\phi^\dagger \Delta\phi \tag{5.52}$$

For fermions, we replace the exterior algebra by the Clifford algebra, and hence we obtain

$$\alpha \to -i\frac{z}{L}\gamma^r\partial_z + \frac{n\beta}{L}\gamma^v + \omega\frac{z^2}{L\beta}(\gamma^0 - \gamma^v) + \frac{z}{L}\not{k} \tag{5.53}$$

This of course is the quantity appearing in the Dirac operator, apart from the spin connection terms. What we learn from this is that the $\not{k}$ term should really be grouped with

$$\mathcal{Q} = z\not{k} + n\beta\gamma^v + 2\omega\frac{z^2}{\beta}\gamma^0 Q_- \tag{5.54}$$

In particular, this combination is Galilean invariant, $[K_i, \mathcal{Q}] = 0$, and also $[D, \mathcal{Q}] = 0$. (Later, it will

play a central role in the renormalizability of the theory.) We also note that

$$\mathcal{Q}^2 = z^2\mathcal{S} + n^2\beta^2 \tag{5.55}$$

which is the scalar invariant noted above, where $\mathcal{S} = q^2 = \vec{k}^2 - 2n\omega$.

Furthermore, when acting on the chiral spinors $\gamma^0\mathbf{u}_\pm$, this simplifies to

$$\mathcal{Q}\gamma^0\mathbf{u}_\pm = n\beta\left(\gamma^0 + \frac{z\not{k}}{n\beta}\right)\gamma^0\mathbf{u}_\pm \tag{5.56}$$

and thus the on-shell spinor can be rewritten

$$\Psi = -\frac{i}{n\beta}z^{1+d/2}\sum_{\varepsilon_r}\left[\varepsilon_r qz K'_{\mu_{\varepsilon_r}}(qz) - (m_0 - \varepsilon_r/2)K_{\mu_{\varepsilon_r}}(qz) - iK_{\mu_{\varepsilon_r}}(qz)\mathcal{Q}\right]\gamma^0\mathbf{u}_{\varepsilon_r} \tag{5.57}$$

We note that $\mathbf{v}_{\varepsilon_r} \equiv \gamma^0\mathbf{u}_{\varepsilon_r}$ are chiral, with $Q_-\mathbf{v}_{\varepsilon_r} = 0$. We note though that the individual pieces of $\mathcal{Q}$ come in with different powers of z, and so going to the boundary is somewhat subtle. What we must do is understand how the generators of the Schrödinger algebra act on the terms in the expansion of the field. This is explained in detail in the Appendix.

5.3 Variational Principle and Boundary Renormalization

As in the relativistic case [33, 34, 35, 36], we need to add a boundary term to the Dirac action, as the bulk part of the Dirac action vanishes on-shell. This boundary term serves to give the proper Dirichlet boundary condition and simultaneously make the on-shell action finite. Since in the variational principle the field variations are off-shell, first of all we have to state clearly what we mean by an off-shell spinor. The on-shell solution (5.57) suggests that an off-shell spinor should have the same z expansion, except that the coefficients are in general full unconstrained Dirac spinors. This off-shell spinor obviously carries a Schrödinger representation through (5.31)-(5.33). However, as established in the appendix C, this representation is reducible. Hence, it is natural that we define the off-shell spinor to be an irreducible representation that encompasses all vacuum solutions (5.57). According to (C.19), it takes the form

$$\Psi = \sum_{\varepsilon_r}\left[z^{\Delta^-_{-\varepsilon_r}}\sum_{k=0}^{\infty}z^{2k}\left(\rho^{\varepsilon_r}_{(2k)} + \mathcal{Q}\rho^{\varepsilon_r}_{(2k+1)}\right) + z^{\Delta^+_{-\varepsilon_r}}\sum_{k=0}^{\infty}z^{2k}\left(\chi^{\varepsilon_r}_{(2k)} + \mathcal{Q}\chi^{\varepsilon_r}_{(2k+1)}\right)\right] \tag{5.58}$$

where $\mathcal{Q}$ is given by (5.54) and

$$\gamma^r \rho^{\varepsilon_r}_{(m)} = \varepsilon_r \rho^{\varepsilon_r}_{(m)}, \qquad Q_- \rho^{\varepsilon_r}_{(m)} = 0 \tag{5.59}$$

similarly for χ.

By comparison to the on-shell solution, one can deduce the on-shell relationship of $\rho^{\varepsilon_r}_{(m)}$ and $\chi^{\varepsilon_r}_{(m)}$ to the independent quantities $\rho^{\varepsilon_r}_{(0)} \sim \mathbf{u}_{\varepsilon_r}$

$$\rho^{\varepsilon_r}_{(2k)} = -ix^{\varepsilon_r}_{-(2k)} \rho^{\varepsilon_r}_{(2k+1)} = \frac{x^{\varepsilon_r}_{-(2k)}}{x^{\varepsilon_r}_{-(0)}} \frac{\Gamma(1-\mu_{-\varepsilon_r})}{k!\Gamma(k+1-\mu_{-\varepsilon_r})} \left(\frac{q}{2}\right)^{2k} \rho^{\varepsilon_r}_{(0)} \tag{5.60}$$

$$\chi^{\varepsilon_r}_{(2k)} = -ix^{\varepsilon_r}_{+(2k)} \chi^{\varepsilon_r}_{(2k+1)} = -\frac{x^{\varepsilon_r}_{+(2k)}}{x^{\varepsilon_r}_{-(0)}} \frac{\Gamma(1-\mu_{-\varepsilon_r})}{k!\Gamma(k+1+\mu_{-\varepsilon_r})} \left(\frac{q}{2}\right)^{2k+2\mu_{-\varepsilon_r}} \rho^{\varepsilon_r}_{(0)}, \tag{5.61}$$

where $x^{\varepsilon_r}_{\pm(2k)} = \varepsilon_r(\frac{1}{2} + \varepsilon_r m_0 \pm \mu_{-\varepsilon_r} + 2k)$.

As is well known, the bulk part of the Dirac action evaluates to zero on the equations of motion. The on-shell action is determined entirely by the boundary term. The renormalized Dirac action must be of the form

$$S_{Lor} = \int_M d^{d+3}x\sqrt{-g}\ \overline{\Psi} i(\not{D} - m_0)\Psi + \frac{1}{L^2}\int_{\partial M} dt\ d\xi\ d^dx\sqrt{\gamma}\ e^z_r \overline{\Psi} T \Psi \tag{5.62}$$

for some matrix T, which must respect the symmetries of the boundary theory. Given that

$$\Psi(z,t,\xi,\vec{x}) = e^{in\xi}\Psi(z,t,\vec{x}) \tag{5.63}$$

the action reduces to

$$R\int d^{d+1}x \int dz\sqrt{-g}\ \overline{\Psi} i(\not{D}_n - m_0)\Psi + R\int dt\ d^dx\sqrt{\gamma}\ z^{-d-2}\ \overline{\Psi} T \Psi \tag{5.64}$$

where γ denotes the spatial induced d-metric of the boundary (which in our case is flat). We absorb this overall factor of R into the normalization. We vary the action subject to the vanishing of the variation of the source. Given our choice of action, we find

$$\delta S = \int \bar{\Psi}(i\gamma^r + T)\delta\Psi + \int \delta\bar{\Psi} T \Psi \tag{5.65}$$

A proper variational principle is obtained by requiring that terms involving $\delta\chi$ not appear in this expression. This will force the variational principle to give the correct Dirichlet condition $\delta\rho = 0$ on the boundary. In addition to this requirement, the resulting on-shell action must be made finite by the addition of suitable boundary counter-terms. As is customary, we will use minimal subtraction. By suitable, we mean any

term that respects the symmetry of the regulated boundary theory. In the case of AdS, the boundary counterterms are Poincaré invariant, which is the symmetry respected by the regulator. In our case, we expect the counterterms to be Galilean invariant. Since these counterterms are all written in terms of the boundary values of bulk fields, upon which the Schrödinger transformations act in the prescribed way, it is appropriate to write the boundary counterterms as boundary values of bulk-invariant terms (that is, using the bulk metric for contractions and the bulk realization of the symmetry generators).

Requiring the boundary term to be Galilean invariant, T has to be written in terms of operators that commute with the Galilean generators, in particular the K_i. Careful consideration of this problem reveals that such invariants may be constructed out of P_{ε_r}, $\gamma^0 Q_-$ and $\mathcal{Q}$ and thus the most general boundary term can be written as (here $L = \mathcal{Q}^2/n^2\beta^2$)[4]

$$T = \sum_{\varepsilon_r} \left[a_{\varepsilon_r}(L) + b_{\varepsilon_r}(L)\frac{i\mathcal{Q}}{n\beta} + \left[c_{\varepsilon_r}(L) + d_{\varepsilon_r}(L)\frac{i\mathcal{Q}}{n\beta}\right]\gamma^0 Q_- \right] P_{\varepsilon_r} \tag{5.66}$$

where $a_{\varepsilon_r}(L), ...$ are functions to be determined. Although we have written the coefficient functions as functions of $\mathcal{Q}^2 \sim L$ for notational brevity, since N is central and the fields are equivariant, this could just as well be replaced by $z^2\mathcal{S} = z^2 q^2$.

This form for T and the field written in the form (5.57) is most convenient to discuss the renormalizability of the theory – it organizes the counterterms in an invariant fashion. What is more complicated here, compared to the relativistic case, is that this organization is not homogeneous in powers of z. It is easy to see in this form however how the renormalization will work – since $\mathcal{Q}^2 \sim L$, we can regard T as an expansion in powers of $\mathcal{Q}$ (rather than z). At any given order, canceling divergences will correspond to conditions on the Taylor coefficients of the functions $a_{\varepsilon_r(L)}, ...$ around $L = 1$. Depending on the values of various parameters (m_o, n, ...), we can terminate the Taylor expansion at some order, as all further contributions to the action will be zero when the cutoff is removed. It remains then to demonstrate that the conditions on the Taylor coefficients can be consistently solved to remove all divergences. We will not construct a general proof, and in fact will work just at lowest order. Experience with these manipulations suggests that no problems will be encountered at higher orders.

Given the form for T, we consider the variational problem; this will place conditions on the lowest order Taylor coefficients of the functions in T. We write (5.65) in terms of $\delta\rho^{\varepsilon_r}_{(m)}$ and $\delta\chi^{\varepsilon_r}_{(m)}$ and their conjugates. Due to the fact that $\mu_- - \mu_+ < 1$ for $n > 0$, the only terms that possibly contain $\delta\chi^{\varepsilon_r}_{(m)}$ are the finite term

[4] the similar expression for AdS would be $\sum_{\varepsilon_r}(a_{\varepsilon_r}(q^2) + \not{k}\, b_{\varepsilon_r}(q^2))P_{\varepsilon_r}$, where P_{ε_r} is the projector along the radial direction.

(z^0 power), which evaluate to

$$(\rho^{\varepsilon_r}_{(0)})^\dagger \delta\chi^{\varepsilon_r}_{(0)} \left[-ib_{\varepsilon_r} - \frac{in\beta}{x^{\varepsilon_r}_{-(0)}}(a_{\varepsilon_r} + i\varepsilon_r) \right] + n\beta(\rho^{\varepsilon_r}_{(0)})^\dagger \delta\chi^{\varepsilon_r}_{(1)} \left[i\varepsilon_r - (a_{-\varepsilon_r} - id_{-\varepsilon_r}) + \frac{n\beta}{x^{\varepsilon_r}_{-(0)}}(b_{-\varepsilon_r} + ic_{-\varepsilon_r}) \right] \quad (5.67)$$

where $a_{\varepsilon_r} \equiv a_{\varepsilon_r}(1)$, etc. To obtain this expression, we have used the on-shell relations for the $\rho^{\varepsilon_r}_{(m)}$. Similarly, the only terms involving $\delta\chi^\dagger$ are

$$-(\delta\chi^{\varepsilon_r}_{(0)})^\dagger \rho^{\varepsilon_r}_{(0)} \left[ib_{\varepsilon_r} + \frac{in\beta}{x^{\varepsilon_r}_{-(0)}}(a_{-\varepsilon_r} - id_{-\varepsilon_r}) \right] + n\beta(\delta\chi^{\varepsilon_r}_{(1)})^\dagger \rho^{\varepsilon_r}_{(0)} \left[a_{\varepsilon_r} - \frac{n\beta}{x^{\varepsilon_r}_{-(0)}}(b_{-\varepsilon_r} + ic_{-\varepsilon_r}) \right] \quad (5.68)$$

The variational principle requires each term to vanish separately, which results in three independent equations

$$b_{\varepsilon_r} = -\frac{n\beta}{x^{\varepsilon_r}_{-(0)}}(a_{\varepsilon_r} + i\varepsilon_r) \quad (5.69)$$

$$b_{\varepsilon_r} = -\frac{n\beta}{x^{\varepsilon_r}_{-(0)}}(a_{-\varepsilon_r} - id_{-\varepsilon_r}) \quad (5.70)$$

$$a_{\varepsilon_r} = \frac{n\beta}{x^{\varepsilon_r}_{-(0)}}(b_{-\varepsilon_r} + ic_{-\varepsilon_r}) \quad (5.71)$$

As argued above, given a specific value of $a_{\varepsilon_r} = a_{\varepsilon_r}(1), ...$ satisfying (5.69)-(5.71), the higher order coefficients in the Taylor expansion can be found successively by requiring the cancelation of subleading divergences. There are, however, two things that those higher order coefficients cannot control, since they involve subleading powers in z. They are the leading divergence, of the form $\rho^{\varepsilon_r\dagger}_{(0)}\rho^{\varepsilon_r}_{(0)}$ [5], and the finite part of the on-shell action. Requiring the leading divergence to be zero sets

$$-ib_{\varepsilon_r} - \frac{in\beta}{x^{\varepsilon_r}_{-(0)}}(a_{-\varepsilon_r} - id_{-\varepsilon_r}) + \frac{in\beta}{x^{\varepsilon_r}_{-(0)}} \left(a_{\varepsilon_r} - \frac{n\beta}{x^{\varepsilon_r}_{-(0)}}(b_{-\varepsilon_r} + ic_{-\varepsilon_r}) \right) = 0, \quad (5.72)$$

which is fortunately automatically satisfied from (5.70) and (5.71). The finite part of the on-shell action is in fact independent of the values of a_{ε_r},... (although the variation of the action is not). Indeed, a short calculation gives

$$\begin{aligned} S_{os} &= \int \frac{d\omega}{2\pi} \int \frac{d^dk}{(2\pi)^d} \sum_{\varepsilon_r} \frac{2\varepsilon_r\mu_{-\varepsilon_r}}{n\beta} (\rho^{\varepsilon_r}_{(0)})^\dagger \chi^{\varepsilon_r}_{(0)} \\ &= -\frac{2\varepsilon_r\mu_{-\varepsilon_r}}{n\beta} \int \frac{d\omega}{2\pi} \int \frac{d^dk}{(2\pi)^d} \sum_{\varepsilon_r} \frac{x^{\varepsilon_r}_{+(2k)}}{x^{\varepsilon_r}_{-(0)}} \frac{\Gamma(1-\mu_{-\varepsilon_r})}{\Gamma(1+\mu_{-\varepsilon_r})} \left(\frac{q^2}{4}\right)^{\mu_{-\varepsilon_r}} (\rho^{\varepsilon_r}_{(0)})^\dagger \rho^{\varepsilon_r}_{(0)}, \end{aligned} \quad (5.73)$$

where we have used the conditions (5.69)-(5.71). Thus, it is scheme independent.

[5] Other possible terms such as $\rho^{\varepsilon_r\dagger}_{(0)} \not{k} \rho^{-\varepsilon_r}_{(0)}$ must be thought of as a piece of $\bar{\rho}^{\varepsilon_r}_{(0)}\gamma^0\mathcal{Q}\rho^{-\varepsilon_r}_{(0)}$, but as we have discussed, this is not K_i invariant, so will not appear.

5.4 Boundary Operators

As we have seen, the leading term in the expansion of the field is proportional to $X^{\varepsilon_r}_{-(0)}\rho^{\varepsilon_r}_{(0)}$, where $X^{\varepsilon_r}_{-(0)}$ is a constant matrix and $\rho^{\varepsilon_r}_{(0)}$ is a (doubly) chiral spinor field. It is convenient to take a basis of boundary quasi-primary operators such that $\rho^{\varepsilon_r}_{(0)}$ act as the sources for operators of charge n and dimension $\Delta^+_{\varepsilon_r}$

$$\int dt \int d^d x \sqrt{\gamma} \ \left[(\rho^{\varepsilon_r}_{(0)})^\dagger(t,\vec{x})\mathcal{O}_{n,\varepsilon_r}(t,\vec{x}) + h.c.\right] \tag{5.74}$$

This is possible because the $X^{\varepsilon_r}_{-(0)}$ are constant matrices. This coupling preserves the Schrödinger invariance at the boundary, obtained from the bulk transformations, for example

$$v^i K_i : \quad \Psi'(t',\vec{x}',z') = e^{in(\vec{v}\cdot\vec{x}+i\vec{v}^2 t/2)}(1+v\cdot\kappa)\Psi(t,\vec{x},z) \tag{5.75}$$

$$cC : \qquad \Psi'(t',\vec{x}',z') = e^{-\frac{inc}{2}\frac{\vec{x}^2+z^2}{1+ct}}(1+c\hat{c})\Psi(t,\vec{x},z), \tag{5.76}$$

at $z=0$. Under, say, a finite C transformation, the coupling (5.74) transforms as

$$\int dt \int d^d x \sqrt{\gamma}\ (\rho^{\varepsilon_r}_{(0)})^\dagger(t,\vec{x})\mathcal{O}_{n,\varepsilon_r}(t,\vec{x}) \to \int \frac{dt d^d x}{(1+ct)^{d+2}}(1+ct)^{\Delta^+_{-\varepsilon_r}+\Delta^-_{-\varepsilon_r}}(\rho^{\varepsilon_r}_{(0)})^\dagger(t,\vec{x})\mathcal{O}_{n,\varepsilon_r}(t,\vec{x}) \tag{5.77}$$

given the appropriate transformation of boundary quasi-primary operators (see for example Ref. [122]). Thus the coupling is invariant, as $\Delta^+_{\varepsilon_r}+\Delta^-_{\varepsilon_r} = d+2$.

Given the form of the on-shell action, we then read off the two-point Euclidean correlator of quasi-primary operators

$$\langle(\mathcal{O}_{n,\varepsilon_r})^\dagger(t,\vec{x})\mathcal{O}_{n',\varepsilon'_r}(t',\vec{x}')\rangle = -\delta_{\varepsilon_r,\varepsilon'_r}\delta_{n,n'}\int\frac{d\omega}{2\pi}\frac{d^d k}{(2\pi)^d}e^{-i\omega(t'-t)}e^{i\vec{k}\cdot(\vec{x}'-\vec{x})}\frac{2\varepsilon_r\mu_{-\varepsilon_r}}{n\beta}\frac{x^{\varepsilon_r}_{+(2k)}}{x^{\varepsilon_r}_{-(0)}}\frac{\Gamma(1-\mu_{-\varepsilon_r})}{\Gamma(1+\mu_{-\varepsilon_r})}\left(\frac{q^2}{4}\right)^{\mu_{-\varepsilon_r}} \tag{5.78}$$

By scaling, it is easy to see that this behaves as

$$(t'-t)^{-\Delta^+_{-\varepsilon_r}} f\left(\frac{(\vec{x}'-\vec{x})^2}{(t'-t)}\right),$$

and in fact this is just proportional to the scalar propagator. We note that this correlator preserves chirality, and in particular no γ-matrix structure is present. This is expected of a non-relativistic theory at zero density, as there is no essential difference between boson and fermion fields.

This is not to say that other correlation functions do not have more interesting structure. The subleading terms in the asymptotic expansion of the field are sources for descendant operators. Given the form of the

generators in the bulk (5.32,5.33), we see that Schrödinger transformations mix the descendant fields in an interesting way. The correlation functions of dual operators will of course display a similar structure, and thus these correlation functions can have non-trivial γ-matrix structure.

5.5 Conclusion

We have investigated carefully the Dirac fermion problem on the spacetime of Schrödinger isometry, which is dual to the vacuum configuration of non-relativistic conformal field theories in d spatial dimensions. The structure of the system is rather intricate, but a sensible Dirichlet problem exists and the boundary theory is renormalizable.

Although the bulk geometry contains a compact null direction (coordinatized by ξ), the metric is of the Bargman type and the usual holographic prescriptions go through more or less unmodified for equivariant operators, with care taken in interpreting the boundary action. The bulk field sources operators of a highest weight module of the Schrödinger algebra and the correct structure of two-point correlation functions is obtained. It would be interesting to extend these computations to higher point functions and to finite density.

Note that the results in this chapter are apparently different from those in [125]. It is because in their paper the spinorial boundary operators carry a different representation of the Schrödinger group. It is the spin-1/2 Levy-Leblond representation [119], in which a spinor consists of two components of dimensions differing by one and transform into each other under the boost and special conformal transformation. In this chapter, we tackle the standard problem of Dirac spinors on curved space-time and it turns out that the boundary operators carry a pretty simple representation, where they transform as scalar fields under the boost and special conformal.

Chapter 6

Vector Fields and the Sch/nrCFT Correspondence

This chapter continues the the topic of non-relativistic holography where the conceptual problem of variational principle and renormalization are tackled by considering vector fields on the Schrödinger background (4.1)

$$ds^2 = \frac{L^2}{z^2}\left(-\frac{\beta^2}{z^2}dt^2 + 2dtd\xi + d\vec{x}^2 + dz^2\right)$$

From now on we set $L = 1$ for simplicity. In this space-time, we may classify vector fields by $\{n, m_0\}$ where n is the eigenvalue of the central generator N (often referred to as the mass operator or the particle number operator) and m_0 is the bulk mass of the field. Because $N = \partial_\xi$ is central, fields can be taken to be equivariant $A(\xi, z, t, \vec{x}) \sim e^{in\xi}A(z, t, \vec{x})$ and hence for $n \neq 0$, the fields are inherently complex. For $n = 0, m_0 = 0$, the vector field is in fact a gauge field, and is expected to be dual to a conserved global current in the dual field theory.

Vector fields in relativistic holography has been studied extensively [28, 116, 34]. There the representation theory is pretty much simple, and normally was not paid much attention. In the Schrödinger case, however, as we have learnt in the last chapter it is crucial to carefully study the representations of the Schödinger group carried by the sources. We will see that for the vector field, there is a significant distinction between $n = 0$ and $n \neq 0$ cases. While the former resembles AdS in many ways, the latter deviates qualitatively to the standard expectation in terms of group representation.

We start the chapter with a general discussion on spin-1 representation of the Schrödinger group and work out the expected 2-point functions for the boundary currents. We then devote the last two sections studying in details vector fields in Schrödinger background, with $n \neq 0$ and $n = 0$ respectively.

6.1 Spin-1 representation of Schrödinger symmetry

6.1.1 bulk representation

The elements $N, H, \vec{P}, D, M_{ij}$ are represented in a straightforward manner on the components of vector fields, so we will not have occasion to focus on them. The explicit realization of these generators in the bulk are given in (5.16)-(5.22). Throughout this note we will focus mainly on the representation of the non-trivial elements of the Schrödinger algebra: the boost $\vec{K}$ and the special conformal transformation C. They act on the bulk coordinates as follows

$$K : \vec{x}' = \vec{x} + \vec{v}t; \quad t' = t; \quad z' = z; \quad \xi' = \xi - \vec{v}\cdot\vec{x} - \frac{1}{2}\vec{v}^2 t$$
$$C : \vec{x}' = \frac{\vec{x}}{1+ct}; \quad t' = \frac{t}{1+ct}; \quad z' = \frac{z}{1+ct}; \quad \xi' = \xi + \frac{c}{2}\frac{\vec{x}^2+z^2}{1+ct}$$

and so the corresponding Killing vectors (acting on scalar functions) are

$$K_i = -t\partial_i + x_i\partial_\xi \tag{6.1}$$
$$C = t(t\partial_t + \vec{x}\cdot\vec{\partial} + z\partial_z) - \frac{1}{2}(\vec{x}^2+z^2)\partial_\xi. \tag{6.2}$$

The special conformal transformation, together with the dilatation, is different from all other elements of the Schrödinger group in that it has a non-trivial Jacobian. The transformation law for a scalar field $\Phi(t,\vec{x},z,\xi)$ of scaling dimension Δ_Φ is simply

$$K: \quad \Phi'(t',\vec{x}',z',\xi') = \Phi(t,x,z,\xi) \tag{6.3}$$
$$C: \quad \Phi'(t',\vec{x}',z',\xi') = \lambda^{\Delta_\Phi}\Phi(t,\vec{x},z,\xi), \tag{6.4}$$

or if we reduce to a field of definite particle number n (that is, an equivariant field), we have effectively

$$K: \quad \Phi'(t',\vec{x}',z') = e^{in\vec{v}\cdot\vec{x}+\frac{i}{2}n\vec{v}^2 t}\Phi(t,x,z) \tag{6.5}$$
$$C: \quad \Phi'(t',\vec{x}',z') = e^{-\frac{inc}{2}\frac{\vec{x}^2+z^2}{\lambda}}\lambda^{\Delta_\Phi}\Phi(t,\vec{x},z), \tag{6.6}$$

where $\lambda = 1 + ct$. Given the coordinate transformation above, we easily deduce the spin-1 representation of the Schrödinger group. For a bulk 1-form field,

$$K: \quad \mathbf{H}'(t', \vec{x}', z', \xi') = \mathbf{H}(t, \vec{x}, z, \xi) \cdot \begin{pmatrix} 1 & 0 & 0 & 0 \\ -v^i & 1 & 0 & 0 \\ 0 & 0 & 1 & 0 \\ -\frac{\vec{v}^2}{2} & v_i & 0 & 1 \end{pmatrix}, \tag{6.7}$$

$$C: \quad \mathbf{H}'(t', \vec{x}', z', \xi') = \mathbf{H}(t, \vec{x}, z, \xi) \cdot \begin{pmatrix} \lambda^{\Delta+2} & 0 & 0 & 0 \\ cx^i\lambda^{\Delta+1} & \lambda^{\Delta+1} & 0 & 0 \\ cz\lambda^{\Delta+1} & 0 & \lambda^{\Delta+1} & 0 \\ -\frac{c^2}{2}(\vec{x}^2 + z^2)\lambda^{\Delta} & -cx_i\lambda^{\Delta} & -cz\lambda^{\Delta} & \lambda^{\Delta} \end{pmatrix}. \tag{6.8}$$

Here $\mathbf{H} = (H_t, H_i, H_z, H_\xi)$ are the components of a generic one-form whose components have scaling dimensions $(\Delta + 2, \Delta + 1, \Delta + 1, \Delta)$ respectively. Notice that since H_ξ transforms into itself under K and C (and eventually under the whole Schrödinger group), the representation (6.7) and (6.8) can be reduced by setting $H_\xi = 0$ and dropping it from the multiplet. We also note that one can drop H_z, but only along with H_ξ, resulting in what we call the *short representation* $\{H_t, H_i\}$. Finally, the *ultra-short representation* $\{H_t\}$ can be obtained by further dropping H_i in the short representation. These representations will be of interest holographically.

6.1.2 Dual Representations and the Source-Operator Coupling

In a holographic context, we are interested both in the representations of the isometry group that we have in the bulk, but also in the representation theory of the dual operators in the dual field theory. The latter can be deduced by consideration of how the source (i.e., the asymptotic of the bulk field) couples to its dual operator. Roughly speaking then, the boundary representation can be obtained from the bulk one by taking the $z \to 0$ limit. We will find that all of the components of a vector field play a role in the boundary, including the ξ-component. The important role played by the ξ-coordinate in the boundary is also clear when we find the Schrödinger invariant source-operator coupling.

This coupling associates a bulk representation of the Schrödinger algebra to a boundary representation of the same algebra. Given a bulk system, as we will construct below, we are handed a definite bulk representation. We need to consider carefully what boundary representation, carried by the dual operators, is induced. The one-form fields that we have discussed above naturally couple to vector operators in the boundary. Let us first consider how such operators transform. In the boundary, the Schrödinger group acts

on the coordinates as

$$K: \quad \vec{x}' = \vec{x} + \vec{v}t; \quad t' = t; \quad \xi' = \xi - \vec{v}\vec{x} - \frac{1}{2}\vec{v}^2 t$$
$$C: \quad \vec{x}' = \frac{\vec{x}}{1+ct}; \quad t' = \frac{t}{1+ct}; \quad \xi' = \xi + \frac{c}{2}\frac{\vec{x}^2}{1+ct},$$

which are generated by

$$K_i = -t\partial_i + x_i\partial_\xi \tag{6.9}$$
$$C = t(t\partial_t + \vec{x}\cdot\vec{\partial} + \Delta) - \frac{1}{2}\vec{x}^2\partial_\xi. \tag{6.10}$$

Note that we interpret ξ here as a boundary coordinate. The vector field ∂_ξ is still central, and so operators can be taken to have definite eigenvalues n.

A one-form operator $\hat{\mathbf{O}} = (\hat{O}_t, \hat{O}_i, \hat{O}_\xi)$ with particle number n and scaling dimension $(\Delta+2, \Delta+1, \Delta)$ would transform as

$$K: \quad \hat{\mathbf{O}}'(t', \vec{x}', \xi') = \hat{\mathbf{O}}(t, \vec{x}, \xi) \cdot \begin{pmatrix} 1 & 0 & 0 \\ -v^i & 1 & 0 \\ -\frac{\vec{v}^2}{2} & v_i & 1 \end{pmatrix}, \tag{6.11}$$

$$C: \quad \hat{\mathbf{O}}'(t', \vec{x}', \xi') = \hat{\mathbf{O}}(t, \vec{x}, \xi) \cdot \begin{pmatrix} \lambda^{\Delta+2} & 0 & 0 \\ cx^i\lambda^{\Delta+1} & \lambda^{\Delta+1} & 0 \\ -\frac{c^2}{2}\vec{x}^2\lambda^\Delta & -cx_i\lambda^\Delta & \lambda^\Delta \end{pmatrix}. \tag{6.12}$$

If we call the matrices appearing here K and C, a vector operator $(\hat{O}^t, \hat{O}^i, \hat{O}^\xi)$ would then transform via ${K^{-1}}^T$ and ${C^{-1}}^T$ respectively. It can be seen that the one-form and vector operators are related by a "boundary metric"

$$\eta = \begin{pmatrix} 0 & 0 & 1 \\ 0 & 1 & 0 \\ 1 & 0 & 0 \end{pmatrix}, \tag{6.13}$$

which is preserved up to a re-scaling under the Schrödinger group, just as the relativistic conformal group preserves up to a re-scaling the Minkovski metric. Similar to bulk representations, we also have *short* and *ultra-short representation* $\{\hat{O}_t, \hat{O}_i\}$ and $\{\hat{O}_t\}$ respectively.

For a simple example, if we had free fermions we could construct the spin-1 current multiplet with components $J_m = i\psi^\dagger\partial_m\psi - i\partial_m\psi^\dagger\psi$, $m = t, i, \xi$ with $(n, \Delta) = (0, d)$ where d is the number of spatial dimensions. In the same model, operators of the form $(\psi^{\dagger p} J_m \psi^q)$ have $(n, \Delta) = (p-q, d + \frac{p+q}{2})$. These operators will have the corresponding dual sources in the bulk, coming from bulk vector fields with different mass m_0 and particle number n.

Now the bulk field **H** give rise to a source **S** for operators in the boundary theory, and we write a source-operator coupling of the general form

$$L_I = \int_{\partial M} S_\mu \hat{O}^\mu \tag{6.14}$$

which should be invariant under the Schrödinger group. If the sources **S** have (n_S, Δ_S), the dual operators should have (n_J, Δ_J) such that $n_S = -n_J$ and $\Delta_S + \Delta_J = d$. However, having written this coupling, it is important to realize that not all of the components of the source are independent. Before proceeding with the discussion, let us pause to note what happens in the more familiar AdS cases. There the z-component of the vector field is either a pure gauge (so that it does not contribute to the on-shell action) for $m_0 = 0$, or being determined by the other components through the equations of motion for $m \neq 0$. In both instances, the z-component does not source an independent operator in the boundary theory. The dual operators always carry a vector representation in the boundary.

In the Schrödinger case, as we will see, for $n = 0$ we have the same situation as AdS. However, for $n \neq 0$, interesting thing happens, where it is the t-component of the vector field that becomes unphysical. The z-component, instead, combines with the ξ-component to source a pair of scalar operators. (In the massless limit, one of the combinations is not gauge invariant and also drops out of the system). In any case, we must look at solutions to the equations of motion as a guide.

6.2 Boundary vector 2-point functions

Let us first consider the general form of the 2-point functions of vector operators, which follow from the representation (6.11) and (6.12). The 2-point correlator of equivariant operators should satisfy

$$G_{mn}(t', \vec{x}') = \langle \hat{O}_m(t', \vec{x}') \hat{O}_n^\dagger(0,0) \rangle = \langle \hat{O}'_m(t', \vec{x}') \hat{O}'^\dagger_n(0,0) \rangle = G'_{mn}(t', \vec{x}') \tag{6.15}$$

in which the right hand side can be converted to a combination of the unprimed 2-point functions using (6.11) and (6.12).

6.2.1 for $n \neq 0$

Given that $\hat{O}_\xi$ transforms as if it were a scalar, we have

$$G_{\xi\xi}(t, \vec{x}) = \alpha \frac{1}{t^\Delta} e^{in\frac{\vec{x}^2}{2t}} \tag{6.16}$$

where Δ is the scaling dimension of $\hat{O}_\xi$ and α an undetermined constant. All other components of G_{mn} can be inferred from $G_{\xi\xi}$ using (6.15) for different symmetries of the Schrödinger group. For example, applying (6.15) for K on $G_{i\xi}$ gives the differential equation

$$v^j(t\partial_j - inx_j)G_{i\xi} = v_i G_{\xi\xi}, \tag{6.17}$$

which gives $G_{i\xi} = \alpha \frac{x_i}{t^{\Delta+1}} e^{in\frac{\vec{x}^2}{2t}}$. It can be checked that this form of $G_{i\xi}$ is also consistent with the finite K and C symmetry. Similar computations yield results

$$G_{mn}(t,\vec{x}) = \begin{pmatrix} -\frac{\vec{x}^4}{4t^{\Delta+4}} & -\frac{\vec{x}^2 x_i}{2t^{\Delta+3}} & -\frac{\vec{x}^2}{2t^{\Delta+2}} \\ -\frac{\vec{x}^2 x_j}{2t^{\Delta+3}} & \frac{x_i x_j}{t^{\Delta+2}} & \frac{x_j}{t^{\Delta+1}} \\ -\frac{\vec{x}^2}{2t^{\Delta+2}} & \frac{x_j}{t^{\Delta+1}} & \frac{1}{t^{\Delta}} \end{pmatrix} \alpha e^{in\frac{\vec{x}^2}{2t}}. \tag{6.18}$$

Hence, all vector 2-point functions are completely determined up to a proportionality constant. This constant can be set to 1 by an appropriate rescaling of the operators.

6.2.2 for $n = 0$

For $n = 0$, one might simply consider the $n \to 0$ limit of the above correlation functions. However, this does not give the general result, and in fact will not be consistent with the correlators that we will obtain holographically. At $n = 0$ there is another possible functional form for the 2-point functions. To see how this comes about, consider the simplest piece of the correlator, $G_{\xi\xi}$, which satisfies the K and C symmetry constraints (6.15)

$$\begin{aligned} t\partial_i G_{\xi\xi} &= 0 \\ -t(t\partial_t + x^i\partial_i)G_{\xi\xi} &= \Delta t G_{\xi\xi} \end{aligned} \tag{6.19}$$

We will also need to consider constraints from other elements of the Schrödinger group but we will not write them explicitly. One solution to these equations is $G_{\xi\xi} \sim \frac{1}{t^\Delta}$, which is the $n \to 0$ limit of (6.18). Because the equations are proportional to t, there is another solution of the following form[1]

$$G_{\xi\xi} = \beta \frac{\delta(t)}{(\vec{x}^2)^{\Delta-1}}, \tag{6.20}$$

[1] The power of $\vec{x}^2$ is determined by D.

which does not exist for $n \neq 0$. If we look at the full system of equations for G_{mn}, we find that in fact $\beta = 0$, but other components can have temporal δ-function support. The general result is

$$G_{mn}(t,\vec{x}) = \begin{pmatrix} -\frac{1}{2\Delta(\Delta-1)}\frac{\delta''(t)}{(x^2)^{\Delta-1}} + U\frac{\delta'(t)}{(x^2)^{\Delta}} + W\frac{\delta(t)}{(x^2)^{\Delta+1}} & \frac{1}{\Delta}\frac{\delta'(t)x_i}{(x^2)^{\Delta}} - \Delta U\frac{\delta(t)x_i}{(x^2)^{\Delta+1}} & \frac{\delta(t)}{(x^2)^{\Delta}} \\ \frac{1}{\Delta}\frac{\delta'(t)x_j}{(x^2)^{\Delta}} - \Delta U\frac{\delta(t)x_j}{(x^2)^{\Delta+1}} & \frac{\delta(t)}{(x^2)^{\Delta+1}}\left(\frac{\Delta+1}{\Delta}\delta_{ij}x^2 - 2x_ix_j\right) & 0 \\ \frac{\delta(t)}{(x^2)^{\Delta}} & 0 & 0 \end{pmatrix}. \quad (6.21)$$

As we will see, this type of solution will be realized in the boundary theory. The current correlators are determined up to two arbitrary constants U and W. It turns out that the U and W terms in (6.21) essentially correspond to the 2-point functions of a short and ultra-short multiplet respectively. This is a result of the fact that given any spin-1 multiplet $\{\hat{O}_t, \hat{O}_i, \hat{O}_\xi\}$, we can always construct out of it a short multiplet $\{\frac{d}{d-\Delta}\partial_t\hat{O}_\xi + \frac{\Delta}{d-\Delta}\partial_i\hat{O}_i, \partial_i\hat{O}_\xi\}$ and an ultra-short one $\{\partial_i^2\hat{O}_\xi\}$. This is a special feature of $n = 0$, which causes an ambiguity in the spin-1 representation. Indeed, define

$$\begin{aligned} \bar{\hat{O}}_\xi &= \hat{O}_\xi \\ \bar{\hat{O}}_i &= \hat{O}_i + \eta\ \partial_i\hat{O}_\xi \\ \bar{\hat{O}}_t &= \hat{O}_t + \frac{\eta d}{d-\Delta}\partial_t\hat{O}_\xi + \frac{\eta\Delta}{d-\Delta}\partial_i\hat{O}_i + \kappa\ \partial_i^2\hat{O}_\xi, \end{aligned} \quad (6.22)$$

then $\{\bar{\hat{O}}_t, \bar{\hat{O}}_i, \bar{\hat{O}}_\xi\}$ also forms a spin-1 multiplet for arbitrary η and κ. The ambiguity can be removed by fixing $U = W = 0$ in (6.21). For $d \neq \Delta$, this is done by choosing $\eta = \frac{(d-\Delta)U}{2(2\Delta-d)}$ and $\kappa = \frac{W}{4\Delta(2\Delta+2-d)}$. The 2-point functions becomes

$$G_{mn}(t,\vec{x}) = \begin{pmatrix} -\frac{1}{2\Delta(\Delta-1)}\frac{\delta''(t)}{(x^2)^{\Delta-1}} & \frac{1}{\Delta}\frac{\delta'(t)x_i}{(x^2)^{\Delta}} & \frac{\delta(t)}{(x^2)^{\Delta}} \\ \frac{1}{\Delta}\frac{\delta'(t)x_j}{(x^2)^{\Delta}} & \frac{\delta(t)}{(x^2)^{\Delta+1}}\left(\frac{\Delta+1}{\Delta}\delta_{ij}x^2 - 2x_ix_j\right) & 0 \\ \frac{\delta(t)}{(x^2)^{\Delta}} & 0 & 0 \end{pmatrix}. \quad (6.23)$$

When $d = \Delta$, there is no short-multiplet ambiguity, so only κ is allowed in (6.22), which helps setting $W = 0$. However, as will be clear later, this case corresponds to the massless limit and so there is an extra constraint on the operators: the continuity equation $\partial_t\hat{O}_\xi + \partial_i\hat{O}_i = 0$. This requires $U = 0$ too.

6.3 Vector fields on Schrödinger background: $n \neq 0$

Now we consider the bulk equations of motion carefully. Because we are on a symmetric background, the equations of motion have exact solutions that we can write in terms of Bessel functions. As above, there are several distinct cases to consider.

6.3.1 On-shell Solution

The bulk action for an $n \neq 0$ complex massive vector field on the Schrödinger background takes the form

$$S = -\int_M dz dt d^d x d\xi \sqrt{|g|}\Big(\frac{1}{4}F_{\mu\nu}F^{\mu\nu *} + \frac{1}{2}m_0^2 A_\mu A^{\mu *}\Big) \tag{6.24}$$

and the equations of motion are

$$\nabla^\mu F_{\mu\nu} - m_0^2 A_\nu = 0. \tag{6.25}$$

Here, μ, ν run over $t, \vec{x}, \xi, z$. Notice that for $m_0 \neq 0$, this equation implies that $\nabla^\nu A_\nu = 0$, which we refer to as the Lorentz condition. For $m_0 = 0$, this does not follow, but we have a choice of gauge fixing condition to make; in fact, $\nabla^\nu A_\nu = 0$ seems to be the sensible gauge condition, as it does not break the Schrödinger symmetry. After Fourier transforming the fields $A_\mu \sim e^{-i\omega t + i\vec{k}\cdot\vec{x} + in\xi}$, one finds that the eqs. (6.25) can be put in the following form using the Lorentz condition

$$0 = z^2 A_t'' - (d-1)zA_t' - z^2 q^2 A_t - m^2 A_t - \frac{2\beta^2}{z}A_\xi' + \frac{2in\beta^2}{z}A_z + 2i\omega z A_z \tag{6.26}$$

$$0 = z^2 A_i'' - (d-1)zA_i' - z^2 q^2 A_i - m^2 A_i - 2ik_i z A_z \tag{6.27}$$

$$0 = z^2 A_z'' - (d+1)zA_z' - z^2 q^2 A_z + (d+1-m^2)A_z - \frac{2in\beta^2}{z}A_\xi \tag{6.28}$$

$$0 = z^2 A_\xi'' - (d-1)zA_\xi' - z^2 q^2 A_\xi - m^2 A_\xi - 2inzA_z, \tag{6.29}$$

where $m^2 = m_0^2 + n^2\beta^2$ and where $q = \sqrt{\vec{k}^2 - 2n\omega}$. We notice that A_z and A_ξ satisfy coupled equations (6.28,6.29) independent of A_t and A_i and they may be solved exactly to give

$$A_\xi = \frac{1}{\beta}\sum_{\eta=\pm} C_\eta\, z^{\frac{d}{2}+1} K_{\nu_\eta}(qz) \tag{6.30}$$

$$A_z = \frac{1}{2in\beta}\sum_{\eta=\pm} C_\eta z^{\frac{d}{2}}\Big(\alpha_\eta K_{\nu_\eta}(qz) - 2zqK_{\nu_\eta+1}(qz)\Big), \tag{6.31}$$

where

$$\nu_\eta = \sqrt{\Big(\frac{d}{2}+1\Big)^2 + m^2 + \gamma_\eta} \tag{6.32}$$

$$\alpha_\eta = d + 2 + 2\nu_\eta + \gamma_\eta \tag{6.33}$$

$$\gamma_\eta = \eta\sqrt{d^2 + 4m_0^2} - d, \tag{6.34}$$

and C_η are arbitrary constants. Given these solutions, we see that A_z, A_ξ act as sources for A_t, A_i. The specific solution to (6.27) can be found by defining $\tilde{A}_i = z^{-\frac{d}{2}} A_i$ and using the ansatz $\tilde{A}_i = \sum_\eta U_\eta z^{V_\eta} K_{\mu_\eta}(qz)$, yielding $U_\eta = C_\eta \frac{k_i}{n\beta}$, $V_\eta = 1$ and $\mu_\eta = \nu_\eta$. Hence we get

$$A_i = C_i z^{\frac{d}{2}} K_{\nu_0}(qz) + \sum_\eta C_\eta \frac{k_i}{n\beta} z^{\frac{d}{2}+1} K_{\nu_\eta}(qz), \tag{6.35}$$

with

$$\nu_0 = \sqrt{\frac{d^2}{4} + m^2}, \tag{6.36}$$

and C_i constant. Similarly, A_t can be found without much difficulty

$$A_t = C_t z^{\frac{d}{2}} K_{\nu_0}(qz) + \sum_\eta C_\eta z^{\frac{d}{2}} \Big(- \frac{\gamma_\eta}{2\nu_\eta \alpha_\eta} q\, K_{\nu_\eta+1}(qz) + \frac{\gamma_\eta}{2\nu_\eta(\alpha_\eta - 4\nu_\eta)} q\, K_{\nu_\eta-1}(qz) - \frac{\omega}{n\beta} z K_{\nu_\eta}(qz) \Big). \tag{6.37}$$

We notice that singularities appear in the solutions as $n \to 0$. We should take greater care then with $n = 0$ and derive the solutions for this case separately. We will do so in the next section.

We also notice that the on-shell solutions (6.30), (6.31), (6.35) and (6.37) suggest the following redefinition of the fields

$$\begin{aligned}
A_\xi &= \frac{1}{\beta} \sum_\eta \bar{A}_\eta \\
A_z &= \frac{1}{2in\beta} \sum_\eta \Big(\frac{\gamma_\eta}{z} \bar{A}_\eta + 2\bar{A}'_\eta \Big) \\
A_i &= \bar{A}_i + \frac{k_i}{n\beta} \sum_\eta \bar{A}_\eta \\
A_t &= \bar{A}_t + \sum_\eta \Big(- \frac{\omega}{n\beta} \bar{A}_\eta + \frac{\gamma_\eta^2}{4n^2\beta z^2} \bar{A}_\eta + \frac{\gamma_\eta}{2n^2\beta z} \bar{A}'_\eta \Big),
\end{aligned} \tag{6.38}$$

with which the equations of motion completely decouple and the on-shell solutions become

$$\bar{A}_\eta = C_\eta z^{\frac{d}{2}+1} K_{\nu_\eta}(qz) \tag{6.39}$$

$$\bar{A}_i = C_i z^{\frac{d}{2}} K_{\nu_0}(qz) \tag{6.40}$$

$$\bar{A}_t = C_t z^{\frac{d}{2}} K_{\nu_0}(qz). \tag{6.41}$$

The transformation properties of the barred fields can be inferred directly from those of the original fields (6.7), (6.8) (with $\Delta = 0$). A simple calculation reveals that under K and C, $\bar{A}_\eta$ *transform as scalars, while* $\{\bar{A}_t, \bar{A}_i\}$ *form a short spin-1 multiplet.* The Lorentz condition simplifies significantly

$$\nabla^\nu A_\nu = -(d+1)zA_z + z^2\Big(\partial_\xi A_t + \frac{\beta^2}{z^2}\partial_\xi A_\xi + \partial_t A_\xi + \partial_i A_i + \partial_z A_z\Big) = 0 = \partial_\xi \bar{A}_t + \partial_i \bar{A}_i,$$

which can be used to eliminate $\bar{A}_t$ in terms of $\bar{A}_i$. This leaves us with only three physical Schrödinger representations $\bar{A}_\eta$, $\bar{A}_i$, all transform as scalars under the boost and special conformal transformation. (Of course, $\bar{A}_i$ transform as a spatial vector under rotations). As anticipated, the bulk action (6.24) written in terms of $\bar{A}_\eta$ and $\bar{A}_i$ (after removing $\bar{A}_t$ and adding appropriate total derivatives) takes a simple form

$$S = -\int_M \sqrt{-g}\Bigg\{\frac{1}{2}\Big(\partial_\mu \bar{A}_i \partial^\mu \bar{A}^{i*} + m_0^2 \bar{A}_i \bar{A}^{i*}\Big) + \sum_\eta \frac{4m_0^2 - d\gamma_\eta}{4n^2\beta^2}\Big(\partial_\mu \bar{A}_\eta \partial^\mu \bar{A}^*_\eta + (m_0^2+\gamma_\eta)\bar{A}_\eta \bar{A}^*_\eta\Big)\Bigg\}. \quad (6.42)$$

This is a free system of a massive spatial vector and two massive scalars on the Schrödinger geometry.

It is important to note that at $m_0 = 0$, $4m_0^2 - d\gamma_+ = 0$ and hence $\bar{A}_+$ completely decouples. This effect of reducing the physical degrees of freedom is expected because of the gauge symmetry present in that case. Indeed, observe that at $m_0 = 0$, $F_{z\xi} = \frac{1}{2z}\sum_\eta \gamma_\eta \bar{A}_\eta \sim \bar{A}_-$, so A_- is gauge invariant. So is $\bar{A}_i$: under a gauge tranformation parameterized by ϕ, we have $\bar{A}'_i = A'_i - \frac{k_i}{n}\sum_\eta \bar{A}'_\eta = A_i + ik_i\phi - \frac{k_i}{n}(\sum_\eta \bar{A}_\eta + in\phi) = \bar{A}_i$. Only $\bar{A}_+$ is not gauge invariant and so is the mode that can be gauged away.

6.3.2 Variational Principle, Renormalization and 2-point Functions

Because of the simple form of the vector field solutions found above, the following will be very much like scalars on the Schrödinger geometry, as studied in [124] [123] [37]. Writing

$$K_\nu(qz) = x_\nu \frac{1}{(qz)^\nu} + \ldots y_\nu (qz)^\nu + \ldots,$$

where $x_\nu = \frac{\Gamma(\nu)}{2^{1-\nu}}$, $y_\nu = \frac{\Gamma(-\nu)}{2^{1+\nu}}$, we define the sources and vev of the dual operators to be the coefficients of the "conjugate" powers of z

$$S^{(0)}_\eta = x_{\nu_\eta} q^{-\nu_\eta} C_\eta; \;\; S^{(0)}_i = x_{\nu_0} q^{-\nu_0} C_i; \quad (6.43)$$

$$V^{(0)}_\eta = y_{\nu_\eta} q^{\nu_\eta} C_\eta; \qquad V^{(0)}_i = y_{\nu_0} q^{\nu_0} C_i, \quad (6.44)$$

As in the scalar case, the transformation properties of these quantities inherit directly from those of $\bar{A}_\eta$ and $\bar{A}_i$. Generically, the dual operators fall into three representations of the boundary Schrödinger group: $\hat{O}_\eta$, carrying the scalar representations with scaling dimension $\Delta_\eta = \frac{d}{2} + 1 + \nu_\eta$, and $\hat{O}_i$, transforming as a spatial vector under spatial rotation, but as scalars under the rest of the generators, having scaling dimension $\Delta = \frac{d}{2} + \nu_0$. At $m_0 = 0$, the dual operators reduce to only $\hat{O}_-$ and $\hat{O}_i$.

The variational principle and renormalization proceed in the same way as scalars on Schrödinger geometry, as discussed in [38], following [32]. We notice that the solutions found above are such that effectively it looks like $\bar{A}_\eta$ can be thought of as two decoupled scalars on relativistic AdS_{d+3}/CFT_{d+2}, whereas for $\bar{A}_i$ (with the lower index), d is shifted by 2 and can be thought of as d decoupled scalars on AdS_{d+1}/CFT_d. Thus, we can immediately deduce the counter terms from the more familiar AdS case, and we find

$$S_{ct} = \int_{\partial M} d^{d+1}x d\xi \sqrt{-\gamma} \Bigg\{ \Big(\frac{d-\Delta}{2} \bar{A}_i \bar{A}^{i*} + \frac{1}{2(\Delta - d - 2)} \bar{A}^{i*} \Box_\gamma \bar{A}_i \Big) + \sum_\eta \frac{4m_0^2 - d\gamma_\eta}{2n^2\beta^2} \Big(\frac{d+2-\Delta}{2} \bar{A}_\eta \bar{A}_\eta^* + \frac{1}{2(\Delta - d - 4)} \bar{A}_\eta^* \Box_\gamma \bar{A}_\eta \Big) \Bigg\}, \tag{6.45}$$

where $\sqrt{-\gamma} = z^{-(d+2)}$ is the $(d+2)$-dimensional induced metric determinant and $\Box_\gamma = z^2(2in\partial_t + \partial_i^2)$ the Schrödinger operator. The renormalized on-shell action hence evaluates to

$$S_{R,os} = -R \int_{\partial M} d^d k d\omega \Bigg\{ \nu_\eta \, \frac{y_{\nu_\eta}}{x_{\nu_\eta}} \frac{4m_0^2 - d\gamma_\eta}{2n^2\beta^2} q^{2\nu_\eta} S_\eta^{(0)} S_\eta^{(0)*} + \nu_0 \, \frac{y_{\nu_0}}{x_{\nu_0}} q^{2\nu_0} S_i^{(0)} S_i^{(0)*} \Bigg\}, \tag{6.46}$$

where R is the compactification radius of ξ direction. The 2-point functions can be read off immediately

$$\langle \hat{O}_\eta^\dagger(k,\omega) \hat{O}_{\eta'}(k,\omega) \rangle = -\delta_{\eta\eta'} R \nu_\eta \, \frac{y_{\nu_\eta}}{x_{\nu_\eta}} \frac{4m_0^2 - d\gamma_\eta}{2n^2\beta^2} q^{2\nu_\eta} \tag{6.47}$$

$$\langle \hat{O}_i^\dagger(k,\omega) \hat{O}_j(k,\omega) \rangle = -\delta_{ij} R \nu_0 \, \frac{y_{\nu_0}}{x_{\nu_0}} q^{2\nu_0}, \tag{6.48}$$

keeping in mind that at $m_0 = 0$ there is no $\hat{O}_+$.

6.4 Vector fields on Schrödinger background: $n = 0$

As mentioned before, the solutions found in the previous section possess singularities as $n \to 0$. The special case $n = 0$ thus has to be treated separately.

6.4.1 On-shell Solutions

For $n = 0$, the bulk vector field can be taken to be real with the standard action

$$S = -\int_M d^d x dt d\xi dz \sqrt{-g}\Big(\frac{1}{4}F_{\mu\nu}F^{\mu\nu} + \frac{1}{2}m^2 A_\mu A^\mu\Big). \tag{6.49}$$

The equations of motion are the $n \to 0$ limit of (6.26)-(6.29) and can be solved exactly to give the general solution

$$A_\xi = C_\xi \; z^{\frac{d}{2}} K_{\nu_0}(kz) \tag{6.50}$$

$$A_z = C_z \; z^{\frac{d}{2}+1} K_{\nu_0}(kz) \tag{6.51}$$

$$A_i = C_i \; z^{\frac{d}{2}} K_{\nu_0}(kz) - i\frac{k_i}{k} C_z \; z^{\frac{d}{2}+1} K_{\nu_0+1}(kz) \tag{6.52}$$

$$\begin{aligned} A_t = {} & C_t \; z^{\frac{d}{2}} K_{\nu_0}(kz) + i\frac{\omega}{k} C_z \; z^{\frac{d}{2}+1} K_{\nu_0+1}(kz) \\ & + C_\xi \; k^2\beta^2 z^{\frac{d}{2}} \Big(\frac{d-2\nu_0}{16\nu_0(\nu_0+1)^2} K_{\nu_0+2}(kz) - \frac{d+2\nu_0}{16\nu_0(\nu_0-1)^2} K_{\nu_0-2}(kz) - \frac{2+d}{4\nu_0(\nu_0^2-1)} \frac{\partial}{\partial \nu_0} K_{\nu_0}(kz) \Big) \end{aligned} \tag{6.53}$$

Note that now $k = \sqrt{\vec{k}^2}$. Observe that there is apparent singularities at $\nu_0 = 0, 1$. The Lorentz condition now takes the form

$$0 = \nabla A \sim (d - 2\nu_0) C_z + 2i\omega C_\xi - 2ik_i C_i \tag{6.54}$$

We notice the qualitative difference from the $n \neq 0$ results. Here A_ξ and A_z decouple from each other in (6.50) and (6.51). C_t is no longer an unphysical degree of freedom and in fact does not even appear in the Lorentz condition. Instead, for generic values of m_0, C_z can be eliminated using the Lorentz condition, as long as $d - 2\nu_0 \neq 0$[2] Furthermore, there is no possible redefinition of the fields to decouple the equations of motion (technically due to the $\frac{\partial}{\partial \nu_0} K_{\nu_0}(kz)$ term in (6.53)). Finally, as will be discussed in detail later, in contrast to the $n \neq 0$ case, the gauge limit $m_0 \to 0$ is not a singular limit. Note also that at this value of m_0, A_z is a pure gauge. Hence, we have the similar situation as in AdS.

6.4.2 Sources and Vevs and their Transformations

The next step is to identify the sources and v.e.v. of the boundary operators and find their transformation properties. They can be identified as the coefficients of the $z^{\frac{d}{2}-\nu_0}$ and $z^{\frac{d}{2}+\nu_0}$ terms in the on-shell solutions

[2]That is, as long as $m_0 \neq 0$. If $m_0 = 0$, the Lorentz condition reduces to $\omega C_\xi = \vec{k} \cdot \vec{C}$, which can clearly be interpreted as a constraint equation, leading to the expected Ward identity in the boundary theory.

(6.50)-(6.53), respectively

$$
\begin{aligned}
S_z^{(0)} &= x_{\nu_0} k^{-\nu_0} C_z \\
S_\xi^{(0)} &= x_{\nu_0} k^{-\nu_0} C_\xi \\
S_i^{(0)} &= x_{\nu_0} k^{-\nu_0} C_i - i2\nu_0\, x_{\nu_0}\, k_i k^{-\nu_0-2} C_z \\
S_t^{(0)} &= x_{\nu_0} k^{-\nu_0} C_t + i2\nu_0\, x_{\nu_0}\, \omega k^{-\nu_0-2} C_z + \kappa^S\, x_{\nu_0} k^{2-\nu_0} \beta^2 C_\xi,
\end{aligned}
\tag{6.55}
$$

$$
\begin{aligned}
V_z^{(0)} &= y_{\nu_0} k^{\nu_0} C_z \\
V_\xi^{(0)} &= y_{\nu_0} k^{\nu_0} C_\xi \\
V_i^{(0)} &= y_{\nu_0} k^{\nu_0} C_i \\
V_t^{(0)} &= y_{\nu_0} k^{\nu_0} C_t + \kappa^V\, y_{\nu_0} k^{2+\nu_0} \beta^2 C_\xi,
\end{aligned}
\tag{6.56}
$$

where κ^S and κ^V are the corresponding momentum independent contributions coming from the last term (proportional to C_ξ) of (6.53), namely

$$
\kappa^S = -\frac{d-2\nu_0}{16(\nu_0+1)^2} + \frac{d+2}{4\nu_0(\nu_0^2-1)}\Big(\pi\cot(\pi\nu_0) - \psi(1-\nu_0)\Big) \tag{6.57}
$$

$$
\kappa^V = -\frac{d+2\nu_0}{16(\nu_0-1)^2} + \frac{d+2}{4\nu_0(\nu_0^2-1)}\Big(\pi\cot(\pi\nu_0) + \psi(1+\nu_0)\Big), \tag{6.58}
$$

with $\psi(x)$ the digamma function. As we will see shortly, in contrast to the $n \neq 0$ case where the sources (and vev) are scalars under the (boundary) boost and special conformal transformations, here they form a spin-1 representation (6.11) and (6.12). The observation made in section 2.2 then implies that the sources and vev are only determined up to a field redefinition (6.22), dual to a redefinition of the boundary operators. The desired redefinition will be determined so that the current 2-point functions take the normalized form (6.23). We will come to this point later.

Throughout this section we adopt a more convenient hybrid representation where $\mathbf{S}^{(0)} = \mathbf{S}^{(0)}(t, \vec{k})$, $\mathbf{S}^{(0)} = (S_t^{(0)}, S_i^{(0)}, S_z^{(0)}, S_\xi^{(0)})$, and likewise for $\mathbf{V}^{(0)}$. Let's find the transformation properties of $\mathbf{S}^{(0)}$ and $\mathbf{V}^{(0)}$. Given the finite boost

$$
z' = z, \;\; k_i' = k_i, \;\; \partial_t' = \partial_t - i v^i k_i, \tag{6.59}
$$

and given that the bulk field A transforms as in (6.7), it is easy to show that vev transform as

$$\begin{aligned}
V_\xi^{(0)'} &= V_\xi^{(0)} \\
V_z^{(0)'} &= V_z^{(0)} \\
V_i^{(0)'} &= V_i^{(0)} + v_i V_\xi^{(0)} \\
V_t^{(0)'} &= V_t^{(0)} - v^i V_i^{(0)} - \frac{v^2}{2} V_\xi^{(0)'}
\end{aligned} \tag{6.60}$$

In other words, $\{V_t^{(0)}, V_i^{(0)}, V_\xi^{(0)}\}$ form a spin-1 representation, while $V_z^{(0)}$ decouples from the rest. Note that here $\mathbf{V}^{(0)'}$ stands for $\mathbf{V}^{(0)'}(t', \vec{k}')$. Under the special conformal transformation, we have

$$z' = z/\lambda, \;\; k_i' = \lambda k_i, \;\; \partial_t' = \lambda^2 \partial_t - c\lambda \frac{\partial}{\partial k_i} k_i + c\lambda z \partial_z. \tag{6.61}$$

From (6.8) and the on-shell solutions (6.50)-(6.53), the transformation law for $V_\xi^{(0)}$ is seen immediately

$$A_\xi' = A_\xi \Leftrightarrow V_\xi^{(0)'} = \lambda^{\frac{d}{2}+\nu_0} V_\xi^{(0)}. \tag{6.62}$$

For $V_z^{(0)}$ we have

$$A_z' = \lambda A_z - cz A_\xi \Leftrightarrow V_z^{(0)'} = \lambda^{\frac{d}{2}+\nu_0+2} V_z^{(0)} - c\lambda^{\frac{d}{2}+\nu_0+1} V_\xi^{(0)}. \tag{6.63}$$

For $V_i^{(0)}$, the transformation law

$$A_i' = \lambda A_i - ic \frac{\partial}{\partial k_i} A_\xi$$

gives

$$\begin{aligned}
&V_i^{(0)'} z^{\frac{d}{2}} k^{-\nu_0} \lambda^{-\frac{d}{2}-\nu_0} K_{\nu_0} - i k_i V_z^{(0)'} z^{\frac{d}{2}+1} k^{-\nu_0-1} \lambda^{-\frac{d}{2}-\nu_0-1} K_{\nu_0+1} \\
&= \lambda \Big(V_i^{(0)} \; z^{\frac{d}{2}} k^{-\nu_0} K_{\nu_0} - i \frac{k_i}{k} V_z^{(0)} \; z^{\frac{d}{2}+1} k^{-\nu_0} K_{\nu_0+1} \Big) - ic \frac{\partial}{\partial k_i} \Big(V_\xi^{(0)} \; z^{\frac{d}{2}} k^{-\nu_0} K_{\nu_0} \Big).
\end{aligned}$$

Using $\frac{\partial}{\partial k_i}\Big(k^{-\nu_0} K_{\nu_0}\Big) = -z k_i k^{-\nu_0-1} K_{\nu_0+1}$ and equations (6.62), (6.63), the above equation implies

$$\begin{aligned}
&V_i^{(0)'} K_{\nu_0} - i k_i z k^{-1} \lambda^{-1} K_{\nu_0+1} \Big(\lambda^{\frac{d}{2}+\nu_0+2} V_z^{(0)} - c\lambda^{\frac{d}{2}+\nu_0+1} V_\xi^{(0)} \Big) \\
&= \lambda \Big(V_i^{(0)} \; \lambda^{\frac{d}{2}+\nu_0} K_{\nu_0} - i \frac{k_i}{k} V_z^{(0)} \; z\lambda^{\frac{d}{2}+\nu_0} K_{\nu_0+1} \Big) - ic \frac{\partial}{\partial k_i} V_\xi^{(0)} \lambda^{\frac{d}{2}+\nu_0} K_{\nu_0} + ic V_\xi^{(0)} \frac{k_i}{k} z \lambda^{\frac{d}{2}+\nu_0} K_{\nu_0+1}
\end{aligned}$$

or

$$V_i^{(0)'} = \lambda^{\frac{d}{2}+\nu_0+1} V_i^{(0)} - ic\lambda^{\frac{d}{2}+\nu_0} \frac{\partial}{\partial k_i} V_\xi^{(0)}. \tag{6.64}$$

For $V_t^{(0)}$, the computation is more involved but straightforward. From

$$A_t' = \lambda^2 A_t + c\frac{i\partial}{\partial k_i}\lambda A_i + cz\lambda A_z - \frac{c^2}{2}(-\frac{\partial^2}{\partial k_i^2} + z^2)A_\xi$$

we get

$$\begin{aligned}
&V_t^{(0)'} z^{\frac{d}{2}} k^{-\nu_0} \lambda^{-\frac{d}{2}-\nu_0} K_{\nu_0} - \kappa^V y_{\nu_0} V_\xi^{(0)'} z^{\frac{d}{2}} k^{2-\nu_0} \beta^2 \lambda^{-\frac{d}{2}-\nu_0+2} K_{\nu_0} - \frac{\partial}{\partial t'}\Big(V_z^{(0)'} z^{\frac{d}{2}+1} k^{-\nu_0-1} \lambda^{-\frac{d}{2}-\nu_0-2} K_{\nu_0+1}\Big) \\
&+ V_\xi^{(0)'} z^{\frac{d}{2}} k^{-\nu_0+2} \lambda^{-\frac{d}{2}-\nu_0+2} X \\
=&\lambda^2\Big(V_t^{(0)} z^{\frac{d}{2}} k^{-\nu_0} K_{\nu_0} - \kappa^V y_{\nu_0} V_\xi^{(0)} z^{\frac{d}{2}} k^{2-\nu_0} \beta^2 K_{\nu_0} - \frac{\partial}{\partial t}\Big(V_z^{(0)} z^{\frac{d}{2}+1} k^{-\nu_0-1} K_{\nu_0+1}\Big) + V_\xi^{(0)} z^{\frac{d}{2}} k^{-\nu_0+2} X\Big) \\
&+ c\lambda\frac{i\partial}{\partial k_i}\Big(V_i^{(0)}\ z^{\frac{d}{2}} k^{-\nu_0} K_{\nu_0} - i\frac{k_i}{k} V_z^{(0)}\ z^{\frac{d}{2}+1} k^{-\nu_0} K_{\nu_0+1}\Big) \\
&+ cz\lambda V_z^{(0)}\ z^{\frac{d}{2}+1} k^{-\nu_0} K_{\nu_0} - \frac{c^2}{2}(z^2 - \frac{\partial^2}{\partial k_i^2})\Big(V_\xi^{(0)}\ z^{\frac{d}{2}} k^{-\nu_0} K_{\nu_0}\Big),
\end{aligned}$$

where $X = \beta^2\Big(\frac{d-2\nu_0}{16\nu_0(\nu_0+1)^2} K_{\nu_0+2} - \frac{d+2\nu_0}{16\nu_0(\nu_0-1)^2} K_{\nu_0-2} - \frac{2+d}{4\nu_0(\nu_0^2-1)} \frac{\partial}{\partial \nu_0} K_{\nu_0}\Big)$. After a careful calculation, this gives

$$V_t^{(0)'} = \lambda^{\frac{d}{2}+\nu_0+2} V_t^{(0)} + ic\lambda^{\frac{d}{2}+\nu_0+1} \frac{\partial}{\partial k_i} V_i^{(0)} + \frac{c^2}{2}\lambda^{\frac{d}{2}+\nu_0} \frac{\partial^2}{\partial k_i^2} V_\xi^{(0)}. \tag{6.65}$$

Thus, (6.62), (6.63), (6.64) and (6.65) confirm that $\{V_t^{(0)}, V_i^{(0)}, V_\xi^{(0)}\}$ belong to a spin-1 (boundary) representation with dimensions $\{\frac{d}{2}+\nu_0+2, \frac{d}{2}+\nu_0+1, \frac{d}{2}+\nu_0\}$. The way in which $V_z^{(0)}$ transforms is unusual, but it is necessary to ensure that the Lorentz condition (6.54) is K and C invariant.

For the sources, the computation is a little bit more complicated but the spirit is the same. What we get is again a spin-1 representation, with dimensions $\{\frac{d}{2}-\nu_0+2, \frac{d}{2}-\nu_0+1, \frac{d}{2}-\nu_0\}$. The dual operators $\{\hat{J}_t, \hat{J}_i, \hat{J}_\xi\}$ therefore carry a spin-1 representation with dimensions $\{\frac{d}{2}+\nu_0+2, \frac{d}{2}+\nu_0+1, \frac{d}{2}+\nu_0\}$. The boundary coupling is

$$S_I = \int d^d x dt\Big(S_t^{(0)}\hat{J}_\xi + S_\xi^{(0)}\hat{J}_t + S_i^{(0)}\hat{J}_i\Big). \tag{6.66}$$

6.4.3 Variational Principle, Renormalization and 2-point Functions

As standard in holography, we need to add counter terms to the bulk action (6.49) to make the variational principle work properly and simultaneously cancel all the divergences. A proper variational principle requires the action's variation to vanish under normalizable fluctuations of the bulk fields [38]. As the fluctuations are necessarily off-shell, first of all we have to define the off-shell bulk fields. As is customary, the off-shell fields are taken to have the same near boundary expansion as the on-shell solutions (6.50)-(6.53), except that the coefficients of different powers of z are completely unrelated. Hence, we postulate the off-shell field to be of the form

$$A_\xi(z) = z^{\frac{d}{2}}\Big(S_\xi^{(0)} z^{-\nu_0} - \frac{1}{4(\nu_0-1)}k^2 S_\xi^{(2)} z^{2-\nu_0} + \cdots + V_\xi^{(0)} z^{\nu_0} + \frac{1}{4(\nu_0+1)}k^2 V_\xi^{(2)} z^{2+\nu_0}\ldots\Big) \tag{6.67}$$

$$A_z(z) = z^{\frac{d}{2}}\Big(S_z^{(0)} z^{-\nu_0} - \frac{1}{4(\nu_0-1)}k^2 S_z^{(2)} z^{2-\nu_0} + \cdots + V_z^{(0)} z^{\nu_0} + \frac{1}{4(\nu_0+1)}k^2 V_z^{(2)} z^{2+\nu_0}\ldots\Big) \tag{6.68}$$

$$A_i(z) = z^{\frac{d}{2}}\Big(S_i^{(0)} z^{-\nu_0} - \frac{1}{4(\nu_0-1)}k^2 S_i^{(2)} z^{2-\nu_0} + \cdots + V_i^{(0)} z^{\nu_0} + \frac{1}{4(\nu_0+1)}k^2 V_i^{(2)} z^{2+\nu_0}\ldots\Big) \tag{6.69}$$

$$\begin{aligned} A_t(z) = z^{\frac{d}{2}}\Big(S_t^{(0)} z^{-\nu_0} - \frac{1}{4(\nu_0-1)}k^2 S_t^{(2)} z^{2-\nu_0} + \cdots + V_t^{(0)} z^{\nu_0} + \frac{1}{4(\nu_0+1)}k^2 V_t^{(2)} z^{2+\nu_0}\ldots\Big) \\ + \frac{2+d}{4\nu_0(\nu_0^2-1)} z^{\frac{d}{2}}\ln(kz)\; k^2\beta^2\Big(S_\xi^{(0)} z^{-\nu_0} + \cdots - V_\xi^{(0)} z^{\nu_0} + \ldots\Big) \\ + z^{\frac{d}{2}-2}\beta^2\Big(\frac{d-2\nu_0}{4(\nu_0+1)} S_\xi^{(0)} z^{-\nu_0} - \frac{d+2\nu_0}{4(\nu_0-1)} V_\xi^{(0)} z^{\nu_0}\Big), \end{aligned} \tag{6.70}$$

where $\mathbf{S}^{(0)}, \mathbf{S}^{(2)}, \mathbf{V}^{(0)}, \mathbf{V}^{(2)}, \ldots$ are independent coefficients. On-shell, for example, $\mathbf{S}^{(0)}$ and $\mathbf{V}^{(0)}$ are given in (6.55) and (6.56) respectively. Notice the logarithmic behavior in (6.70), coming from the ν-derivative term in the solution (6.53). Generically we do not have this kind of behavior in the $n \neq 0$ case, even in the relativistic counterpart. However, as we will see, these terms will disappear in the renormalized on-shell action.

The on-shell action (6.49) evaluates to

$$S_{os} = -\frac{R}{4}\int_{z=\epsilon} d^d x dt \sqrt{-g} A_\mu F^{z\mu}. \tag{6.71}$$

As is customary [37, 38], the counter terms consist of Galilean invariant combinations of induced field at the boundary. The most general form of this type is

$$S_{ct} = -\frac{R}{4}\int_{z=\epsilon} d^d k d\omega \sqrt{-\gamma}\Big(a(q)\; z^2(2A_t A_\xi + A_i A_i) + b(q)\; A_\xi A_\xi + c(q)\; z^2(-i\omega A_\xi + i k_i A_i)^2\Big), \tag{6.72}$$

where γ is the $d+2$-dimensional induced metric and $a(q)$, $b(q)$, $c(q)$ are polynomials of $q = k^2 z^2$ [3], of which the coefficients are to be determined. It is physically illuminating to divide S_{ct} into two pieces. One piece involves the first few order of $a(q)$, $b(q)$ and $c(q)$, responsible for ensuring a proper variational principle plus canceling the leading divergences in the renormalized action. We will call this piece the Gibbons-Hawking term, after the same name in gravity. At first sight, solving for the Gibbons-Hawking term always involves an over-determined system of equations. The success of the variational principle and renormalization procedure depends crucially on whether or not this system of equations is actually reducible to a solvable system. This is what happens in the fermion case, where the system in fact turns out to be under-determined [38]. In the case at hand, as we will see, the system is critical for $\nu_0 > 1$ and the Gibbons-Hawking term is unique. For $\nu_0 < 1$, the system is over-determined. As discussed later, this might be related to the fact that there is a singular point $\nu_0 = 1$.

The other piece consists of higher order terms in $a(q)$, $b(q)$ and $c(q)$ so that no normalizable fluctuation survives the $z \to 0$ limit. This piece thus only takes care of the cancelation of (subleading) divergences. We call it the counter-term. Since S_{ct} is the most general Galilean invariant combination, at any order of z the requirement of divergence cancelation leads at most to a critical system of equations. As a result, in principle the counter-term can always be solved. Also, in contrast to the Gibbons-Hawking term, the counter-term, along with the number of divergences in the bulk action, depends greatly on dimensionality and the mass. Finally, it does not have any finite contribution, since if it had, so would its variation, which contradicts its defining property. We will not discuss the counterterms much further.

Determining the Gibbons-Hawking term is indeed the central task in the variational principle and renormalization procedure. Using for (6.67)-(6.70) for the field and their variation (with $\mathbf{V}$ replaced by $\delta\mathbf{V}$ appropriately), we collect the divergent and finite terms in δS that involve the normalizable fluctuation $\delta\mathbf{V}$

$$\begin{aligned}
\delta S &= -\frac{R}{2}\sqrt{-g}\delta A_\mu F^{z\mu} \\
&= \left\{ \frac{R(d^2-4\nu_0^2)}{8z^2(\nu_0^2-1)} - \frac{Rk^2(\nu_0^2 d^2+\nu_0 d^2-8d+4\nu_0^2 d+16\nu_0 d-4d\nu_0^3-12\nu_0^3+4\nu_0^4+32\nu_0-16)}{64\nu_0(\nu_0-1)^2(\nu_0+1)} \right\}\times \\
&\times S_\xi^{(0)}\delta V_\xi^{(0)} - \frac{R(d-2\nu_0)}{4}\Big(S_t^{(0)}\delta V_\xi^{(0)} + S_\xi^{(0)}\delta V_t^{(0)} + S_i^{(0)}\delta V_i^{(0)}\Big) - \frac{R(d^2-4\nu_0^2)}{64(\nu_0+1)^2} S_\xi^{(0)}\delta V_\xi^{(2)} \\
&+ z^{2\nu_0-2}\frac{R\nu_0^2(d+2)}{2(\nu_0^2-1)} V_\xi^{(0)}\delta V_\xi^{(0)}
\end{aligned} \tag{6.73}$$

(the integral over the transverse momentum is implied). These terms have to be cancelled against terms

[3] Should $a(q)$, $b(q)$ and $c(q)$ contain $\ln(kz)$ to take care of the logarithmic terms in the bulk action? Fortunately not. Since $\partial_{\nu_0} K_{\nu_0} C_\xi \sim (I_{-\nu_0}+I_{\nu_0})\ln(kz) C_\xi$ and $K_{\nu_0} C_t \sim (I_{-\nu_0}-I_{\nu_0})C_t$, a cancelation of terms schematically of the form $\sim X_t X'_\xi$ will automatically ensure the cancelation of $\sim \ln(kz) X_\xi X'_\xi$, where X and X' stand for any coefficients $S^{(k)}$, $V^{(k)}$ and their variations

coming from the variation of the Gibbons-Hawking term. As there is k^2 in δS, the Gibbons-Hawking term is parametrized by four unknowns

$$S_{GH} = -\frac{R}{4}\int_{z=\epsilon} d^d k d\omega \sqrt{-\gamma}\Big(a_0\ z^2(2A_tA_\xi + A_iA_i) + b_0\ A_\xi A_\xi + a_1\ k^2 z^4(2A_tA_\xi + A_iA_i) + b_1\ k^2 z^2 A_\xi A_\xi\Big) \tag{6.74}$$

These unknowns are subjected to further constraints that the leading (up to k^2) divergences of S_{GH} have to cancel those of S_{os}. The latter evaluates to

$$\begin{aligned} S_{os}^{div} &= z^{-2\nu_0}\left\{\frac{Rd(2\nu_0-d)}{z^2 16(\nu_0+1)} + \frac{Rk^2(\nu_0 d^2 + 4\nu_0 d - 4d - 8 - 4\nu_0^3 + 8\nu_0)}{64\nu_0(\nu_0-1)(\nu_0+1)} - \frac{Rk^2(d+2)(d-2\nu_0)}{16\nu_0(\nu_0-1)(\nu_0+1)}\ln z\right\} S_\xi^{(0)} S_\xi^{(0)} \\ &+ z^{-2\nu_0}\Big(-\frac{R(d-2\nu_0)}{8} - \frac{R(2\nu_0-d-2)}{16(\nu_0-1)}k^2 z^2\Big)\Big(2S_t^{(0)}S_\xi^{(0)} + S_i^{(0)}S_i^{(0)}\Big) + \frac{R(d^2-4\nu_0^2)}{16z^2(\nu_0^2-1)} S_\xi^{(0)} V_\xi^{(0)} \\ &+ z^{2\nu_0-2}\frac{R\nu_0^2(d+2)}{4(\nu_0^2-1)} V_\xi^{(0)} V_\xi^{(0)} + o(k^4). \end{aligned} \tag{6.75}$$

Computing similarly δS_{GH} and S_{GH}^{div} in terms of a_0, a_1, b_0 and b_1, we obtain a highly over-determined system: twelve conditions (five for the variational principle and seven for the leading divergences) with four unknowns. This system is not solvable for generic values of ν_0. However, for $\nu_0 > 1$ the last term in (6.73) and (6.75) becomes irrelevant, and the system collapses to a critical one, giving a unique Gibbons-Hawking term

$$\begin{aligned} S_{GH} = -\frac{R}{4}\int_{z=\epsilon} d^d k d\omega \sqrt{-\gamma}\Big(&\frac{d-2\nu_0}{2} z^2(2A_tA_\xi + A_iA_i) + \frac{\nu_0(d-2\nu_0)}{2(\nu_0+1)} A_\xi A_\xi \\ &- \frac{1}{2(\nu_0-1)}k^2 z^4(2A_tA_\xi + A_iA_i) + \frac{d+2-2\nu_0^2-2\nu_0}{4\nu_0(\nu_0^2-1)}k^2 z^2 A_\xi A_\xi\Big). \end{aligned} \tag{6.76}$$

The renormalized on-shell action takes the form

$$\begin{aligned} S_{R,os} = -\frac{R}{4}\int_{z=\epsilon} d^d k d\omega \sqrt{-\gamma}\Big\{&2\nu_0\Big(S_t^{(0)}V_\xi^{(0)} + S_\xi^{(0)}V_t^{(0)} + S_i^{(0)}V_i^{(0)}\Big) \\ &+ \Big(\frac{\nu_0^4 d - 5\nu_0^2 d - 8\nu_0^2 + 2d + 4}{4\nu_0(\nu_0^2-1)^2}\Big)k^2 S_\xi^{(0)} V_\xi^{(0)}\Big\}. \end{aligned} \tag{6.77}$$

Now we can use the Lorentz condition (6.54) to write C_z in terms of the sources

$$C_z = \frac{2ik^{\nu_0}}{x_{\nu_0}(d+2\nu_0)}\Big(k_i S_i^{(0)} - \omega S_\xi^{(0)}\Big). \tag{6.78}$$

Using (6.55) and (6.56), the renormalized on-shell action can be rewritten as

$$S_{R,os} = -\frac{R\nu_0 y_{\nu_0}}{2x_{\nu_0}} \int_{z=\epsilon} d^d k d\omega \sqrt{-\gamma}\, k^{2\nu_0} \Big\{ 2S_t^{(0)} S_\xi^{(0)} + \Big(\delta_{ij} - \frac{4\nu_0}{d+2\nu_0}\frac{k_i k_j}{k^2}\Big) S_i^{(0)} S_j^{(0)} \\ + \frac{8\nu_0}{d+2\nu_0}\frac{\omega k_i}{k^2} S_i^{(0)} S_\xi^{(0)} + \Big(-\frac{4\nu_0}{d+2\nu_0}\frac{\omega^2}{k^4} + (\kappa^V - \kappa^S) + \frac{\nu_0^4 d - 5\nu_0^2 d - 8\nu_0^2 + 2d + 4}{8\nu_0^2(\nu_0^2-1)^2}\Big) k^2 S_\xi^{(0)} S_\xi^{(0)} \Big\}.$$

As repeatedly mentioned, we have a freedom (6.22) to redefine the sources to simplify the current 2-point functions. Taking the new $S_t^{(0)}$ to be

$$S_t^{(0)} \equiv S_t^{(0)} + \Big(\frac{\kappa^V - \kappa^S}{2} + \frac{\nu_0^4 d - 5\nu_0^2 d - 8\nu_0^2 + 2d + 4}{16\nu_0^2(\nu_0^2-1)^2}\Big) k^2 S_\xi^{(0)} \tag{6.79}$$

we finally get

$$S_{R,os} = -\frac{R\nu_0 y_{\nu_0}}{2x_{\nu_0}} \int_{z=\epsilon} d^d k d\omega \sqrt{-\gamma}\, k^{2\nu_0} \Big\{ 2S_t^{(0)} S_\xi^{(0)} + \Big(\delta_{ij} - \frac{4\nu_0}{d+2\nu_0}\frac{k_i k_j}{k^2}\Big) S_i^{(0)} S_j^{(0)} \\ + \frac{8\nu_0}{d+2\nu_0}\frac{\omega k_i}{k^2} S_i^{(0)} S_\xi^{(0)} - \frac{4\nu_0}{d+2\nu_0}\frac{\omega^2}{k^2} S_\xi^{(0)} S_\xi^{(0)} \Big\}.$$

The 2-point functions can be deduced immediately

$$G_{mn} = -\frac{R\nu_0 y_{\nu_0}}{x_{\nu_0}} k^{2\nu_0} \begin{pmatrix} -\frac{4\nu_0}{d+2\nu_0}\frac{\omega^2}{k^2} & \frac{4\nu_0}{d+2\nu_0}\frac{\omega k_i}{k^2} & 1 \\ \frac{4\nu_0}{d+2\nu_0}\frac{\omega k_j}{k^2} & \delta_{ij} - \frac{4\nu_0}{d+2\nu_0}\frac{k_i k_j}{k^2} & 0 \\ 1 & 0 & 0 \end{pmatrix}, \tag{6.80}$$

The Fourier transform (along with re-scaling of the operators appropriately) gives the form that we anticipated above, (6.23). Notice that in contrast to the $n \neq 0$ case, the $m_0 \to 0$ limit is nowhere singular and there is no apparent reduction of degrees of freedom. This is because in this limit, the Lorentz condition (6.54) does not fix the gauge completely. The remaining gauge freedom instead imposes the continuity relation on the boundary currents

$$\partial_t J_\xi + \partial_i J_i = 0$$

.

6.5 Conclusions

In this chapter, we have carefully considered the representation theory of vector fields and the corresponding vector operators in the spacetime with Schrödinger isometry, and worked out the boundary renormalization

and determination of boundary 2-point functions. We have found that the case of non-zero particle number is quite different from that of zero particle number. In the latter case, we have the same situation as in AdS where the z-component of the vector field is unphysical holographically, leaving the sources to form a spin-1 representation of the boundary Schrödinger group. In the former case, however, it is the t-component of the vector field that becomes unphysical. The z and ξ-components, corresponding to the two extra dimensions, combine to source a pair of scalar operators. The dual operator content is a spatial vector multiplet and either a pair of scalar multiplets (for $m_0 \neq 0$) or a single scalar multiplet (for $m_0 = 0$). In any cases, the 2-point functions for the dual operators are computed.

The variational principle and renormalization procedure is also carried out deliberately for any values of n following the method set out in [38]. In the case where $n = 0$, we found that the procedure only works for $\nu_0 > 1$. We believe this is related to the apparent singularity at $\nu_0 = 1$, which seems to signal the fact that for $\nu_0 < 1$ things should be treated quite differently. These cases are definitely interesting and will be left for future study.

Appendix A

Free energies of possible bulk backgrounds

Following [48] we use the notation adopted in [130] to compute the free energy of possible finite temperature Dq-brane backgrounds for type IIA and IIB supergravity, both compact and non-compact x^q-direction.

A.1 Compact x^q

The relevant parts of the supergravity action (in string frame) are

$$\begin{aligned} S &= -(S_{\rm EH} + S_\phi + S_{\rm RR} + S_{\rm NS}), \\ &= -\int e^{-2\phi}\sqrt{g}(\mathcal{R} + 4\partial\phi\partial\phi) + \frac{1}{2}\sum_q \int F_{(q+2)} \wedge *F_{(q+2)} + \frac{1}{2}\int e^{-2\phi} H_{(3)} \wedge *H_{(3)}. \end{aligned} \tag{A.1}$$

We are interested in backgrounds with $H_{(3)}$ not turned on, and choose the following ansatz for the metric and the RR q-form C_{q+1}

$$ds^2 = d\tau^2 + e^{2\lambda(\tau)} dx_\parallel^2 + e^{2\tilde{\lambda}(\tau)} dx_c^2 + e^{2\nu(\tau)} d\Omega_k^2, \tag{A.2}$$

$$C_{(q+1)} = A\, dx^1 \wedge ... \wedge dx^{q-1} \wedge dx^{q-c} \wedge dx^c, \tag{A.3}$$

where $k = 8 - q$, and $d\Omega_k^2$ is the line element of unit k-sphere. Again, we have set $l_s = 1$. The equation of motion for $C_{(q+1)}$ has the solution

$$\dot{A} e^{-q\lambda - \tilde{\lambda} + k\nu} = \text{const.} \tag{A.4}$$

The RR action then becomes

$$-S_{\rm RR} = \int Q^2 e^{q\lambda + \tilde{\lambda} - k\nu} d\tau, \tag{A.5}$$

where, again, we denoted the integration constant by Q^2. For convenience, we change the variable from τ to ρ defined by $d\rho = -e^{\varphi}d\tau$, where

$$\varphi = 2\phi - q\lambda - \tilde{\lambda} - k\nu. \tag{A.6}$$

Then

$$-S_{\rm RR} = -\int Q^2 e^{q\lambda+\tilde{\lambda}-k\nu-\varphi}d\rho. \tag{A.7}$$

Following the same argument as we did for $q = 6$, it is not hard to see that the action (A.1) takes the form

$$S = \int \Big(k(k-1)e^{-2\nu-2\varphi} - q\lambda'^2 - \tilde{\lambda}'^2 - k\nu'^2 + \varphi'^2 - Q^2 e^{q\lambda+\tilde{\lambda}-k\nu}\Big)d\rho. \tag{A.8}$$

Having put the action in the above form, the equations of motion are now in order

$$\lambda'' = \frac{Q^2}{2}e^{-2\phi+2q\lambda+2\tilde{\lambda}} \tag{A.9}$$

$$\tilde{\lambda}'' = \frac{Q^2}{2}e^{-2\phi+2q\lambda+2\tilde{\lambda}} \tag{A.10}$$

$$\nu'' = (k-1)e^{-2\nu-2\varphi} - \frac{Q^2}{2}e^{-2\phi+2q\lambda+2\tilde{\lambda}} \tag{A.11}$$

$$\phi'' = \frac{(5-k)Q^2}{2}e^{-2\phi+2q\lambda+2\tilde{\lambda}}, \tag{A.12}$$

Define $\Phi = -2\phi + 2q\lambda + 2\tilde{\lambda}$, (A.9), then (A.10) and (A.12) result in

$$\Phi'' = 4Q^2 e^{\Phi}, \tag{A.13}$$

which yields the following solution

$$\Phi = -2\ln\big(\frac{\sqrt{2}Q}{CC_1}\sinh C_1\rho\big) - 2\ln C. \tag{A.14}$$

The last term is there just for convenience. Solving for λ, $\tilde{\lambda}$ and ϕ in (A.9), (A.10) and (A.12), we obtain

$$\lambda = -\frac{1}{4}\ln\Big(\frac{\sqrt{2}Q}{g_s C_1}\sinh C_1\rho\Big) + C_2^{\lambda}\rho, \tag{A.15}$$

$$\tilde{\lambda} = -\frac{1}{4}\ln\Big(\frac{\sqrt{2}Q}{g_s C_1}\sinh C_1\rho\Big) + C_2^{\tilde{\lambda}}\rho, \tag{A.16}$$

$$\phi = -\frac{5-k}{4}\ln\Big(\frac{\sqrt{2}Q}{g_s C_1}\sinh C_1\rho\Big) + C_2^{\phi}\rho + \ln g_s, \tag{A.17}$$

with $qC_2^\lambda + C_2^{\tilde{\lambda}} - C_2^\phi = 0$. The constants C_1, C_2^λ, $C_2^{\tilde{\lambda}}$ and C_2^ϕ are to be determined. Define $\Phi_0 = \Phi + 2\ln g_s$, then the equation of motion for ν becomes

$$\nu'' = (k-1)e^{\frac{7-q}{4}\Phi_0 - 2C_2^\phi \rho - 4\ln g_s + 2(k-1)\nu} - \frac{1}{2}Q^2 e^{\Phi}. \tag{A.18}$$

If we take $2(k-1)\nu = \frac{q-3}{4}\Phi_0 + 2C_2^\phi \rho + C_\nu$, then the above equation is satisfied if

$$C_\nu = \ln \frac{2Q^2 g_s^2}{(k-1)^2}. \tag{A.19}$$

Thus, we obtain

$$\nu = -\frac{5-k}{4(k-1)} \ln\Big(\frac{\sqrt{2}Q}{g_s C_1}\sinh C_1 \rho\Big) + \frac{C_2^\phi \rho}{k-1} + \frac{1}{k-1}\ln\frac{\sqrt{2}Qg_s}{k-1}. \tag{A.20}$$

We now check whether the near horizon geometry of non-extremal Dq-branes satisfies (A.15), (A.16), (A.17) and (A.20). This geometry takes the form

$$\begin{aligned} ds^2 &= f_q^{-1/2}\Big(dx_\parallel^2 + h dx_c^2\Big) + f_q^{1/2}\Big(\frac{1}{h}du^2 + u^2 d\Omega_k^2\Big), & \text{(A.21)} \\ e^{-2\phi} &= g_s^{-2} f_q^{(q-3)/2}, & \text{(A.22)} \end{aligned}$$

where $f_q = \frac{d_q' g_s N_c}{(l_s u)^{7-q}}$, $d_p' = (2\sqrt{\pi})^{5-q}\Gamma(\frac{7-q}{2})$ and $h = 1 - (u_c/u)^{7-q}$.The relation between u and pho can is inferred from (A.15) and (A.16)

$$e^{2(\tilde{\lambda}-\lambda)} = e^{2\rho(C_2^{\tilde{\lambda}} - C_2^\lambda)} = h, \tag{A.23}$$

which gives

$$\rho = \frac{1}{2\Delta C_2}\ln h \qquad \Rightarrow \qquad d\rho = \frac{(7-q)u_c^{7-q}u^{q-8}}{2\Delta C_2}\frac{1}{h}du, \tag{A.24}$$

where $\Delta C_2 = C_2^{\tilde{\lambda}} - C_2^{\lambda}$. Calculating $e^{2\lambda}$ from (A.15), we have

$$\begin{aligned} e^{2\lambda} &= \frac{e^{2C_2^{\lambda}\rho}}{\sqrt{\left(\frac{\sqrt{2}Q}{g_s C_1}\right)\sinh C_1\rho}} \\ &= \sqrt{\frac{\sqrt{2}C_1 g_s}{Q}}\frac{h^{\frac{C_2^{\lambda}}{\Delta C_2}}}{\sqrt{h^{\frac{C_1}{2\Delta C_2}} - h^{\frac{-C_1}{2\Delta C_2}}}} \\ &= \sqrt{\frac{\sqrt{2}C_1 g_s}{Q}}\frac{h^{\frac{C_2^{\lambda}}{\Delta C_2}-\frac{C_1}{4\Delta C_2}}}{\sqrt{1-h^{\frac{-C_1}{\Delta C_2}}}}. \end{aligned} \tag{A.25}$$

The only way to make $e^{2\lambda}$ in (A.25) to be equal to $f_q^{1/2}$ is by imposing $-C_1 = \Delta C_2$ and $C_1 = 4C_2^{\lambda}$, or

$$C_1 = 4C_2^{\lambda}; \qquad C_2^{\tilde{\lambda}} = -3C_2\lambda. \tag{A.26}$$

Thus, we have

$$e^{2\lambda} = \sqrt{\frac{\sqrt{2}C_1 g_s}{Q}}\Big(\frac{u}{u_c}\Big)^{\frac{7-q}{2}} \equiv f_q^{-1/2} \qquad \Rightarrow \qquad C_2^{\lambda} = \frac{Q(u_c l_s)^{7-q}}{4\sqrt{2}g_s^2 N_c d_q'}. \tag{A.27}$$

Also, the dilaton can be matched to (A.22) as long as we take $C_2^{\phi} = (5-k)C_2^{\lambda}$ resulting in

$$e^{2\phi} = e^{2\lambda(5-k)+2\ln g_s} = g_s^2 f_q^{-\frac{q-3}{2}}. \tag{A.28}$$

Furthermore, from (A.20), we have

$$e^{2\nu} = \Big(\frac{\sqrt{2}Qg_s}{k-1}\Big)^{\frac{2}{k-1}} e^{2\lambda\frac{5-k}{k-1}} \equiv f_q^{1/2}u^2 \qquad \Rightarrow \qquad N_c = \frac{\sqrt{2}Ql_s^{k-1}}{(k-1)d_q'}. \tag{A.29}$$

The final check is the g_{uu} component. To do that, we first need to compute $e^{-2\varphi}$ which gives

$$\begin{aligned} e^{-2\varphi} &= e^{-4\phi+2q\lambda+2\tilde{\lambda}+2k\nu} \\ &= e^{\frac{6k+2}{k-1}\lambda - 8C_2^{\lambda}\rho + \frac{2k}{k-1}\ln(\frac{\sqrt{2}Qg_s}{k-1}) - 4\ln g_s}. \end{aligned} \tag{A.30}$$

Hence

$$\begin{aligned} d\tau^2 &= e^{-2\varphi}d\rho^2 \\ &= \frac{(7-q)^2 u_c^{2(7-q)} u^{2(q-8)}}{64(C_2^\lambda)^2}\frac{1}{h^2}e^{\frac{6k+2}{k-1}\lambda - 8C_2^\lambda\rho + \frac{2k}{k-1}\ln(\frac{\sqrt{2}Qg_s}{k-1}) - 4\ln g_s}du^2 \\ &= f_q^{1/2}\frac{1}{h}du^2, \end{aligned} \tag{A.31}$$

where we have used (A.27) and (A.29) to simplify the expression. Therefore, the exact solution we just found indeed corresponds to the near horizon geometry of non-extremal N_c Dq-branes.

With (A.15), (A.16), (A.17) and (A.20) at hand, it is now straightforward to plug them into (A.8) to get the on-shell action. Changing back to the u coordinate and being careful about the fact that $d\rho/du$ is negative, we obtain (here prime denotes u derivative.)

$$\begin{aligned} S &= -V_9\int_{u_c}^{\infty}\Big\{\Big(-q\lambda'^2 - \tilde{\lambda}'^2 - k\nu'^2 + \varphi'^2\Big)\frac{du}{d\rho} + \Big(k(k-1)e^{-2\nu-2\varphi} - Q^2 e^{q\lambda+\tilde{\lambda}-k\nu}\Big)\frac{d\rho}{du}\Big\}du \\ &= \frac{9-q}{g_s^2}V_9\int_{u_c}^{\Lambda}(7-q)\ u^{6-q}du \\ &= \frac{9-q}{g_s^2}V_9\Big(\Lambda^{7-q} - u_c^{7-q}\Big), \end{aligned} \tag{A.32}$$

where Λ is the cutoff, and $V_9 = \beta R_c \mathrm{Vol}(\mathrm{S}^{8-q})\mathrm{Vol}(\mathbb{R}^{q-1})$ (in units where string length $l_s = 1$). For $q \leq 4$, it is not hard to see from (A.32) that the geometry given in (2.35) for which $u_c = 0$ has more free energy than the geometries given in (2.32) and (2.36). The difference in free energies of the thermal and black Dq-brane geometries is given by

$$S_{\text{thermal}} - S_{\text{black brane}} = \frac{9-q}{g_s^2}V_9\Big(u_T^{7-q} - u_{\text{KK}}^{7-q}\Big), \tag{A.33}$$

which using (2.34) and (2.38) can be equivalently expresses as

$$S_{\text{thermal}} - S_{\text{black brane}} = \frac{9-q}{g_s^2}V_9\left(\frac{4\pi}{7-q}R_{q+1}^{\frac{1}{2}(7-q)}\right)^{2\frac{7-q}{5-q}}\left(\beta^{2\frac{q-7}{5-q}} - \beta_c^{2\frac{q-7}{5-q}}\right). \tag{A.34}$$

Thus, for $q \leq 4$ there is a phase transition at $\beta = 2\pi R_c$. For $\beta > 2\pi R_c$ the thermal geometry (2.32) dominates whereas for $\beta < 2\pi R_c$ it is the black brane geometry (2.36) which dominates the Euclidean path integral. The case of D5-branes and any associated phase transition has been discussed in section 5.

A.2 Non-compact x^q

When x^q is not compact, and $q \neq 5$, there are only two geometries with the same asymptotic boundary condition: the thermal geometry (2.7) and the black brane geometry (2.2) . The difference in free energies of the two geometries is obtained by first setting $u_c = 0$ in (A.32) for the thermal and $u_c = u_T$ for the black brane geometry, then subtracting the results

$$S_{\text{thermal}} - S_{\text{black brane}} = \frac{9-q}{g_s^2} V_9 u_T^{7-q}, \tag{A.35}$$

where $V_9 = \text{Vol}(\text{S}^{8-q})\text{Vol}(\mathbb{R}^q)\text{Vol}(\text{S}^1_\beta)$ in units where $l_s = 1$. The difference in free energies (2.8) is positive indicating that independent of temperature the black brane geometry is always dominant and determines the vacuum. The case of D5-branes has been discussed in section 2.

Appendix B

Parity breaking in three dimensions

The qualitative behavior of the holographic dual of the torsion vortex solution found in chapter 3 could be captured by the three dimensional Gross-Neveu model coupled to abelian gauge fields. The Euclidean action of this model is[1]

$$I = -\int d^3x \left[\bar{\psi}^a \left(\not{\partial} - \mathrm{i}e\not{A}\right)\psi^a + \frac{G}{2N}\left(\bar{\psi}^a\psi^a\right)^2 + \frac{1}{4M}F_{\mu\nu}F_{\mu\nu}\right]. \tag{B.1}$$

M is an UV mass scale. Introducing the usual Lagrange multiplier field σ, whose equation of motion is $\sigma = \frac{-2G}{N}\bar{\psi}^a\psi^a$ we can make the action quadratic in the fermions

$$I = -\int d^3x \left[\bar{\psi}^a \left(\not{\partial} + \sigma - \mathrm{i}e\not{A}\right)\psi^a - \frac{N}{2G}\sigma^2 - \frac{1}{4M}F^{\mu\nu}F_{\mu\nu}\right]. \tag{B.2}$$

The model possesses two parity breaking vacua distinguished by the value of the pseudoscalar order parameter $\langle\sigma\rangle$. This is seen as follows: switching off the gauge fields momentarily one integrates over the fermions to produce a large-N effective action as

$$\mathcal{Z} = \int (\mathcal{D}\sigma) e^{N\left[\mathrm{tr}\log(\not{\partial}+\sigma) - \frac{1}{2G}\int d^3x\sigma^2\right]}. \tag{B.3}$$

The path integral has a non-zero large-N extremum σ_* found by setting $\sigma = \sigma_* + \frac{1}{\sqrt{N}}\lambda$

$$\mathcal{Z} = \int (\mathcal{D}\lambda) e^{N\left[\mathrm{tr}\log(\not{\partial}+\sigma_*) - \frac{1}{2G}\int d^3x\sigma_* + \frac{1}{\sqrt{N}}\left\{\mathrm{tr}\frac{\lambda}{\not{\partial}+\sigma_*} - \frac{\sigma_*}{G}\int d^3x\lambda\right\} + O(1/N)\right]} \tag{B.4}$$

The term in the curly brackets is the gap equation. To study it one considers a uniform momentum cutoff Λ to obtain

$$\frac{1}{G} = \int^{\Lambda} \frac{d^3p}{(2\pi)^3}\frac{2}{p^2+\sigma_*^2} = (\mathrm{tr}1)\left[\frac{\Lambda}{\pi^2} - \frac{|\sigma_*|}{\pi^2}\arctan\frac{\Lambda}{|\sigma_*|}\right]. \tag{B.5}$$

[1] We use $\bar{\psi}^i$, ψ^i $(a = 1, 2, ..., N)$ two-component Dirac fermions. The γ-matrices are defined in terms of the usual Pauli matrices as $\gamma^i = \sigma^i$ $i = 1, 2, 3$.

Defining the critical coupling as

$$\frac{1}{G_*} = \frac{\Lambda}{\pi^2}\,, \tag{B.6}$$

(B.5) possesses a non-zero solution for σ_* when $G > G_*$ given by

$$|\sigma_*| = \frac{2\pi}{G}\left(\frac{G}{G_*} - 1\right) \equiv m\,. \tag{B.7}$$

The two distinct parity breaking vacua then have

$$\sigma_* = -\frac{2G}{N}\langle\bar{\psi}^a\psi^a\rangle = \pm m\,. \tag{B.8}$$

Going back to (B.2) one can tune $G > G_*$ and start in any of the two parity breaking vacua. Suppose we start from $\sigma_* = +m$. To leading order in N we have

$$\mathcal{Z} = \int (\mathcal{D}A_\mu)(\mathcal{D}\bar{\psi}^a)(\mathcal{D}\psi^a) e^{\int d^3x\left[\bar{\psi}^a(\not{\partial}+m-\mathrm{i}e\not{A})\psi^a - \frac{N}{2G}m^2 + O(1/\sqrt{N}) - \frac{1}{4M}F^{\mu\nu}F_{\mu\nu}\right]} \tag{B.9}$$

As is well known [131, 132] for an odd number N of fermions the path integral (B.9) yields an effective action for the gauge fields which for low momenta is dominated by the Chern-Simons term i.e.

$$\mathcal{Z} \approx \int e^{S_{CS}}\,, \tag{B.10}$$

with

$$S_{CS} = \mathrm{i}\frac{ke^2}{4\pi}\int d^3x \epsilon^{\mu\nu\rho}A_\mu\partial_\nu A_\rho\,, \qquad k = \frac{N}{2}\,. \tag{B.11}$$

Had we started from the $\sigma_* = -m$ vacuum, we would have found again (B.10), however with $k = -\frac{N}{2}$, i.e. the vacuum with $\sigma_* = -m$ yields an effective Chern-Simons action with $k = -\frac{N}{2}$.

Consider now deforming the action (B.9) by the Chern-Simons term with a fixed coefficient as

$$\mathcal{Z} = \int (\mathcal{D}A_\mu)(\mathcal{D}\bar{\psi}^i)(\mathcal{D}\psi^i) e^{\int d^3x\left[\bar{\psi}^i(\not{\partial}+m-\mathrm{i}e\not{A})\psi^i - \frac{N}{2G}m^2 + O(1/\sqrt{N}) - \frac{1}{4M}F^{\mu\nu}F_{\mu\nu} - \mathrm{i}q\int d^3x\epsilon^{\mu\nu\rho}A_\mu\partial_\nu A_\rho\right]}\,. \tag{B.12}$$

If q is fixed to

$$q = \frac{Ne^2}{4\pi}\,, \tag{B.13}$$

the effective action for the gauge fields resulting from the fermionic path integrals in (B.12) is going to be *exactly equal* the one obtained when we start at the $\sigma_* = -m$ vacuum. In other words, deforming the

$\sigma_* = +m$ vacuum with a Chern-Simons term with a fixed coefficient is equivalent to being in the $\sigma_* = -m$ vacuum. This is exactly analogous to the holographic interpretation of our torsion vortex.

Appendix C

Off-shell fermions on Schrödinger geometry

In this appendix, we would like to identify the appropriate functional space for the off-shell fermion on Schrödinger geometry. The criteria is that the off-shell fermion should carry an irreducible representation of the bulk Schrödinger symmetry that encompass all vacuum solutions (5.57).

C.1 off-shell transformation

As a reminder, the realization in the bulk of the boost K_i and special conformal transformation C acting on fermions is

$$K_i = - t\partial_i + x_i\partial_\xi + \frac{z}{\beta}\gamma^0\gamma_i Q_- \tag{C.1}$$

$$=K_i^{(0)} + \frac{z}{\beta}\gamma^0\gamma_i Q_- \tag{C.2}$$

$$C =t(z\partial_z + \vec{x}\vec{\partial} + t\partial_t) - \frac{1}{2}(\vec{x}^2 + z^2)\partial_\xi + \frac{z}{\beta}(\not{x} + z\gamma^r)\gamma^0 Q_- \tag{C.3}$$

$$=C^{(0)} - \frac{1}{2}z^2\partial_\xi + \frac{z}{\beta}(\not{x} + z\gamma^r)\gamma^0 Q_-. \tag{C.4}$$

Motivated by the general solution of the Dirac equation, the off-shell spinors are assumed to have the near boundary expansion

$$\begin{aligned}\Psi =&z^{\Delta_+^-}\sum_{k=0}^{\infty} z^{2k}(\Psi^I_{(2k)} + z\Psi^I_{(2k+1)}) + z^{\Delta_+^+}\sum_{k=0}^{\infty} z^{2k}(\Psi^{II}_{(2k)} + z\Psi^{II}_{(2k+1)})\\ &+ z^{\Delta_-^-}\sum_{k=0}^{\infty} z^{2k}(\Psi^{III}_{(2k)} + z\Psi^{III}_{(2k+1)}) + z^{\Delta_-^+}\sum_{k=0}^{\infty} z^{2k}(\Psi^{IV}_{(2k)} + z\Psi^{IV}_{(2k+1)})\end{aligned} \tag{C.5}$$

containing four power series of z, in which the $\Psi_{(m)}$'s are in general full Dirac spinors. For generic values of d, m_0 and n these series do not talk to each other under Schrödinger transformations. Each of them form a separate representation of the Schrödinger group. As our purpose is to work out the transformation laws, it is sufficient to focus on just one of them, say the one with Δ_+^-. Results for the other series are inferred

immediately.

Let's re-parametrize the first series in terms of P and Q chiral spinors as follows

$$\Psi^I = \sum_{k,\varepsilon_r',\varepsilon_\ell'} z^{\Delta_+^- + 2k} \Big(\rho_{(2k)}^{\varepsilon_r'\varepsilon_\ell'} + \mathcal{Q}\, \rho_{(2k+1)}^{\varepsilon_r'\varepsilon_\ell'} \Big), \tag{C.6}$$

where $\gamma^r \rho_{(m)}^{\varepsilon_r\varepsilon_\ell} = \varepsilon_r \rho_{(m)}^{\varepsilon_r\varepsilon_\ell}$ and $\gamma^v\gamma^0 \rho_{(m)}^{\varepsilon_r\varepsilon_\ell} = \varepsilon_\ell \rho_{(m)}^{\varepsilon_r\varepsilon_\ell}$.

Our task is to find the transformation laws of $\rho_{(m)}^{\varepsilon_r\varepsilon_\ell}$ under the Schrödinger algebra, restricted to the non-trivial isometries K_i and C. We will then argue that it is possible to consistently reduce the representation by setting half of the fields to zero, leaving the $\rho_{(m)}^{\varepsilon_r +}$ untouched. At this point, the remaining fields $\rho_{(m)}^{++}$ and $\rho_{(m)}^{-+}$ transform independently, so one of them can be further set to zero under the criteria that the left-over representation should include all on-shell solutions. In particular, a suitable irreducible representation corresponds to keeping $\rho_{(m)}^{-+}$ for Ψ^I, Ψ^{II} and $\rho_{(m)}^{++}$ for Ψ^{III}, Ψ^{IV}.

Transformations of $\rho_{(m)}^{\varepsilon_r\varepsilon_\ell}$ are straightforwardly found by acting with K_i and C on (C.6) and reading off the coefficients of different powers of z. Projecting further by $P_{\varepsilon_r} Q_{\varepsilon_\ell}$ we get

$$\not{k}\delta_{K_i}\rho_{(2k+1)}^{\bar\varepsilon_r\varepsilon_\ell} = \not{k} K_i^{(0)} \rho_{(2k+1)}^{\bar\varepsilon_r\varepsilon_\ell} + \frac{1}{\beta}\gamma^0\gamma_i \rho_{(2k)}^{\varepsilon_r -}\delta_{\varepsilon_\ell,+} - n\gamma_i \rho_{(2k+1)}^{\bar\varepsilon_r -}\delta_{\varepsilon_\ell,-} \tag{C.7}$$

$$\not{k}\delta_C\rho_{(2k+1)}^{\bar\varepsilon_r\varepsilon_\ell} = C^{(0)}\not{k}\,\rho_{(2k+1)}^{\bar\varepsilon_r\varepsilon_\ell} + \frac{\not{x}}{\beta}\gamma^0\rho_{(2k)}^{\varepsilon_r -}\delta_{\varepsilon_\ell,+} - \frac{in}{2}\not{k}\,\rho_{(2k-1)}^{\bar\varepsilon_r\varepsilon_\ell} - n\not{x}\,\rho_{(2k+1)}^{\bar\varepsilon_r +}\delta_{\varepsilon_\ell,+} + \frac{1}{\beta}\gamma^r\gamma^0\not{k}\,\rho_{(2k-1)}^{\varepsilon_r -}\delta_{\varepsilon_\ell,+} \tag{C.8}$$

and

$$\begin{aligned}\delta_{K_i}\rho_{(2k)}^{\varepsilon_r\varepsilon_\ell} + n\beta\gamma^v\delta_{K_i}\rho_{(2k+1)}^{\bar\varepsilon_r\bar\varepsilon_\ell} + \frac{2\omega}{\beta}\gamma^0\delta_{K_i}\rho_{(2k-1)}^{\bar\varepsilon_r -}\delta_{\varepsilon_\ell,+} &= K_i^{(0)}\Big(\rho_{(2k)}^{\varepsilon_r\varepsilon_\ell} + n\beta\gamma^v\rho_{(2k+1)}^{\bar\varepsilon_r\bar\varepsilon_\ell} + \frac{2\omega}{\beta}\gamma^0\rho_{(2k-1)}^{\bar\varepsilon_r -}\delta_{\varepsilon_\ell,+}\Big) \\ &\quad - \frac{1}{\beta}\not{k}\gamma^0\gamma_i\rho_{(2k-1)}^{\bar\varepsilon_r -}\delta_{\varepsilon_\ell,+}\end{aligned} \tag{C.9}$$

$$\begin{aligned}\delta_C\rho_{(2k)}^{\varepsilon_r\varepsilon_\ell} + n\beta\gamma^v\delta_C\rho_{(2k+1)}^{\bar\varepsilon_r\bar\varepsilon_\ell} + \frac{2\omega}{\beta}\gamma^0\delta_C\rho_{(2k-1)}^{\bar\varepsilon_r -}\delta_{\varepsilon_\ell,+} &= C^{(0)}\Big(\rho_{(2k)}^{\varepsilon_r\varepsilon_\ell} + n\beta\gamma^v\rho_{(2k+1)}^{\bar\varepsilon_r\bar\varepsilon_\ell} + \frac{2\omega}{\beta}\gamma^0\rho_{(2k-1)}^{\bar\varepsilon_r -}\delta_{\varepsilon_\ell,+}\Big) \\ &\quad - \frac{in}{2}\rho_{(2k-2)}^{\varepsilon_r\varepsilon_\ell} + \frac{1}{\beta}\gamma^r\gamma^0\rho_{(2k-2)}^{\bar\varepsilon_r -}\delta_{\varepsilon_\ell,+} - \frac{in^2\beta}{2}\gamma^v\rho_{(2k-1)}^{\bar\varepsilon_r\bar\varepsilon_\ell} \\ &\quad - \frac{in\omega}{\beta}\gamma^0\rho_{(2k-3)}^{\bar\varepsilon_r -}\delta_{\varepsilon_\ell,+} + \frac{\not{x}}{\beta}\gamma^0\not{k}\,\rho_{(2k-1)}^{\bar\varepsilon_r -}\delta_{\varepsilon_\ell,+} - \varepsilon_r n\rho_{(2k-1)}^{\varepsilon_r +}.\end{aligned} \tag{C.10}$$

Here $\bar\varepsilon_{r,\ell} = -\varepsilon_{r,\ell}$ and $\rho_{(m)}^{\varepsilon_r'\varepsilon_\ell'}$, $m < 0$ are defined to be zero. It is also important to note that the action of $C^{(0)}$ (the part of C acting on functions), due to the term $z\partial_z$, depends on the dimension of the fields it acts

on. From (C.7) and (C.8), we see that $\rho^{\bar{\varepsilon}_r-}_{(2k-1)}$ transform into themselves

$$\not{k}\delta_{K_i}\rho^{\bar{\varepsilon}_r-}_{(2k+1)} = \not{k}K^{(0)}_i\rho^{\bar{\varepsilon}_r-}_{(2k+1)} - n\gamma_i\rho^{\bar{\varepsilon}_r-}_{(2k+1)} \tag{C.11}$$

$$\not{k}\delta_C\rho^{\bar{\varepsilon}_r-}_{(2k+1)} = C^{(0)}\not{k}\,\rho^{\bar{\varepsilon}_r-}_{(2k+1)} - \frac{in}{2}\not{k}\,\rho^{\bar{\varepsilon}_r-}_{(2k-1)}, \tag{C.12}$$

hence can be consistently set to zero. With that in mind, the transformations of $\rho^{\varepsilon_r-}_{(2k)}$ can be deduced from (C.7), (C.8), (C.9) and (C.10) to read

$$\not{k}\delta_{K_i}\rho^{\varepsilon_r-}_{(2k)} = \not{k}K^{(0)}_i\rho^{\varepsilon_r-}_{(2k)} - n\gamma_i\rho^{\varepsilon_r-}_{(2k)} \tag{C.13}$$

$$\not{k}\delta_C\rho^{\varepsilon_r-}_{(2k)}) = \not{k}C^{(0)}\rho^{\varepsilon_r-}_{(2k)} - \frac{in}{2}\not{k}\,\rho^{\varepsilon_r-}_{(2k-2)} + n\not{x}\,\rho^{\varepsilon_r-}_{(2k)}. \tag{C.14}$$

Again, they only transform into themselves. Thus, we have shown that the representation can be reduced by setting $\rho^{\varepsilon_r-}_{(m)} = 0$. The transformations of the remaining fields are simplified significantly

$$\delta_{K_i}\rho^{\varepsilon_r+}_{(2k+1)} = K^{(0)}_i\rho^{\varepsilon_r+}_{(2k+1)} \tag{C.15}$$

$$\delta_C\rho^{\varepsilon_r+}_{(2k+1)} = C^{(0)}\rho^{\varepsilon_r+}_{(2k+1)} - \frac{in}{2}\,\rho^{\varepsilon_r+}_{(2k-1)} \tag{C.16}$$

$$\delta_{K_i}\rho^{\varepsilon_r+}_{(2k)} = K^{(0)}_i\rho^{\varepsilon_r+}_{(2k)} \tag{C.17}$$

$$\delta_C\rho^{\varepsilon_r+}_{(2k)} = C^{(0)}\rho^{\varepsilon_r+}_{(2k)} - \frac{in}{2}\,\rho^{\varepsilon_r+}_{(2k-2)} - \varepsilon_r n\rho^{\varepsilon_r+}_{(2k-1)} \tag{C.18}$$

Looking at (C.15)-(C.18), we notice that fields with opposite ε_r index do not mix under the transformations as well. Thus, the representation can be maximally reduced by setting one of the two $\rho^{\varepsilon_r+}_{(m)}$ to zero. The criteria is obvious: the leftover representation must include all solutions of the Dirac equation. Thus, in (C.5) it corresponds to keeping only $\rho^{\bar{\varepsilon}_r+}_{(m)}$ in the series with leading order $z^{\Delta^{\pm}_{\varepsilon_r}}$. This gives the off-shell spinor

$$\Psi = \sum_{\varepsilon_r}\left[z^{\Delta^-_{-\varepsilon_r}}\sum_{k=0}^{\infty}z^{2k}\left(\rho^{\varepsilon_r}_{(2k)} + \mathcal{Q}\rho^{\varepsilon_r}_{(2k+1)}\right) + z^{\Delta^+_{-\varepsilon_r}}\sum_{k=0}^{\infty}z^{2k}\left(\chi^{\varepsilon_r}_{(2k)} + \mathcal{Q}\chi^{\varepsilon_r}_{(2k+1)}\right)\right], \tag{C.19}$$

where $\rho^{\varepsilon_r} = \rho^{\varepsilon_r+}$, etc.

C.2 Massless limit

In the massless limit, $\mu_+ = \mu_- = \mu$, $\Delta^{\pm}_- = \Delta^{\pm}_+ = \Delta^{\pm}$ and the expansion (C.5) collapses into just two series. However, for each series all the analysis carried out above is still valid. The only difference is that now to include all solutions of the Dirac equation in the reduced representation, for each series we must keep both

$\rho^{\varepsilon_r +}_{(m)}$ rather than just one of them. The transformation laws are the same as (C.15)-(C.18). Again, fields with opposite ε_r index do not mix under the transformations. Each series then contains two irreducible representations of the Schrödinger group, labeled by ε_r.

References

[1] Maldacena, Juan Martin, "*The large N limit of superconformal field theories and supergravity,*" *Adv. Theor. Math. Phys.* **2** (1998) 231-252, arXiv:hep-th/9711200.

[2] Itzhaki, Nissan and Maldacena, Juan Martin and Sonnenschein, Jacob and Yankielowicz, Shimon, "*Supergravity and the large N limit of theories with sixteen supercharges,*" *Phys. Rev.* **D58** (1998) 046004, arXiv:hep-th/9802042.

[3] C. P. Herzog, M. Rangamani, and S. F. Ross, "*Heating up Galilean holography,*" *JHEP* **11** (2008) 080, arXiv:0807.1099.

[4] J. Maldacena, D. Martelli, and Y. Tachikawa, "*Comments on string theory backgrounds with non-relativistic conformal symmetry,*" *JHEP* **10** (2008) 072, arXiv:0807.1100.

[5] A. Adams, K. Balasubramanian, and J. McGreevy, "*Hot Spacetimes for Cold Atoms,*" *JHEP* **11** (2008) 059, arXiv:0807.1111.

[6] D. T. Son, "*Toward an AdS/cold atoms correspondence: a geometric realization of the Schroedinger symmetry,*" *Phys. Rev.* **D78** (2008) 046003, arXiv:0804.3972.

[7] K. Balasubramanian and J. McGreevy, "*Gravity duals for non-relativistic CFTs,*" *Phys. Rev. Lett.* **101** (2008) 061601, arXiv:0804.4053.

[8] Karch, Andreas and Katz, Emanuel, "*Adding flavor to AdS/CFT,*" *JHEP* **06** (2002) 043, arXiv:hep-th/0205236.

[9] Kruczenski, Martin and Mateos, David and Myers, Robert C. and Winters, David J., "*Meson spectroscopy in AdS/CFT with flavour,*" *JHEP* **07** (2003) 049, arXiv:hep-th/0304032.

[10] Kirsch, Ingo , "*Spectroscopy of fermionic operators in AdS/CFT,*" *JHEP* **09** (2006) 052, arXiv:hep-th/0607205.

[11] Babington, J. and Erdmenger, J. and Evans, Nick J. and Guralnik, Z. and Kirsch, I., "*Chiral symmetry breaking and pions in non-supersymmetric gauge/gravity duals,*" *Phys. Rev.* **D69** (2004) 077007, arXiv:hep-th/0306018.

[12] Evans, Nick J. and Shock, Jonathan P., "*Chiral dynamics from AdS space,*" *Phys. Rev.* **D70** (2004) 046002, arXiv:hep-th/0403279.

[13] T. Sakai and S. Sugimoto, "Low energy hadron physics in holographic QCD," Prog. Theor. Phys. **113**, 843 (2005), [hep-th/0412141].

[14] Edalati, Mohammad and Leigh, Robert G. and Hoang, Nam Nguyen, "*Transversely-intersecting D-branes at finite temperature and chiral phase transition,*" *JHEP* **05** (2009) 035, arXiv:hep-th/0803.1277.

[15] Erdmenger, Johanna and Evans, Nick and Kirsch, Ingo and Threlfall, Ed, "*Mesons in Gauge/Gravity Duals - A Review,*" *Eur. Phys. J.* **A35** (2008) 81-133, arXiv:hep-th/0711.4467.

[16] Erlich, Joshua and Katz, Emanuel and Son, Dam T. and Stephanov, Mikhail A., "*QCD and a Holographic Model of Hadrons,*" *Phys. Rev. Lett.* **95** (2005) 261602, arXiv:hep-th/0501128.

[17] Karch, Andreas and Katz, Emanuel and Son, Dam T. and Stephanov, Mikhail A. , "*Linear Confinement and AdS/QCD,*" *Phys. Rev.* **D74** (2006) 015005, arXiv:hep-th/0602229.

[18] Gursoy, U. and Kiritsis, E. , "*Exploring improved holographic theories for QCD: Part I,*" *JHEP* **02** (2008) 032, arXiv:hep-th/0707.1324.

[19] Gursoy, U. and Kiritsis, E. and Nitti, F. , "*Exploring improved holographic theories for QCD: Part II,*" *JHEP* **02** (2008) 019, arXiv:hep-th/0707.1349.

[20] Evans, Nick and Shock, Jonathan P. and Waterson, Tom , "*Towards a perfect QCD gravity dual,*" *Phys. Lett.* **B622** (2005) 165-171, arXiv:hep-th/0505250.

[21] Leigh, Robert G. and Hoang, Nam N. and Petkou, Anastasios C., "*Torsion and the Gravity Dual of Parity Symmetry Breaking in AdS4/CFT3 Holography,*" *JHEP* **03** (2009) 033, arXiv:hep-th/0809.5258.

[22] Hartnoll, Sean A. and Herzog, Christopher P. and Horowitz, Gary T., "*Building a Holographic Superconductor,*" *Phys. Rev. Lett.* **101** (2008) 031601, arXiv:hep-th/0803.3295.

[23] Gubser, Steven S. and Pufu, Silviu S., "*The gravity dual of a p-wave superconductor,*" *JHEP* **11** (2008) 033, arXiv:hep-th/0805.2960.

[24] Herzog, C. P. and Kovtun, P. K. and Son, D. T., "*Holographic model of superfluidity,*" *Phys. Rev.* **D79** (2009) 066002, arXiv:hep-th/0809.4870.

[25] Keski-Vakkuri, Esko and Kraus, Per, "*Quantum Hall Effect in AdS/CFT,*" *JHEP* **09** (2008) 130, arXiv:hep-th/0805.4643.

[26] Davis, Joshua L. and Kraus, Per and Shah, Akhil, "*Gravity Dual of a Quantum Hall Plateau Transition,*" *JHEP* **11** (2008) 020, arXiv:hep-th/0809.1876.

[27] Kachru, Shamit and Liu, Xiao and Mulligan, Michael, "*Gravity Duals of Lifshitz-like Fixed Points,*" *Phys. Rev.* **D78** (2008) 106005, arXiv:hep-th/0808.1725.

[28] E. Witten, "*Anti-de Sitter space and holography,*" *Adv. Theor. Math. Phys.* **2** (1998) 253-291, arXiv:hep-th/9802150.

[29] D. T. Son and A. O. Starinets, "*Minkowski-space correlators in AdS/CFT correspondence: Recipe and applications,*" *JHEP* **09** (2002) 042, arXiv:hep-th/0205051.

[30] K. Skenderis and B. C. van Rees, "*Real-time gauge/gravity duality: Prescription, Renormalization and Examples,*" arXiv:0812.2909.

[31] K. Skenderis and B. C. van Rees, "*Real-time gauge/gravity duality,*" *Phys. Rev. Lett.* **101** (2008) 081601, arXiv:0805.0150.

[32] K. Skenderis "*Lecture notes on holographic renormalization,*" *Class. Quant. Grav.* **19** (2002) 5849, arXiv:0209067.

[33] M. Henningson and K. Sfetsos, "*Spinors and the AdS/CFT correspondence,*" *Phys. Lett.* **B431** (1998) 63-68, arXiv:hep-th/9803251.

[34] W. Mueck and K. S. Viswanathan, "*Conformal field theory correlators from classical field theory on anti-de Sitter space. II: Vector and spinor fields,*" *Phys. Rev.* **D58** (1998) 106006, arXiv:hep-th/9805145.

[35] M. Henneaux, "*Boundary terms in the AdS/CFT correspondence for spinor fields,*" arXiv:hep-th/9902137.

[36] G. C. Giecold, "*Fermionic Schwinger-Keldysh Propagators from AdS/CFT,*" arXiv:0904.4869.

[37] Leigh, Robert G. and Hoang, Nam Nguyen, "*Real-Time Correlators and Non-Relativistic Holography,*" *JHEP* **11** (2009) 010, arXiv:hep-th/0904.4270.

[38] Leigh, Robert G. and Hoang, Nam Nguyen, "*Fermions and the Sch/nrCFT Correspondence,*" *JHEP* **03** (2010) 027, arXiv:hep-th/0909.1883.

[39] Leigh, Robert G. and Hoang, Nam Nguyen, "*The Non-Relativistic Holography of Vector Operators,*" to be appeared.

[40] J. M. Maldacena, "The large N limit of superconformal field theories and supergravity," Adv. Theor. Math. Phys. **2** (1998) 231; Int. J. Theor. Phys. **38** (1999) 1113, [hep-th/9711200].

[41] S. S. Gubser, I. R. Klebanov and A. M. Polyakov, "Gauge theory correlators from non-critical string theory," Phys. Lett. B **428**, 105 (1998), [hep-th/9802109].

[42] E. Witten, "Anti-de Sitter space and holography," Adv. Theor. Math. Phys. **2**, 253 (1998), [hep-th/9802150].

[43] O. Aharony, S. S. Gubser, J. Maldacena, H. Ooguri and Y. Oz, "Large N field theories, string theory and gravity," Phys. Rept. **323** (2000) 183, [hep-th/9905111].

[44] E. Witten, "Anti-de Sitter space, thermal phase transition, and confinement in gauge theories," Adv. Theor. Math. Phys. **2**, 505 (1998), [hep-th/9803131].

[45] A. Brandhuber, N. Itzhaki, J. Sonnenschein and S. Yankielowicz, "Wilson loops in the large N limit at finite temperature," Phys. Lett. B **434**, 36 (1998), [hep-th/9803137].

[46] E. Antonyan, J. A. Harvey, S. Jensen and D. Kutasov, "NJL and QCD from string theory," [hep-th/0604017].

[47] Y. Nambu and G. Jona-Lasinio, "Dynamical model of elementary particles based on an analogy with superconductivity. I," Phys. Rev. **122**, 345 (1961).

[48] O. Aharony, J. Sonnenschein and S. Yankielowicz, "A holographic model of deconfinement and chiral symmetry restoration," Annals Phys. **322**, 1420 (2007), [hep-th/0604161].

[49] A. Parnachev and D. A. Sahakyan, "Chiral phase transition from string theory," Phys. Rev. Lett. **97**, 111601 (2006), [hep-th/0604173].

[50] E. Antonyan, J. A. Harvey and D. Kutasov, "Chiral symmetry breaking from intersecting D-branes," Nucl. Phys. B **784**, 1 (2007), [hep-th/0608177].

[51] N. Itzhaki, J. M. Maldacena, J. Sonnenschein and S. Yankielowicz, "Supergravity and the large N limit of theories with sixteen supercharges," Phys. Rev. D **58**, 046004 (1998), [hep-th/9802042].

[52] O. Aharony, "A brief review of 'little string theories'," Class. Quant. Grav. **17**, 929 (2000), [hep-th/9911147].

[53] M. Kruczenski, D. Mateos, R. C. Myers and D. J. Winters, "Towards a holographic dual of large-N(c) QCD," JHEP **0405**, 041 (2004), [hep-th/0311270].

[54] N. Horigome, M. Nishimura and Y. Tanii, "Chiral Symmetry Breaking in Brane Models," arXiv:0710.4900 [hep-th].

[55] Y. h. Gao, W. s. Xu and D. f. Zeng, "NGN, QCD(2) and chiral phase transition from string theory," JHEP **0608**, 018 (2006), [hep-th/0605138].

[56] D. J. Gross and A. Neveu, "Dynamical Symmetry Breaking In Asymptotically Free Field Theories," Phys. Rev. D **10**, 3235 (1974).

[57] J. J. Friess, S. S. Gubser, G. Michalogiorgakis and S. S. Pufu, "Stability of strings binding heavy-quark mesons," JHEP **0704**, 079 (2007), [hep-th/0609137].

[58] N. Horigome and Y. Tanii, "Holographic chiral phase transition with chemical potential," JHEP **0701**, 072 (2007), [hep-th/0608198].

[59] O. Bergman, G. Lifschytz and M. Lippert, "Holographic Nuclear Physics," JHEP **0711**, 056 (2007), arXiv:0708.0326 [hep-th].

[60] J. L. Davis, M. Gutperle, P. Kraus and I. Sachs, "Stringy NJL and Gross-Neveu models at finite density and temperature," JHEP **0710**, 049 (2007), arXiv:0708.0589 [hep-th].

[61] M. Rozali, H. H. Shieh, M. Van Raamsdonk and J. Wu, "Cold Nuclear Matter In Holographic QCD," JHEP **0801**, 053 (2008), arXiv:0708.1322 [hep-th].

[62] O. Bergman, G. Lifschytz and M. Lippert, "Response of Holographic QCD to Electric and Magnetic Fields," arXiv:0802.3720 [hep-th].

[63] C. V. Johnson and A. Kundu, "External Fields and Chiral Symmetry Breaking in the Sakai-Sugimoto Model," arXiv:0803.0038 [hep-th].

[64] K. Y. Kim, S. J. Sin and I. Zahed, "Dense and Hot Holographic QCD: Finite Baryonic E Field," arXiv:0803.0318 [hep-th].

[65] R. Casero, E. Kiritsis and A. Paredes, "Chiral symmetry breaking as open string tachyon condensation," Nucl. Phys. B **787**, 98 (2007), [hep-th/0702155].

[66] O. Bergman, S. Seki and J. Sonnenschein, "Quark mass and condensate in HQCD," arXiv:0708.2839 [hep-th].

[67] A. Dhar and P. Nag, "Sakai-Sugimoto model, Tachyon Condensation and Chiral symmetry Breaking," arXiv:0708.3233 [hep-th].

[68] M. R. Garousi, "D-brane anti-D-brane effective action and brane interaction in open string channel," JHEP **0501**, 029 (2005), [hep-th/0411222].

[69] M. Edalati, R. G. Leigh and N. Nguyen, work in progress.

[70] U. H. Danielsson, A. Guijosa and M. Kruczenski, "Brane-antibrane systems at finite temperature and the entropy of black branes," JHEP **0109**, 011 (2001), [hep-th/0106201].

[71] K. Hotta, "Brane-antibrane systems at finite temperature and phase transition near the Hagedorn temperature," JHEP **0212**, 072 (2002), [hep-th/0212063].

[72] V. Calo and S. Thomas, "Phase Transitions in Separated D_{p-1} and anti-D_{p-1} Branes at Finite Temperature," arXiv:0802.2453 [hep-th].

[73] C. P. Herzog, P. Kovtun, S. Sachdev, and D. T. Son, "*Quantum critical transport, duality, and M-theory,*" *Phys. Rev.* **D75** (2007) 085020, `arXiv:hep-th/0701036`.

[74] S. A. Hartnoll, P. K. Kovtun, M. Muller, and S. Sachdev, "*Theory of the Nernst effect near quantum phase transitions in condensed matter, and in dyonic black holes,*" *Phys. Rev.* **B76** (2007) 144502, `arXiv:0706.3215`.

[75] S. A. Hartnoll and P. Kovtun, "*Hall conductivity from dyonic black holes,*" *Phys. Rev.* **D76** (2007) 066001, `arXiv:0704.1160`.

[76] S. A. Hartnoll and C. P. Herzog, "*Ohm's Law at strong coupling: S duality and the cyclotron resonance,*" *Phys. Rev.* **D76** (2007) 106012, `arXiv:0706.3228`.

[77] E. Keski-Vakkuri and P. Kraus, "*Quantum Hall Effect in AdS/CFT,*" `arXiv:0805.4643`.

[78] J. L. Davis, P. Kraus, and A. Shah, "*Gravity Dual of a Quantum Hall Plateau Transition,*" arXiv:0809.1876.

[79] S. A. Hartnoll, C. P. Herzog, and G. T. Horowitz, "*Building a Holographic Superconductor,*" *Phys. Rev. Lett.* **101** (2008) 031601, arXiv:0803.3295.

[80] D. Minic and J. J. Heremans, "*High Temperature Superconductivity and Effective Gravity,*" arXiv:0804.2880.

[81] E. Nakano and W.-Y. Wen, "*Critical magnetic field in a holographic superconductor,*" *Phys. Rev.* **D78** (2008) 046004, arXiv:0804.3180.

[82] T. Albash and C. V. Johnson, "*A Holographic Superconductor in an External Magnetic Field,*" arXiv:0804.3466.

[83] S. S. Gubser and S. S. Pufu, "*The gravity dual of a p-wave superconductor,*" arXiv:0805.2960.

[84] C. P. Herzog, P. K. Kovtun, and D. T. Son, "*Holographic model of superfluidity,*" arXiv:0809.4870.

[85] P. Basu, A. Mukherjee and H. H. Shieh, "*Supercurrent: Vector Hair for an AdS Black Hole,*" arXiv:0809.4494.

[86] S. S. Gubser, "*Breaking an Abelian gauge symmetry near a black hole horizon,*" arXiv:0801.2977.

[87] S. S. Gubser, "*Colorful horizons with charge in anti-de Sitter space,*" arXiv:0803.3483.

[88] S. S. Gubser and F. D. Rocha, "*The gravity dual to a quantum critical point with spontaneous symmetry breaking,*" arXiv:0807.1737.

[89] R. G. Leigh and A. C. Petkou, "*Gravitational Duality Transformations on (A)dS4,*" *JHEP* **11** (2007) 079, arXiv:0704.0531.

[90] S. de Haro and A. C. Petkou, "*Holographic Aspects of Electric-Magnetic Dualities,*" *J. Phys. Conf. Ser.* **110** (2008) 102003, arXiv:0710.0965.

[91] D. S. Mansi, A. C. Petkou, and G. Tagliabue, "*Gravity in the 3+1-Split Formalism I: Holography as an Initial Value Problem,*" arXiv:0808.1212.

[92] D. S. Mansi, A. C. Petkou, and G. Tagliabue, "*Gravity in the 3+1-Split Formalism II: Self-Duality and the Emergence of the Gravitational Chern-Simons in the Boundary,*" arXiv:0808.1213.

[93] S. de Haro, "*Dual Gravitons in AdS4/CFT3 and the Holographic Cotton Tensor,*" arXiv:0808.2054.

[94] J. Bagger and N. Lambert, "*Modeling multiple M2's,*" *Phys. Rev.* **D75** (2007) 045020, arXiv:hep-th/0611108.

[95] J. Bagger and N. Lambert, "*Gauge Symmetry and Supersymmetry of Multiple M2-Branes,*" *Phys. Rev.* **D77** (2008) 065008, arXiv:0711.0955.

[96] J. Bagger and N. Lambert, "*Comments On Multiple M2-branes,*" *JHEP* **02** (2008) 105, arXiv:0712.3738.

[97] A. Gustavsson, "*Algebraic structures on parallel M2-branes,*" arXiv:0709.1260.

[98] K. Hosomichi, K. M. Lee, S. Lee, S. Lee and J. Park, *"N=4 Superconformal Chern-Simons Theories with Hyper and Twisted Hyper Multiplets,*" *JHEP* **0807** (2008) 091 arXiv:0805.3662.

[99] O. Aharony, O. Bergman, D. L. Jafferis, and J. Maldacena, "*N=6 superconformal Chern-Simons-matter theories, M2-branes and their gravity duals,*" arXiv:0806.1218.

[100] I. L. Shapiro, "*Physical aspects of the space-time torsion,*" *Phys. Rept.* **357** (2002) 113, arXiv:hep-th/0103093.

[101] O. Chandia and J. Zanelli, "*Torsional topological invariants (and their relevance for real life),*" arXiv:hep-th/9708138.

[102] L. Freidel, D. Minic, and T. Takeuchi, "*Quantum gravity, torsion, parity violation and all that,*" *Phys. Rev.* **D72** (2005) 104002, arXiv:hep-th/0507253.

[103] S. Mercuri, *"From the Einstein-Cartan to the Ashtekar-Barbero canonical constraints, passing through the Nieh-Yan functional,*" *Phys. Rev.* D **77** (2008) 024036 arXiv:0708.0037.

[104] F. Canfora, *"Some solutions with torsion in Chern-Simons gravity and observable effects,*" arXiv:0706.3538.

[105] S. B. Giddings and A. Strominger, "*Axion Induced Topology Change in Quantum Gravity and String Theory,*" *Nucl. Phys.* **B306** (1988) 890.

[106] M. Gutperle and W. Sabra, "*Instantons and wormholes in Minkowski and (A)dS spaces,*" *Nucl. Phys.* **B647** (2002) 344-356, arXiv:hep-th/0206153.

[107] R. D'Auria and T. Regge, "*Gravity Theories with Asymptotically Flat Instantons,*" *Nucl. Phys.* **B195** (1982) 308.

[108] R. Jackiw, "*Topological Investigations of Quantized Gauge Theories,*". Presented at Les Houches Summer School on Theoretical Physics: Relativity Grops and Topology, Les Houches, France, Jun 27 - Aug 4, 1983.

[109] R. G. Leigh and A. C. Petkou, "*SL(2,Z) action on three-dimensional CFTs and holography,*" *JHEP* **12** (2003) 020, arXiv:hep-th/0309177.

[110] G. W. Gibbons, M. B. Green, and M. J. Perry, "*Instantons and Seven-Branes in Type IIB Superstring Theory,*" *Phys. Lett.* **B370** (1996) 37-44, arXiv:hep-th/9511080.

[111] V. Balasubramanian and P. Kraus, "*A stress tensor for anti-de Sitter gravity,*" *Commun. Math. Phys.* **208** (1999) 413-428, arXiv:hep-th/9902121.

[112] P. Kraus, F. Larsen, and R. Siebelink, "*The gravitational action in asymptotically AdS and flat spacetimes,*" *Nucl. Phys.* **B563** (1999) 259-278, arXiv:hep-th/9906127.

[113] E. Witten, "*SL(2,Z) action on three-dimensional conformal field theories with Abelian symmetry,*" arXiv:hep-th/0307041.

[114] R. G. Leigh, N. Nguyen-Hoang and A. C. Petkou, to appear.

[115] M. Tinkham, *Introduction to Superconductivity.* Dover Publications, 2nd ed., 1996.

[116] D. Z. Freedman, S. D. Mathur, A. Matusis, and L. Rastelli, "*Correlation functions in the CFT(d)/AdS(d + 1) correspondence,*" *Nucl. Phys.* **B546** (1999) 96-118, arXiv:hep-th/9804058.

[117] C. P. Herzog and D. T. Son, "*Schwinger-Keldysh propagators from AdS/CFT correspondence,*" *JHEP* **03** (2003) 046, arXiv:hep-th/0212072.

[118] N. Iqbal and H. Liu, "*Real-time response in AdS/CFT with application to spinors,*" arXiv:0903.2596.

[119] J.-M. Lévy-Leblond, "*Nonrelativistic particles and wave equations,*" *Comm. Math. Phys.* **6** (1967), no. 4, 286-311.

[120] C. R. Hagen, "*Scale and conformal transformations in galilean-covariant field theory,*" *Phys. Rev.* **D5** (1972) 377-388.

[121] M. Perroud, "*Projective Representations of the Schrödinger Group,*" *Helv. Phys. Acta* **50** (1977) 233-252.

[122] M. Henkel and J. Unterberger, "*Schroedinger invariance and space-time symmetries,*" *Nucl. Phys.* **B660** (2003) 407–435, arXiv:hep-th/0302187.

[123] C. A. Fuertes and S. Moroz, "*Correlation functions in the non-relativistic AdS/CFT correspondence,*" *Phys. Rev.* **D79** (2009) 106004, arXiv:0903.1844.

[124] A. Volovich and C. Wen, "*Correlation Functions in Non-Relativistic Holography,*" *JHEP* **05** (2009) 087, arXiv:0903.2455.

[125] A. Akhavan, M. Alishahiha, A. Davody, and A. Vahedi, "*Fermions in non-relativistic AdS/CFT correspondence,*" arXiv:0902.0276.

[126] C. Duval, M. Hassaine, and P. A. Horvathy, "*The geometry of Schródinger symmetry in gravity background/non-relativistic CFT,*" *Annals Phys.* **324** (2009) 1158–1167, arXiv:0809.3128.

[127] C. Duval, P. A. Horvathy, and L. Palla, "*Spinors in non-relativistic Chern-Simons electrodynamics,*" *Annals Phys.* **249** (1996) 265–297, arXiv:hep-th/9510114.

[128] C. Duval, G. W. Gibbons, and P. Horvathy, "*Celestial Mechanics, Conformal Structures, and Gravitational Waves,*" *Phys. Rev.* **D43** (1991) 3907–3922, arXiv:hep-th/0512188.

[129] E. Witten, "*Fermion Quantum Numbers in Kaluza-Klein Theory,*" in *Shelter Island II: Proceedings of the 1983 Shelter Island Conference on Quantum Field Theory and the Fundamental Problems of Physics*, R. Jackiw, N. N. Khuri, S. Weinberg, and E. Witten, eds., pp. 227–277. M.I.T. Press, 1983. Lecture given at Shelter Island II Conf., Shelter Island, N.Y., 1-2 Jun 1983.

[130] Kuperstein, Stanislav and Sonnenschein, Jacob, *"Non-critical supergravity (d ¿ 1) and holography,*" *JHEP* **07** (2004) 049, arXiv:hep-th/0403254.

[131] A. J. Niemi and G. W. Semenoff, *"Axial Anomaly Induced Fermion Fractionization And Effective Gauge Theory Actions In Odd Dimensional Space-Times,*" *Phys. Rev. Lett.* **51** (1983) 2077.

[132] A. N. Redlich, "*Parity Violation and Gauge Noninvariance of the Effective Gauge Field Action in Three-Dimensions,*" *Phys. Rev.* **D29** (1984) 2366–2374.

Author's Biography

Nam Nguyen Hoang was born in Ho Chi Minh city, Vietnam, on February 2, 1981. He completed his B.Sc. in Physics from Hanoi University of Science, Hanoi, Vietnam. While a graduate student at the University of Illinois at Urbana-Champaign, he studied theoretical High Energy Physics under the direction of Robert Leigh.

Publications

1. *The Non-Relativistic Holography of Vector Operators*
   (with R. G. Leigh)
   In preparation

2. *Fermions and the Sch/nrCFT Correspondence*
   (with R. G. Leigh)
   JHEP **03** 27 (2010) (hep-th/0909.1883)

3. *Real-Time Correlators and Non-Relativistic Holography*
   (with R. G. Leigh)
   JHEP **11** 10 (2009) (hep-th/0904.4270)

4. *Torsion and the Gravity Dual of Parity Symmetry Breaking in AdS(4)/CFT(3) Holography*
   (with R. G. Leigh and Anastasios C. Petkou)
   JHEP **03** 33 (2009) (hep-th/0809.5258)

5. *Transversely-intersecting D-branes at finite temperature and chiral phase transition*
   (Mohammad Edalati and R. G. Leigh)
   JHEP **05** 35 (2009) (hep-th/0803.1277)